A Dissertation for the Degree of Doctor of Philosophy

Enhancement of therapeutic efficacy by immunomodulation in human mesenchymal stem cells

인간 중간엽 줄기세포의 면역 조절능을 통한 치료 효율 향상 연구

By

Byung-Chul Lee

February 2019

Major of Veterinary Pathobiology and Preventive Medicine,

Department of Veterinary Medicine,

Graduate School of Seoul National University

ABSTRACT

Enhancement of therapeutic efficacy by immunomodulation in human mesenchymal stem cells

Byung-Chul Lee

Major of Veterinary Pathobiology and Preventive Medicine,
Department of Veterinary Medicine,
Graduate School of Seoul National University

Supervisor: Kyung-Sun Kang, D.V.M., Ph.D.

Human mesenchymal stem cells (hMSCs) have recently been considered a promising alternative treatment for diverse immune disorders due to their unique biomedical potentials including the immunomodulatory property and ability to promote tissue regeneration. However, despite many years of research and pre-clinical studies, results from clinical trials using these cells have been diverse and conflicting. This discrepancy is caused by several factors such as poor engraftment, low survival rate and donor-dependent variation of the cells. Enhancement of consistency and efficacy of hMSCs remains a challenge to overcome the current obstacles to

hMSC-based therapy and subsequently achieve improved therapeutic outcomes.

Human umbilical cord blood- (hUCB) and adipose tissue-derived (hAD)-MSCs suppress various lineage of immune cells. Many studies have elucidated the clinical efficacy and underlying mechanisms of MSCs in immune disorders. Although immunoregulatory factors, such as prostaglandin E_2 (PGE_2), and their mechanisms of action on immune cells have been revealed, their effects on MSCs and regulation of their production by the culture environment are less clear. Therefore, in the first part of this study, I investigated the autocrine effect of PGE_2 on human adult stem cells from cord blood or adipose tissue, and the regulation of its production by cell-to-cell contact, followed by the determination of its immunomodulatory properties. MSCs were treated with specific inhibitors to suppress PGE_2 secretion, and proliferation was assessed. PGE_2 exerted an autocrine regulatory function in MSCs by triggering E-Prostanoid (EP) 2 receptor. Inhibiting PGE_2 production led to growth arrest, whereas addition of MSC-derived PGE_2 restored proliferation. The level of PGE_2 production from an equivalent number of MSCs was down-regulated via gap junctional intercellular communication. This cell contact-mediated decrease in PGE_2 secretion down-regulated the suppressive effect of MSCs on immune cells. Taken together, PGE_2 produced by MSCs contributes to maintenance of self-renewal capacity through EP2 in an autocrine manner, and PGE_2 secretion is down-regulated by cell-to-cell contact, attenuating its immunomodulatory potency.

Administration of assistant materials such as small molecules, growth factors and biocompatible particles is known to enhance the therapeutic function of hMSCs against various diseases. MIS416, a novel microparticle which consists of MDP and bacterial DNA for an activation of cytoplasmic receptors NOD2 and TLR9, is phagocytized *in vivo* and changes

immune milieu to resist the pathophysiological environment. In the second part of present study, I investigated whether administration of MIS416 could enhance the therapeutic efficacy of hUCB-MSCs against experimental colitis, using dextran sulfate sodium (DSS)-induced colitis model. Colitis was experimentally induced in mice and mice were examined grossly, and blood, spleen and colon tissues were subsequently collected for further *ex vivo* analyses. To explore the effects of MIS416 on the therapeutic process, hUCB-MSCs and primary isolated immune cells were cultured with MIS416, and *in vitro* assays were performed. Compared to the single administration of hUCB-MSCs, co-administration with MIS416 improved the therapeutic efficiency of the stem cells by significantly alleviating the symptoms of inflammatory bowel disease. Interestingly, MIS416 did not exert any direct effect on the immunomodulatory capacity of hUCB-MSCs. Instead, systemically injected MIS416 altered the immune milieu in the colon which caused hUCB-MSCs to be more readily recruited towards the lesion site and to suppress inflammation more efficiently. In addition, considerable numbers of regulatory immune cells were stimulated as a result of the cooperation of MIS416 and hUCB-MSCs. These findings indicate that co-administration with MIS416 enhances the therapeutic potential of hUCB-MSCs by systemically regulating the immune response, which might be an effective strategy for overcoming the current obstacles to stem cell therapy in clinical practice.

In conclusion, these findings imply that (i) cell proliferation and immunosuppression of hMSCs are augmented by autocrine PGE_2 and its subtype receptor EP2, of which secretion and expression are impeded by cell-to-cell contact and this physiological feature may be applied to preconditioning process of the cells or cell-cultured medium, and (ii) co-administration of microparticle MIS416 changes systemic immune milieu to improve migration into lesion sites and immune suppressive capacity of

hUCB-MSCs. Consequently, this study suggests preconditioning related to cell contact status and co-administration of MIS416 as enhancement strategies for therapeutic efficacy of hMSCs.

Keywords: Mesenchymal stem cells, Cell contact, PGE_2, Proliferation, Immunosuppression, MIS416, Inflammatory bowel disease, Migration

Student number : 2012-21544

TABLE OF CONTENTS

CHAPTER I

PGE_2 maintains self-renewal of human adult stem cells via EP2-mediated autocrine signaling and its production is regulated by cell-to-cell contact

LIST OF ABBREVIATIONS

hMSCs	Human mesenchymal stem cells
hUCB-MSCs	Human umbilical cord blood-derived MSCs
hAD-MSCs	Human adipose tissue-derived MSCs
COX-2	Cyclooxygenase-2
PGE_2	Prostaglandin E_2
mPGES	Membrane associated PGE synthase
CPDL	Cumulative population doubling level
CM	Conditioned medium
siRNA	Small interfering RNA
EP	E prostanoid
CX	Connexin
GJIC	Gap junction intercellular communication
NO	Nitric oxide
TGF	Transforming growth factor
IFN	Interferon
TNF	Tumor necrosis factor
IDO	Indoleamine-2,3-dioxygenase
MLR	Mixed lymphocyte reaction
MNC	Mononuclear cell
IBD	Inflammatory bowel disease
DSS	Dextran sulfate sodium
MAPK	Mitogen-activated protein kinase
NF-κB	Nuclear factor-κB
Th	Helper T lymphocyte
MCP-1	Monocyte chemoattractant protein-1

LIST OF FIGURES

LITERATURE REVIEW

CHAPTER I

CHAPTER Ⅱ

GENERAL DISCUSSION

LIST OF TABLES

LITERATURE REVIEW

CHAPTER I

CHAPTER II

LITERATURE REVIEW

A. Mesenchymal stem cells and therapeutic function

Mesenchymal stem cells (MSCs) reside in most of the tissues in human body and can be isolated from those tissues. MSCs are defined as their capacity, so-called ‘stemness’, to proliferate continuously (self-renewal) and differentiate into mesodermal lineages including osteogenic-, adipogenic- and chondrogenic differentiation (da Silva Meirelles et al., 2006). From the beginning stage of research, a major source for MSCs has been a bone marrow (BM). However, harvesting procedure of BM is too invasive and expensive. In addition, yield and cell viability vary depending on the condition of recipients such as an age (Mueller and Glowacki, 2001). Thus, alternative sources for MSCs have been continuously proposed. Umbilical cord blood (UCB) and adipose tissue (AD) are introduced as promising sources for the BM substitute (Kern et al., 2006). UCB can be easily obtained during childbirth without any harm to both newborns and mothers. AD would be acquired through liposuction less invasively and it contains a greater quantity of cells than BM (Zhu et al., 2008). Of note, there are no crucial differences between MSCs derived from BM, AD and UCB (Kim et al., 2010). Furthermore, it is reported that hMSCs can be isolated from other tissues including umbilical cord (UC), placenta, dental pulp, periodontal ligament, synovial membrane, dermis and endometrium (Baksh et al., 2007; Huang et al., 2009; Lv et al., 2014; Scherjon et al., 2004; Seo et al., 2004).

MSCs have unique biomedical properties (Figure 1). Localization to the lesion site is important for therapeutic mechanisms of MSCs such as suppression of activated immune cells and tissue regeneration. Thus, homing

of MSCs into inflamed sites would be a key factor for MSC-based therapy. It has been reported that injected MSCs migrate to injured site of animal model and ameliorate symptoms of disease (da Silva Meirelles et al., 2008). Migratory ability of MSCs can be influenced by expression level of chemokine receptors, proteases and growth factors. For example, hMSCs expressing CXCR4, specific receptor for chemokine stromal-derived factor-1 (SDF-1) readily settle in BM after transplantation and perform a role for hematopoietic niche (Kortesidis et al., 2005; Wynn et al., 2004).

MSCs has a pro-angiogenic potential, thus the cells were considered as a promising tool for treating cardiovascular diseases such as a peripheral artery disease (PAD) (Kim et al., 2006). It is reported that MSCs have the potential to re-vascularize and protect the ischemic limb (Perin et al., 2017). Among secretory factors of MSCs, vascular endothelial growth factor (VEGF) plays a crucial role in MSC-mediated angiogenic promotion and cardioprotection (Boomsma and Geenen, 2012; Markel et al., 2008; Tang et al., 2006). In addition, MSC-derived MCP-1, IGF-1, FGF, PGE_2 and PGI_2 are also involved in promoting the production of vascular-like structure *in vitro* and *in vivo* (Hung et al., 2007a; Kinnaird et al., 2004; Masferrer et al., 2000).

It has been demonstrated that MSCs accelerate wound repair through multiple studies (An et al., 2018; Chen et al., 2008; Wu et al., 2007; Zhang et al., 2015). Wound healing is a quite complicated physiological phenomenon, and MSCs comprehensively attribute to the recovery process by using therapeutic functions mentioned above. MSCs enhance the rebuilding of extracellular matrix (Jeon et al., 2010) and skin regeneration by promoting the proliferation, differentiation, positioning of cellular constitutes for skin (Luo et al., 2010; Nie et al., 2011). Moreover, MSCs prevent fibrosis during wound healing (Suga, 2009). In addition to the described properties, MSCs carry out the supportive role for other stem

and progenitor cells (Sugiyama et al., 2006), anti-apoptosis (Block et al., 2009) and chemoattraction (da Silva Meirelles et al., 2008).

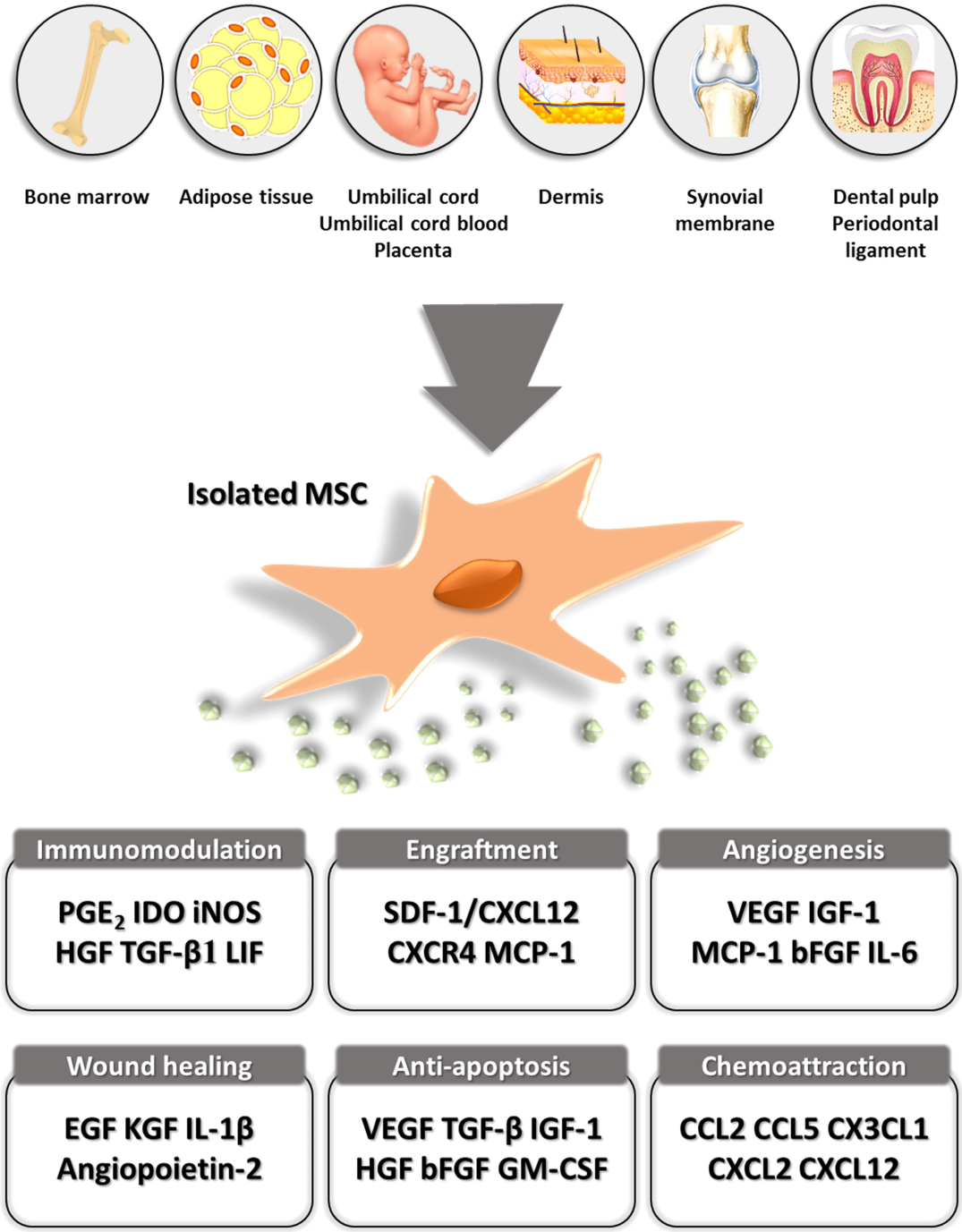

Figure 1. Isolation sources and therapeutic function of MSCs.

A schematogram illustrates various sources for the isolation of MSCs and biological properties associated with their therapeutic effects.

B. MSC-mediated immunomodulation and the role of PGE_2 in therapeutic function

A most important feature of MSCs is the immunomodulatory function for their clinical feasibility. It is reported that MSCs can regulate various immune cell subsets, thus attenuate the severity of the immune-related diseases (Corcione et al., 2006; Le Blanc and Davies, 2015; Zappia et al., 2005). MSCs efficiently suppress excessive effector T cell proliferation and subsequent inflammation by upregulating the expression of immunomodulatory factors such as PGE_2, NO, IDO-1 and FAS ligand, and inducing T cell anergy (Akiyama et al., 2012; Croitoru-Lamoury et al., 2011; Najar et al., 2010; Sato et al., 2007; Zappia et al., 2005). Importantly, hMSCs promote regulatory T cells during the polarization process of Th1 and Th17 cells to maintain systemic immune balance (Ghannam et al., 2010; Luz-Crawford et al., 2013). MSCs also suppress excessive activation of effector B lymphocytes and promote the regulatory type of B cells (Franquesa et al., 2015; Luz-Crawford et al., 2016; Shin et al., 2017). In addition, MSCs can inhibit proliferation of NK cells and DCs, and contribute to polarization of macrophages (Spaggiari et al., 2009; Spaggiari et al., 2006; Zhang et al., 2010).

Among the secretory factors, PGE_2 has an immense power for regulating the physiological behaviors of MSCs (Figure 2), thus COX-2~PGE_2 signaling pathway becomes an attractive target to increase their yield and functionality. Most important role of PGE_2 is a major mediator in immunosuppression of MSCs on various type of immune cells. For example, MSCs exerts anti-proliferative effects on T (Sheng et al., 2008), dendritic (Djouad et al., 2007) and NK cells (Sotiropoulou et al., 2006) through secreted PGE_2. On the other hand, PGE_2 is involved in the lineage determination of alternative type of macrophages (Shin et al., 2016).

In addition, MSC-mediated protection against various autoimmune disease was connected to the promotion of regulatory T cells and subsequent secretion of IL-10 (Kim et al., 2013; Kim et al., 2015; Lee et al., 2016; Luz-Crawford et al., 2013). Furthermore, proliferation of MSCs is considerably affected by autocrine signaling of PGE_2 (Lee et al., 2016). PGE_2 activates FAK and ERK1/2 pathway to promote the migratory capacity of MSCs (Lu et al., 2017). Given these definitive beneficial effects, consistent and stable secretion of PGE_2 is an invaluable target for the enhancement of MSC application.

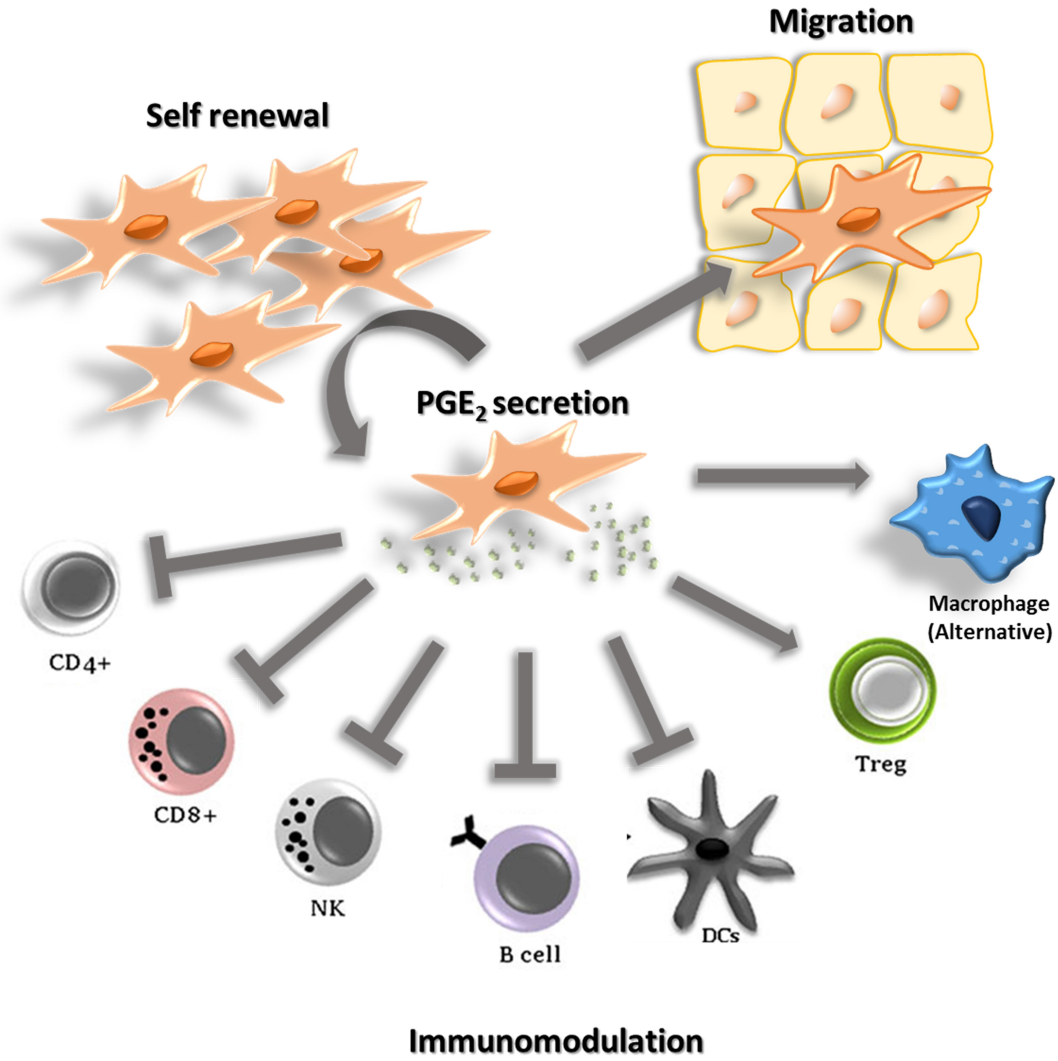

Figure 2. Functional role of PGE_2 in maintaing the property of MSCs.
Secretion of PGE_2 from MSCs is involved in the regulation of cell growth through autocrine signaling and promotes proper delivery of infused MSCs to inflamed sites. Importantly, the cytokine carries out a distinct role for each lineage of immune cells, resulting in restoration of immune homeostasis.

C. Clinical application of MSCs

Given their unique therapeutic potentials, MSCs have been applied to the treatment of several rare diseases for decades. Since the first clinical trial using MSCs performed in 1995 (Lazarus et al., 1995), a number of clinical trials have been conducted and 838 interventional type of studies targeting a very wide range of diseases are enrolled on the public clinical database (http://www.clinicaltrials.gov). In Korea, 35 cases of phase 2 or 3 clinical trials for various diseases have been conducted by using MSCs (Table 1).

Although the mechanisms for the therapeutic effects of MSCs are not fully elucidated, it can be assumed how the cells suppress activated immune cells and accelerate recovery process through many previous studies. Two means of cellular behavior supporting therapeutic mechanisms are suggested, direct cell-mediated action and environmental change mediated by soluble factors (Yagi et al., 2010). As described above, MSCs can regulate various immune cell subsets by direct cell-to-cell interaction to resolve excessive inflammation in immune-related diseases (Corcione et al., 2006; Le Blanc and Davies, 2015; Zappia et al., 2005). Directly infused MSCs present the therapeutic effect on chronic and inflammatory autoimmune diseases including refractory systemic lupus erythematous (Wang et al., 2013) and Crohn's disease (Forbes et al., 2014). Furthermore, MSCs has the potential to directly differentiate into another type of functioning cells such as chondroblasts and pancreatic islet cells (Chen et al., 2004). Given that potential, MSCs have been clinically applied in bone and cartilage diseases (Orozco et al., 2013; Wong et al., 2013) and Diabetes Mellitus (DM) (Haller et al., 2008). Moreover, considerable numbers of studies have demonstrated the therapeutic efficacy of MSC to neurodegenerative diseases and acute brain injury (Lee et al., 2010).

Paracrine property of MSCs is become a powerful weapon after *in vivo* administration. In addition, isolated MSCs consistently emit certain soluble factors into culture medium during the period of *in vitro* expansion. Among the soluble factors, cytokine IL-6 is helpful to maintain the undifferentiated state of stem cells and VEGF plays a pivotal role for vascular neogenesis (Sriramulu et al., 2018). With these secretory factors, conditioned medium (CM) of hMSCs has a therapeutic potential and can be administered to various diseases. It is reported that CM treatment reduces cartilage defects and modulates immune balance in animal model of arthritis (Kay et al., 2017), and enhances endothelial cell growth and cell mobilization from BM resulting in salvation of ischemic hindlimb of mice (Bhang et al., 2014). Importantly, recent studies have demonstrated that the secretory molecules derived from MSCs are encapsulated in the vesicle termed as ‘exosome’ (Figure 3), which exerts therapeutic effects on various diseases including cancer (Katakowski et al., 2013) and myocardial infarction (Lai et al., 2010).

Table 1. Phase 2 & 3 clinical trials in Korea

	Study	Target disease	Lead sponsor	phase	NCT ID
1	Safety and Efficacy of Autologous Mesenchymal Stem Cells in Chronic Spinal Cord Injury	Spinal Cord Injury	Pharmicell Co., Ltd.	2 &3	NCT01676441
2	Mesenchymal Stem Cell in Patients With Acute Severe Respiratory Failure	Respiratory Distress Syndrome, Adult	Asan Medical Center	2	NCT02112500
3	The Effectiveness and Safety for Mesenchymal Stem Cell for Alcoholic Liver Cirrhosis	Alcoholic Liver Cirrhosis	Yonsei University	2	NCT01741090
4	Trial of Autologous Mesenchymal Stem Cells in Patients With Multiple System Atrophy	Multiple System Atrophy	Yonsei University	2	NCT00911365
5	The STem Cell Application Researches and Trials In NeuroloGy-2 (STARTING-2) Study	Stroke, Ischemic	Samsung Medical Center	3	NCT01716481
6	Treatment of Intractable Common Extensor Tendon Injury Using Mesenchymal Stem Cells (Allo-ASC)	Lateral Epicondylitis	Seoul National University Hospital	2	NCT03449082
7	RELIEF(A Randomized, Open labEled, muLticenter Trial for Safety and Efficacy of Intracoronary Adult Human Mesenchymal stEm Cells Acute Myocardial inFarction)	Acute Myocardial Infarction	Pharmicell Co., Ltd.	3	NCT01652209
8	Treatment of Tendon Injury Using Allogenic Adipose-derived Mesenchymal Stem Cells (Rotator Cuff Tear)	Rotator Cuff Tear	Seoul National University Hospital	2	NCT02298023
9	Safety and Efficacy of Intracoronary Adult Human Mesenchymal Stem Cells After Acute Myocardial Infarction	Acute Myocardial Infarction	Yonsei University	2 &3	NCT01392105
10	REVIVE (Randomized Exploratory Clinical Trial to Evaluate the Safety and Effectiveness of Stem Cell Product in Alcoholic Liver Cirrhosis Patient)	Alcoholic Liver Cirrhosis	Pharmicell Co., Ltd.	2	NCT01875081
11	Umbilical Cord Blood-derived Mesenchymal Stem Cells for the Treatment of Steroid-refractory Acute or Chronic Graft-versus-host-disease	GVHD	Samsung Medical Center	1 & 2	NCT01549665
12	Safety and Efficacy Study of Umbilical Cord Blood-Drived Mesenchymal Stem Cells to Promote Engraftment of Unrelated Hematopoietic Stem Cell Transplantation	Acute Leukemia	Medipost Co Ltd.	1 & 2	NCT00823316
13	Safety and Effect of Adipose Tissue Derived Mesenchymal Stem Cell Implantation in Patients With Spinal Cord Injury	Spinal Cord Injury	Biostar	1 & 2	NCT01769872
14	Follow-up Study for Participants Jointstem Clinical Trial	Knee Osteoarthritis	Biostar	2	NCT03509025
15	Autologous Adipose Tissue Derived Mesenchymal Stem Cells Transplantation in Patient With Degenerative Arthritis	Degenerative Arthritis	Biostar	1 & 2	NCT01300598
16	Autologous Adipose Tissue Derived Mesenchymal Stem Cells Transplantation in Patient With Buerger's Disease	Buerger's Disease	Biostar	1 & 2	NCT01302015
17	Efficacy and Safety of Pneumostem® for IVH in Premature Infants (Phase 2a)	Cell Transplantation	Samsung Medical Center	2	NCT02890953
18	A Clinical Trial to Evaluate the Safety and Efficacy of ALLO-ASC-DFU for Second Deep Degree Burn Injury Subjects	Burn Injury	Anterogen Co., Ltd.	2	NCT02619851

19	The Effect of Human Adipose Tissue-derived MSCs in Romberg's Disease	Romberg's Disease	Biostar	2	NCT01309061
20	Clinical Study to Evaluate Efficacy and Safety of ALLO-ASC-DFU in Patients With Diabetic Foot Ulcers	Diabetic Foot Ulcer	Anterogen Co., Ltd.	3	NCT03370874
21	Safety and Effect of Adipose Tissue Derived Mesenchymal Stem Cells Implantation in Patients With Critical Limb Ischemia	Critical Limb Ischemia	Biostar	1 & 2	NCT01663376
22	Safety and Exploratory Efficacy Study of NEUROSTEM® Versus Placebo in Patients With Alzheimer's Disease	Alzheimer's Disease	Medipost Co Ltd.	1 & 2	NCT02054208
23	Follow-up Safety and Efficacy Evaluation on Subjects Who Completed PNEUMOSTEM® Phase-II Clinical Trial	Bronchopulmonary Dysplasia	Medipost Co Ltd.	2	NCT01897987
24	Efficacy and Safety Evaluation of Pneumostem® Versus a Control Group for Treatment of BPD in Premature Infants	Bronchopulmonary Dysplasia	Medipost Co Ltd.	2	NCT01828957
25	Evaluation of the Safety and Potential Therapeutic Effects After Intravenous Transplantation of Cordstem-ST in Patients With Cerebral Infarction	Cerebral Infarction	CHABiotech CO., Ltd	1 & 2	NCT02378974
26	Follow-up Study of Safety and Efficacy in Subjects Who Completed NEUROSTEM® Phase-I/IIa Clinical Trial.	Alzheimer's Disease	Medipost Co Ltd.	1 & 2	NCT03172117
27	Clinical Study to Evaluate Efficacy and Safety of ALLO-ASC-DFU in Patients With Diabetic Foot Ulcers	Diabetic Foot Ulcer	Anterogen Co., Ltd.	2	NCT02619877
28	Clinical Trial to Evaluate Efficacy and Safety of JOINTSTEM in Patients With Degenerative Arthritis	Degenerative Arthritis	Biostar	2	NCT02658344
29	PNEUMOSTEM for the Prevention and Treatment of Severe BPD in Premature Infants	Bronchopulmonary Dysplasia	Medipost Co Ltd.	2	NCT03392467
30	Study to Evaluate the Safety of ALLO-ASC-DFU in the Subjects With Dystrophic Epidermolysis Bullosa	Dystrophic Epidermolysis Bullosa	Anterogen Co., Ltd.	1 & 2	NCT02579369
31	Evaluation of the Safety and Potential Therapeutic Effects After Intravenous Transplantation of CB-AC-02 in Patients With Alzheimer's Disease	Alzheimer's Disease	CHABiotech CO., Ltd	1 & 2	NCT02899091
32	Clinical Trials of Autologous Cultured Adipose-derived Stem Cells (ANTG-ASC) on Complex Fistula	Perianal Fistula	Anterogen Co., Ltd.	2	NCT01314092
33	Study to Compare Efficacy and Safety of Cartistem and Microfracture in Patients With Knee Articular Cartilage Injury	Osteoarthritis	Medipost Co Ltd.	3	NCT01041001
34	Follow-Up Study of CARTISTEM® Versus Microfracture for the Treatment of Knee Articular Cartilage Injury or Defect	Osteoarthritis	Medipost Co Ltd.	3	NCT01626677
35	Safety and Efficacy of FURESTEM-CD Inj. in Patients With Moderately Active Crohn's Disease(CD)	Crohn's Disease	Kang Stem Biotech Co., Ltd.	1 & 2	NCT02000362

This table is organized by transcribing the data from public clinical database (http://www.clinicaltrials.gov).

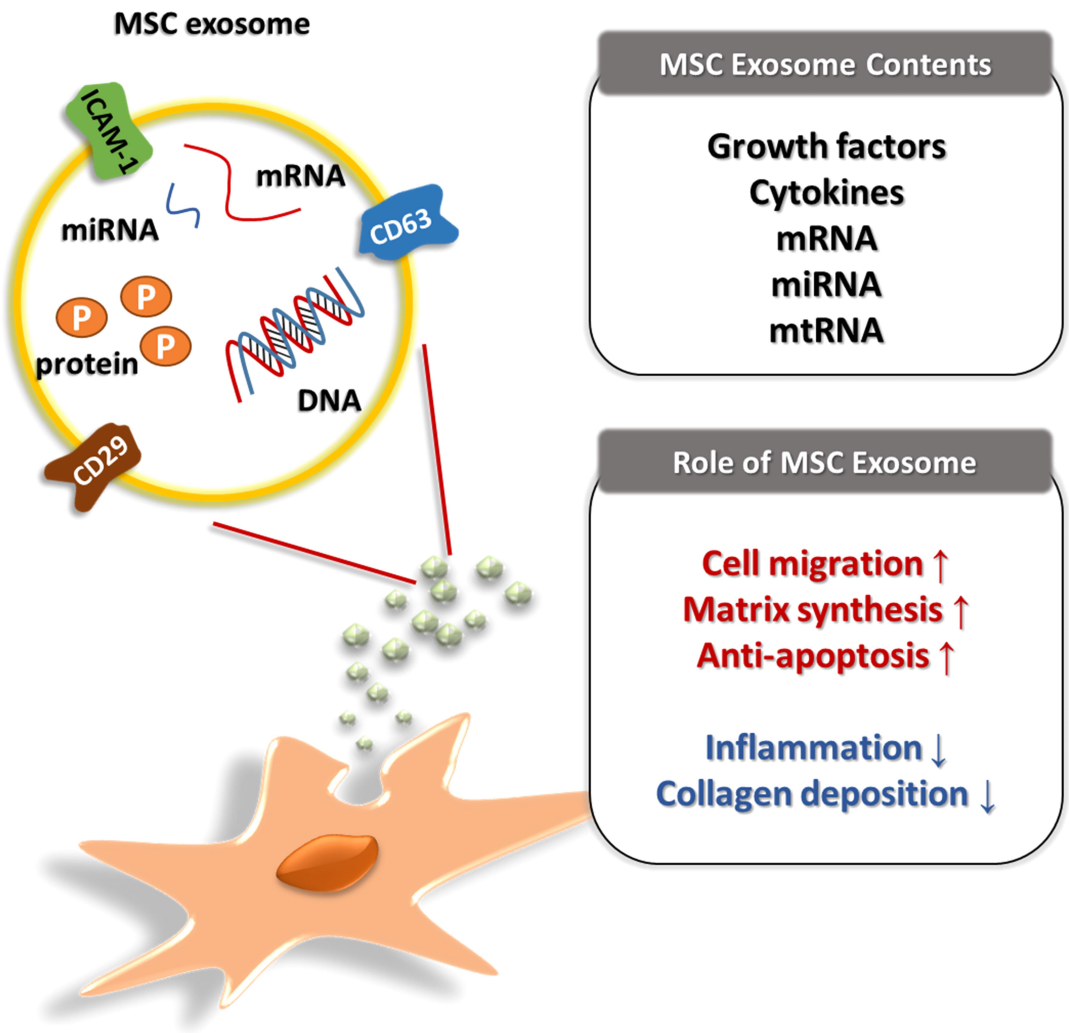

Figure 3. Structure and role of MSC-derived exosome.

MSC-derived exosomes are generated by an endocytic process and released into the extracellular space by using a cellular structure termed as a multivesicular body (MVB). Exosomes contains cytokines, growth factors and genetic materials such as DNA, mRNA and miRNA, wrapped by phospholipid bilayer outer membrane. MSC-Exosomes stimulate target cells, thus alleviates disease-related condition. This figure is modified from Zhou et al. (2018).

D. Current limitations of MSC-based therapy

Although the results of current preclinical studies and some clinical trials using MSCs were very successful and promising, the outcomes from certain cell applications did not show any significant change, or rather it worsens the disease severity. In fact, MSC-based therapies showed diverse and controversial outcomes. In case of cell application for vascular defects, the cells improved in revascularization and led to less amputation, whereas many other trials did not show any clinical benefits (Raval and Losordo, 2013). Even the same source and injection route of the cells targeting the same disease exerted different consequences (Table 2). This discrepancy can be caused by several factors.

Poor engraftment of transferred MSCs is a major reason for the failure of the therapeutic application. Stem cell homing is attributed to very low survival rate and integration into the host cells after transplantation (Li et al., 2016a). Some researchers argue that survival or presence of MSCs in injured site are not important for therapeutic effects (Sala et al., 2015), whereas the others claim that inaccurate delivery of the stem cells to the damaged sites caused a decrease in the therapeutic efficiency (Karp and Teo, 2009). In addition, the remedial effect of infused MSCs persists arbitrarily, so a biologic half-life of the cells can not be accurately defined (Haller et al., 2011).

To achieve a sufficient number of cells for actual transplantation, *ex vivo* expansion step is necessarily required. During culture expansion, senescence of MSCs is inevitable. As MSCs get aged, the osteogenic potentials gradually decreased in line with impaired bone formation ability in the aged (Atashi et al., 2015), while adipogenic differentiation and the expression of its related transcription factors such as PPARγ are enhanced (Xu et al., 2016). Senescent cells are known to display a

senescence-associated secretory phenotype (SASP) that contributes to progress of aging of neighboring cells, impaired regenerative function and immune cell recruitment after administration (Turinetto et al., 2016).

Donor-dependent variation of MSCs is one of the causes dampening the feasibility of the cells (Siegel et al., 2013). To employ MSCs as a reliable cell source for cell-based therapy, the strikingly variable functions of MSCs isolated from each individual donor must be understood. Comparing BM-MSCs from various donors, significant differences in cell growth rates and alkaline phosphatase enzyme activity are founded (Phinney et al., 1999). Differentiation capacity also varies between MSCs from different donors (Siddappa et al., 2007). Furthermore, angiogenic potential of MSCs is also influenced by individual differences mediated by donors (Kang et al., 2018).

Table 2. Controversial clinical outcomes of MSC applications

Disease	Phase	MSC source	Route	Result	Reference
SLE	1	Allo-BM	IV	Improved	(Liang et al., 2010)
SLE	1	Allo-BM	IV	No change	(Carrion et al., 2010)
Multiple sclerosis	1	Allo-BM	Intrathecal	Conflicting	(Mohyeddin Bonab et al., 2007)
Multiple sclerosis	1 & 2	Allo-BM	Intrathecal	Conflicting	(Karussis et al., 2010)
Hematopoietic stem cell transplantation	1	Allo-BM	Cotransplantation	Improved	(Lazarus et al., 2005)
Hematopoietic Stem cell transplantation	1	Allo-BM	Cotransplantation	Improved, but higher recurrence rate of hematologic malignancy	(Ning et al., 2008)

This table is organized by transcribing the data from Kim and Cho (2013).

E. Enhancement strategies for MSC-based therapy

To guarantee consistent and stable therapeutic effects for each recipient, the standardization of methods and enhancement strategies are needed (Fehrer and Lepperdinger, 2005). The tactics should be developed targeting current hurdles such as low *in vivo* survival, inaccurate delivery to inflamed lesion and donor-to-donor variations.

Optimal number of MSCs to be set for each disease respectively (Fossett and Khan, 2012). Furthermore, injection route was considered depending on the pathophysiology and injury site of diseases. In case of atopic dermatitis (AD), local injection to inflamed skin showed more improved results compared to systemic injection in experimental mice model (Kim et al., 2015). In addition, regeneration of the vascular system in different experimental models can be improved by cell applications through various injection routes (Ikegame et al., 2011; Li et al., 2016b). Establishment of optimal cell number and administration route might be connected to successful engraftment of MSCs. Of note, considerable improvements in engraftment are required to achieve a clinical benefit from MSC application (Nitzsche et al., 2017). Many researchers are still trying to enhance the therapeutic efficacy of MSCs by improving their migration into the lesion (Duijvestein et al., 2011; Fan et al., 2012). Most importantly, MSC-mediated immune modulation in different clinical settings and diverse immune environments must be understood and utilized (Prasanna et al., 2010).

To accomplish successful therapeutic outcomes, several advanced strategies for MSC application have been proposed. Preconditioning of MSCs before application by treating cytokines or modifying the culture method is one of promising therapeutic strategies, which augment immunosuppressive capacity or *in vivo* cell survival through paracrine effects (Saparov et al.,

2016). Next, genetic modification would be a therapeutic strategy (Garcia et al., 2014). The last one is a co-administration with bioactive materials including immunosuppressant or a cell scaffold to enhance *in vivo* cell survival and homing (Zippel et al., 2010).

F. Preconditioning of MSCs

Priming with growth factors or cytokines released under proinflammatory condition is archetypical preconditioning method to improve the therapeutic effect of MSCs (Polchert et al., 2008; Su et al., 2015). The crosstalk between MSCs and disease risk factors can be utilized to investigate therapeutic mechanism of MSCs and develop enhancement strategies (Ravanidis et al., 2017). Pretreatment with representative proinflammatory cytokines, TNF-α and IFN-γ improves the therapeutic efficacy of transferred MSCs by mediating resolution of inflammation and expressing vascular protective potential (Duijvestein et al., 2011; Kavanagh et al., 2015; Kwon et al., 2013; Su et al., 2015). It is reported that NF-κB signaling pathway plays a crucial role in TNF-α-mediated stimulation (Crisostomo et al., 2008). In addition, IL-1β primed MSCs more efficiently attenuates experimental colitis by adjusting *in vivo* immune balance and improving stem cell migration (Fan et al., 2012). Treatment with TGF-α significantly increases immunosuppressive capacity and VEGF production of MSCs, subsequently recovers myocardial injury (Herrmann et al., 2010). In line with these studies, priming with bacterial substance, muramyl dipeptide (MDP) promotes the immunomodulatory function of MSCs through stimulation of NOD2~COX-2 signaling and subsequently improved therapeutic effects against the experimental colitis (Kim et al., 2013)

Hypoxic preconditioning is frequently applied to strengthen the therapeutic effect of MSCs. As previous studies reported, administration of hypoxic cultured MSCs more remarkably improves disease symptoms compared to normoxic cells (Boyette et al., 2014; HoWangYin et al., 2014; Hu et al., 2014; Saraswati et al., 2015). MSCs increases their therapeutic potentials by promoting expression of chemokine receptors and subsequent *in vivo* engraftment when exposed to hypoxic condition (Annabi et al., 2003;

Hung et al., 2007b). Furthermore, hypoxic culture facilitates an increase in stemness of MSCs (Saller et al., 2012). Hypoxia inducible factor-1α (HIF-1 α) plays a pivotal role in upregulation of therapeutic function of MSCs or its conditioned medium (Gonzalez King et al., 2017; Kanichai et al., 2008). However, donor-dependent variation such as gene expression pattern must be considered even if MSCs are cultured in hypoxic condition (Kang et al., 2018).

In addition to pretreatment of cytokines and hypoxia, modification of cell culture method could improve the stemness and therapeutic potential of MSCs. It is well known that contact status during cell culture causes spontaneous cell death. In case of MSCs, cell-to-cell contact status influences its differentiation potential (Wang et al., 2006) and immunomodulation (Lee et al., 2016). Furthermore, 3-dimensional culture system mimicked original physiological property of stem cells improved therapeutic function as well as yield (McKee and Chaudhry, 2017). Of note, the simplest method for 3D culture is a spheroid culture. Spheroid culture of MSCs is known to enhance their anti-inflammatory property (Bartosh et al., 2010), pro-angiogenic function (Bhang et al., 2014) and therapeutic outcomes (Frith et al., 2009). Importantly, this method has the advantage that can be applied combined with other enhancement strategies. For example, by the combinatorial treatment of IFN-γ and TNF-α, the immunosuppressive effect of MSC spheroids on the functional macrophages is markedly augmented (Zimmermann and Mcdevitt, 2014). In addition, 3D spheroid culture on biocompatible substances elicits improved differentiation efficiency of MSCs (Wang et al., 2009a).

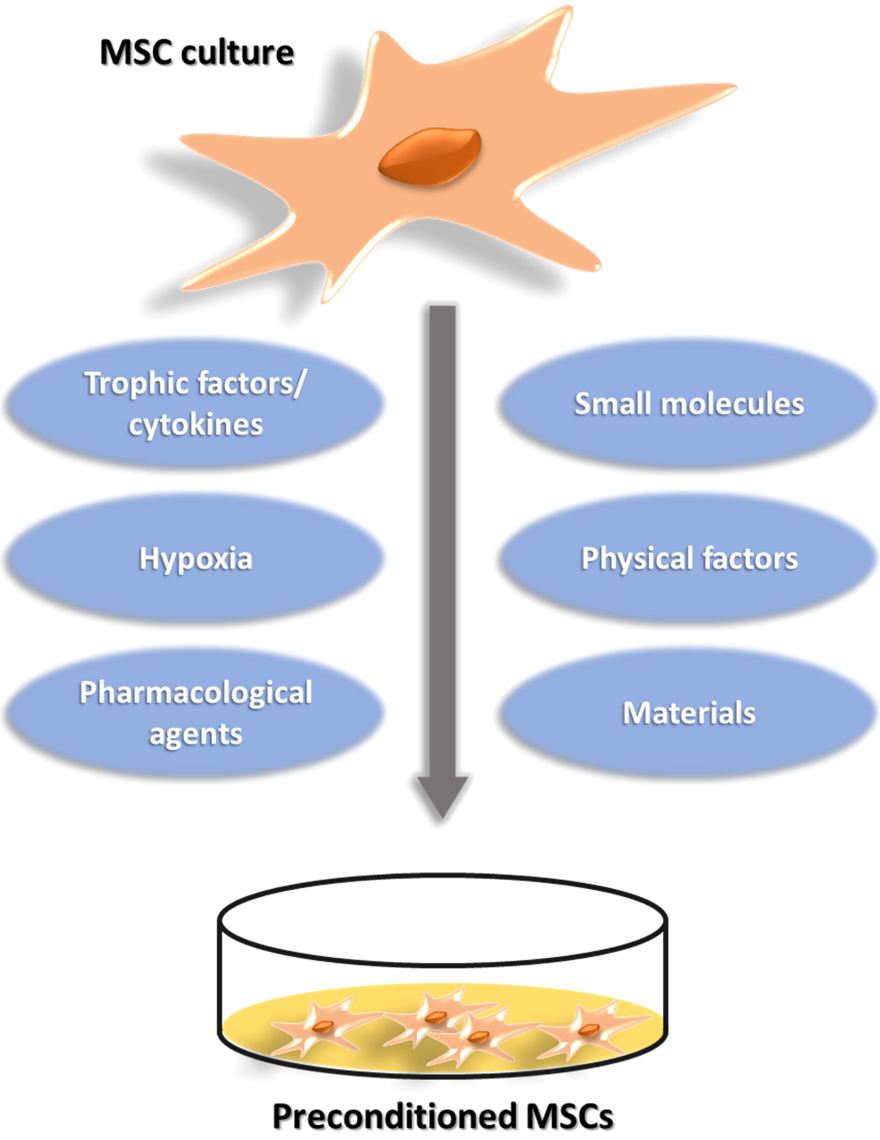

Figure 4. Preconditioning methods to improve the therapeutic effects of MSCs.

MSCs are administrated into a harsh microenvironment created by disease inducing factors such as proinflammatory factors or ROS. Preconditioning methods described in the diagram are key strategies to overcome obstacles such as senescence or apoptosis after the transplantation. This figure is modified from Zhao et al. (2018).

G. Genetic manipulation of MSCs

Genetic modification of hMSCs can be employed to improve the therapeutic potency of MSCs independently with exogenous stimuli. A number of genes related to therapeutic function of MSCs can be a target for sustained and enhanced expression. It is reported that overexpression of VEGF in MSCs promotes angiogenesis and ameliorates brain infarction (Garcia et al., 2014; Lai et al., 2012). With Bcl-2, VEGF overexpression improves cell survival and paracrine effect of the cells (Ni et al., 2017). To ensure the effect of hypoxic preconditioning, HIF-1α can be transduced to MSCs and emulate the therapeutic effects without any exposure process (Hnatiuk et al., 2016). In addition to these, therapeutic genes including IL-4, IL-10, TGF-β1, GATA-4 and CXCR4 are utilized to increase cell survival and therapeutic effects (Choi et al., 2008; Kim et al., 2014; Payne et al., 2012; Yang et al., 2015; Yu et al., 2013). However, although stable and intensive potency can be guaranteed, genetic manipulation of MSCs is unfit to be applied to an actual application in the clinical field. Critical safety issues may be raised for the clinical use of genetically modified MSCs. Consistent activation of specific gene would be a major cause for the development of stem cell-derived malignant tumor. Therefore, efforts to transiently improve therapeutic potential are still needed.

H. Co-administration with supportive materials

Although MSCs had been considered as an auxiliary measure for the transplantation of hematopoietic stem cells (HSCs) to exert a role for niche, the focus of recent studies moves to development of co-administrative substances to increase the therapeutic function of MSCs. Co-administration with immunosuppressants or advanced materials is strongly recommendable because it does not require additional preparatory steps, such as cell priming or genetic manipulation, thus it is convenient to apply for clinical use. Moreover, potent risks with such as tumor formation and contamination of a heterogeneous population can be reduced. It is reported that the co-application of MSCs with immunosuppressants including rapamycin and tacrolimus showed improved therapeutic outcomes through the synergism of each remedy by extending the survival time of transplanted MSCs and reducing the adverse effects of medicines (Ge et al., 2009; Peng et al., 2013). Importantly, application of bioactive reagents which facilitates homeostasis of *in vivo* immune balance stabilizes the mode of action of MSCs. For example, innate immune stimulator, MIS416 improves the immunomodulation of MSCs, recovers immune homeostasis in the gut, and thus, boosts the therapeutic function of MSCs against experimental colitis (Lee et al., 2018). In addition, preclinical studies using biocompatible advanced materials such as gold nanoparticle and graphene derivatives have been actively conducted (Kang et al., 2015a; Park et al., 2015).

Bio-engineering with scaffold takes a big part of improvement methods for MSC-based therapy. Bioactive reagents such as ECM and hydrogel are used to build a structure of tissue or organ using 2D patches or 3D printed architecture. The method encourages cell-to-cell communication as shown in the spheroid culture (Zippel et al., 2010). In addition, the use of scaffold could increase biophysical properties of MSCs such as homing

(Shao et al., 2012) and lineage determination (Caliari and Harley, 2014) (Figure 5).

GENERAL PURPOSE

Although therapeutic functions of hMSCs have been demonstrated through preclinical researches, several consequences from clinical trials could not satisfy the patients. These discrepancies are mediated from the limitations such as a functional quiescence after the application and donor-dependent variation. Hence, various enhancement strategies have been suggested to maintain the stemness of hMSCs and augment the therapeutic efficacy. In the present study, I investigated enhancement methods by using an immunomodulatory function of hMSCs for the successful therapeutic application. To accomplish the advancement of adult stem cell-based therapy, different points in the preparatory process were aimed for the integrated management. Furthermore, I examined whether the enhancement methods could prevent involuntary changes during *ex vivo* culture period and achieve improved clinical outcomes without any artificial manipulations to hMSCs.

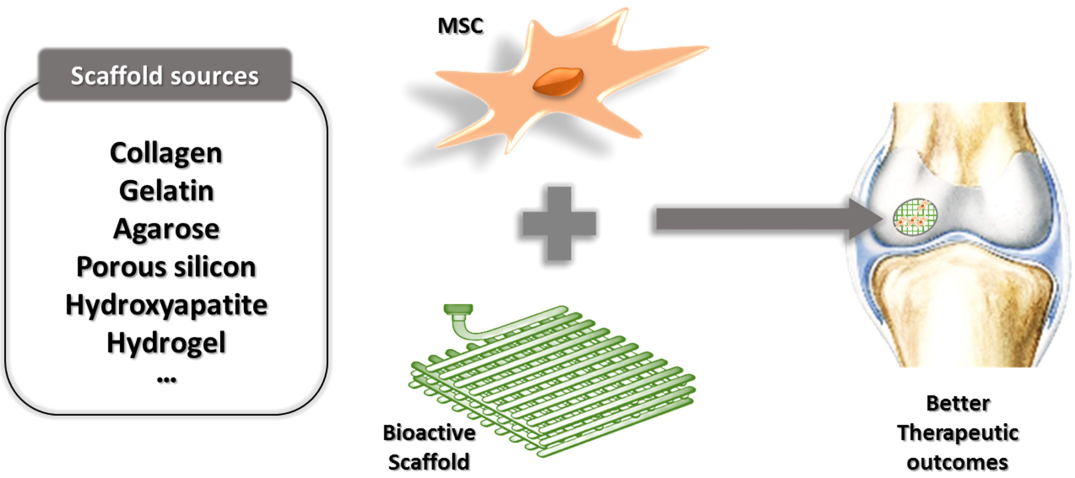

Figure 5. Sources for scaffold and co-administration with MSCs.

Biomaterials have been applied as a component for the scaffold to improve the therapeutic efficacy of MSCs targeting destructive diseases such as an osteoarthritis. The strategy takes advantages that the scaffold supports structural defects and *in vivo* survival of MSCs.

CHAPTER I

PGE_2 maintains self-renewal of human adult stem cells via EP2-mediated autocrine signaling and its production is regulated by cell-to-cell contact

1.1 INTRODUCTION

Mesenchymal stem cells (MSCs) are potential candidates for the treatment of immune disorders such as graft-versus-host disease, rheumatoid arthritis, inflammatory bowel disease and multiple sclerosis (Uccelli et al., 2008). Recently, many researchers have elucidated the safety and distinct functions related to the therapeutic application of MSCs, including paracrine factor-mediated immunomodulatory ability and stemness, which is defined as exhibiting stem cell properties represented by the ability to generate daughter cells identical to themselves (self-renewal) and to differentiate into multiple cell lineages (multipotency) (Bianco et al., 2013). Although a number of researchers have established methods for expanding MSCs in the laboratory and uncovered most of the mechanisms underlying MSC stemness, further studies are required to develop the most efficient procedure to harvest sufficient numbers of stem cells and to fully elucidate any unknown mechanisms for therapeutic application (Bernstein and Delaney, 2012). Moreover, the development of novel approaches to improve the therapeutic efficacy of MSCs is a major topic in the MSC research field. To improve therapeutic efficacy, several groups have manipulated the cells by pre-treating MSCs with growth factors and cytokines or by genetic modification (Cho et al., 2012; Hahn et al., 2008). However, these approaches are controversial because the precise mechanisms based on selected candidate factors such as NO, IDO, IL-10, and PGE_2 from MSCs in specific diseases are not yet fully described. To address these issues, more detailed studies are required to explore the production and functions of candidate factors individually and link their function with the cellular properties.

Prostaglandin E_2 (PGE_2) is a subtype of the prostaglandin family, which includes lipid mediators with physiological effects such as uterine

contraction, cervix softening, fever induction, muscle relaxation and vasodilation. PGE_2 is synthesized from arachidonic acid (AA) released from membrane phospholipids through sequential enzymatic reactions. Cyclooxygenase-2 (COX-2), known as prostaglandin- endoperoxidase synthase, converts AA to prostaglandin H_2 (PGH_2), and PGE_2 synthase isomerizes PGH_2 to PGE_2 (Scholich and Geisslinger, 2006). As a rate-limiting enzyme, COX-2 controls PGE_2 synthesis in response to physiological conditions, including stimulation by growth factors, inflammatory cytokines and tumour promoters (Eibl et al., 2003; Kalinski, 2012). PGE_2 is secreted to the extracellular environment by multidrug-resistant protein 4 (MRP4)-mediated active transport and binds to specific E-Prostanoid (EP) receptors on target cells (Park et al., 2006). EP receptor is a G-protein coupled receptor (GPCR), and these receptors can be classified into 4 subclasses. EP2 receptor enhances cell proliferation and neovascularisation by increasing vascular endothelial growth factor (VEGF) secretion in several cancers (Castellone et al., 2005; Eibl et al., 2003; Seno et al., 2002). In contrast, EP3 receptor-mediated signalling regulates cell proliferation by decreasing cAMP levels, consequently suppressing tumour development. In tumour-progressing cells, EP2 receptor is highly expressed, while the EP3 receptor expression level is relatively low (Shoji et al., 2004; Sung et al., 2005). This COX-2/PGE_2 axis forms an autocrine/paracrine loop, affecting the cell cycle and apoptosis to regulate cell proliferation and viability via the activation of one or more EP receptors (Dohadwala et al., 2002). Using several *in vitro* and *in vivo* models of immune disorders, including Crohn's disease and atopic dermatitis, it have been shown that COX-2 signalling and PGE_2 production in MSCs are crucial factors in the immunomodulatory ability of hMSCs (Kim et al., 2013; Kim et al., 2010; Kim et al., 2015; Lee et al., 2015; Yu et al., 2014). Therefore, studies investigating the detailed regulatory mechanisms that focus on PGE_2

production and function in MSCs are required to further develop therapeutic approaches.

Most eukaryotic cells assemble and construct 3D structures in organs, communicating with each other in response to intra- and extracellular stimuli. Gap junctions form intercellular connections via membrane-incorporated hexamers composed of connexin proteins in cell-to-cell contact. They control cell death and electrophysiology by delivering electrical currents, ions and small molecules. Connexin 43 (CX43) protein expression and gap junction intercellular communication (GJIC) were augmented by PGE_2 produced by mechanical stress via EP2 receptor signalling in an autocrine manner (Cherian et al., 2003). However, the GJIC-mediated regulation of the COX-2/PGE_2 axis is not yet reported.

In the present study, I assessed the role of PGE_2 produced by human adult stem cells in the regulation of self-renewal and immunomodulation in an autocrine/paracrine manner using MSCs from two different sources, umbilical cord blood and adipose tissue. Furthermore, this study was designed to reveal the regulatory mechanism of PGE_2 production in adult stem cells by gap junction intercellular communication (GJIC) when intimate cell-to-cell contact is allowed. Given that the basal level of PGE_2 synthesis in human bone marrow-derived MSCs (hBM-MSCs) is significantly lower than in human umbilical cord blood-derived MSCs (hUCB-MSCs) or human adipose tissue-derived MSCs (hAD-MSCs), as proven in the previous study, I used hUCB-MSCs and hAD-MSCs in the present study to generalize PGE_2-mediated regulation of adult stem cell functions. Moreover, hBM-MSCs are larger than hUCB-MSCs or hAD-MSCs, making it difficult to include hBM-MSCs in the determination of cell proliferation and secretion under the same experimental environment. Therefore, I generalized the PGE_2-mediated novel properties of human adult stem cells using hUCB-MSCs and hAD-MSCs.

1.2 MATERIALS AND METHODS

1.2.1 Isolation and culture of hUCB-MSCs

All experiments involving human umbilical cord blood (UCB) or UCB-derived cells were carried out in accordance with the approved guidelines of the Boramae Hospital Institutional Review Board (IRB) and the Seoul National University IRB (IRB No. 0603/001-002-10C4). The UCB samples were provided immediately after birth with informed consent and parent approval. The UCB from a donor was mixed with HetaSep solution (Stem Cell Technologies, Vancouver, Canada) at a ratio of 5:1 and incubated at room temperature for approximately one hour to remove red blood cells. Then, supernatant was collected using Ficoll, and mononuclear cells were separated after centrifugation at 2,500 rpm for 20 min. The cells were washed twice in phosphate-buffered saline (PBS). Isolated cells were seeded in growth media consisting of D-media (Formula No. 78-5470EF, Gibco BRL, NY, USA) containing EGM-2 SingleQuot and 10% foetal bovine serum (Gibco BRL, NY, USA). After 3 days, unattached cells were washed out, and adherent cell colonies were cultured to consistently establish sharp and spindle-shaped hUCB-MSCs.

1.2.2 Isolation and culture of hUCB-MNCs

The UCB samples were mixed with HetaSep solution (Stem Cell Technologies, Vancouver, Canada) at a ratio of 5:1 and incubated at room temperature for approximately one hour to remove red blood cells. Then, supernatant was collected with Ficoll, and mononuclear cells were separated after centrifugation at 2,500 rpm for 20 min. The cells were washed twice in PBS. Isolated cells were seeded in growth media consisting of RPMI 1640 (Gibco BRL, Grand Island, NY, USA) containing 10% foetal bovine serum.

1.2.3 Isolation and culture of hAD-MSCs

All procedures using human adipose tissue or adipose tissue-derived mesenchymal stem cells were conducted in accordance with guidelines approved by Seoul National University IRB (IRB No. 0611/001-001). Freshly excised human mammary fat tissue, the waste from reduction mammoplasty, was digested for 2 hours with 1 mg/mL of type IA collagenase (≥125 CDU/mg solid, Sigma, St. Louis, MO, USA) at 37°C. After washing in PBS and centrifugation at 1,000 rpm for 5 min, the tissue pellet was filtered through 100 μm nylon mesh and incubated in DMEM (Gibco BRL, NY, USA) containing 10% foetal bovine serum at 37°C with 5% CO_2. After 24 hours of incubation, unattached cells were washed out, and adherent cell colonies were cultured consistently in K-NAC media supplemented with 2 mM N-acetyl-L-cysteine (NAC; Sigma, St. Louis, MO, USA) and 0.2 mM L-ascorbic acid.

1.2.4 Reagents

Cay10526 and prostanoid receptor antagonists for EP1 (SC-51089) and EP2 (AH-6809) were purchased from Cayman Chemical Company (Ann Arbor, MI, USA). Celecoxib, butaprost, sulprostone, carbenoxolone, concanavalin A (ConA) from Canavalia ensiformis (Jack Bean) and the EP3 antagonist L-798106 were purchased from Sigma-Aldrich (St. Louis, MO, USA). The EP4 selective antagonist L-161,982 was purchased from Tocris Bioscience (Moorend Farm Ave., Bristol, UK). Recombinant human IFN-γ and TNF-α were obtained from Peprotech (Rocky Hill, NJ, USA).

1.2.5 Western blot analysis

The cells were washed twice in PBS and lysed in buffer containing 1% Nonidet-P40 supplemented with a complete protease inhibitor ‘cocktail’ (Roche, Indianapolis, IN, USA) and 2 mM dithiothreitol. The protein

samples were separated by 10% SDS-PAGE and transferred to nitrocellulose membranes. After blocking with 3% bovine serum albumin (BSA) solution, proteins on the membrane were incubated with primary antibodies against COX-2, mPGES-1 (Abcam, Cambridge, MA, USA), EP1, EP2, EP3, EP4 (Cayman, Ann Arbor, MI, USA), iNOS and IDO-1 (Millipore, Billerica, MI, USA) more than 12 hours at 4°C and then incubated with secondary antibodies. Detailed information for all antibodies is provided in Table 3. Protein and antibody complexes were detected using the ECL Western blotting detection reagent and analysis system.

1.2.6 BrdU assay

For this assay, the cell proliferation ELISA kit (Roche, Indianapolis, IN, USA) was used. After the indicated treatment, cells were washed twice in PBS and incubated in growth media containing 100 μM bromodeoxyuridine (BrdU) labelling reagent for 2 hours at 37°C in a humidified atmosphere with 5% CO_2. After removing media and drying the cell surface, cells were fixed with the provided FixDenat solution for 30 minutes and incubated in peroxidase-conjugated anti-BrdU antibody (anti-BrdU-POD) solution for 90 minutes at room temperature. Cells were then washed three times in diluted washing solution and incubated with the provided substrate (tetramethyl-benzidine; TMB) solution for 5 to 30 minutes. After sufficient reaction and stop solution addition, the reaction products, which demonstrated cell proliferation levels, were quantified by measuring absorbance at the wavelength 450 nm and 690 nm (as a reference) using spectrophotometer.

1.2.7 Cumulative population doubling level (CPDL) analysis

Cell proliferation was also measured by CPDL analysis. Estimated growth rates and proliferation levels were determined through the formula

Table 3. Antibody information

	Primary antibody	Dilution	Source	Cat. #
Western blotting	Rabbit anti-COX-2	1:1000	Abcam, Cambridge, MA, USA	ab15191
	Rabbit anti-mPGES-1	1:1000	Abcam, Cambridge, MA, USA	ab62050
	Mouse anti-iNOS	1:100	Santa Cruz Biotechnology, Santa Cruz, CA, USA	sc-7271
	Mouse anti-IDO-1	1:500	Merck-Millipore, Darmstadt, Germany	MAB5412
	Rabbit anti-EP1	1:1000	Cayman, Ann Arbor, MI, USA	101740
	Rabbit anti-EP2	1:1000	Cayman, Ann Arbor, MI, USA	101750
	Rabbit anti-EP3	1:1000	Cayman, Ann Arbor, MI, USA	101760
	Rabbit anti-EP4	1:1000	Cayman, Ann Arbor, MI, USA	101770
FACS	PE Mouse Anti-Human CD31	1:50	BD Bioscience, San Jose, CA, USA	340297
	FITC Mouse Anti-Human CD34	1:50	BD Bioscience, San Jose, CA, USA	555821
	PE Mouse Anti-Human CD44	1:50	BD Bioscience, San Jose, CA, USA	550989
	FITC Mouse Anti-Human CD45	1:50	BD Bioscience, San Jose, CA, USA	555482
	PE Mouse anti-Human CD73	1:50	BD Bioscience, San Jose, CA, USA	550257
	FITC Mouse anti-Human CD105 (Endoglin)	1:50	BD Bioscience, San Jose, CA, USA	561443
IHC	Rabbit anti-COX-2	1:100	Abcam, Cambridge, MA, USA	ab15191
	Rabbit mPGES-1	1:1000	Abcam, Cambridge, MA, USA	ab62050

CPDL = ln (Nf/Ni) ln2, where Ni is the initial number of cells seeded, Nf is the final number of harvested cells, and ln is the natural log. First, 3 x 10^5 cells isolated from different donors were seeded with or without indicated treatments, and the number of cells was counted after 3 to 5 days. Then, 3 x 10^5 cells were seeded again with the same treatment. To determine the CPDL, population doublings for each passage were calculated and added.

1.2.8 Cell cycle assay

After indicated treatments, cells were harvested, washed twice in PBS, and fixed with ice-cold 70% ethanol at -20°C for more than 30 min. Fixed cells were washed in PBS and incubated with 400 µl of PBS containing RNase A (7.5 µg/ml) and propidium iodide (50 µg/ml) at 37°C for 30 min. Cell cycles were analysed by flow cytometry, which was performed on a FACScalibur using the Cell Quest software (BD Bioscience, San Jose, CA, USA).

1.2.9 Apoptosis assay

For the apoptosis assay, commercially available Apoptosis Detection Kits (BD Bioscience, San Jose, CA, USA) were used. After indicated treatments, the cells were washed twice in PBS and resuspended in 100 µl of 1X binding buffer at a concentration of 1 x 10^5. Then, 5 µl of FITC annexin V and 5 µl propidium iodide (PI) were added. The mixtures were gently vortexed and incubated for 15 min at room temperature in the dark. Then, 400 µl of 1X binding buffer was added to the mixtures, and all samples were analysed by flow cytometry, which was performed on a FACScalibur using Cell Quest software (BD Bioscience, San Jose, CA, USA).

1.2.10 Immunocytochemistry

Cells at different confluencies were washed in PBS and fixed with 4% paraformaldehyde (PFA) at room temperature for 10 min. For permeabilization, the cells were incubated with 0.05% Triton X-100 solution at room temperature for 10 min and blocked with 5% normal goat serum (NGS) at room temperature for 1 hour. Then, the cells were stained with specific primary antibodies against COX-2 and mPGES-1 (Abcam, Cambridge, MA, USA) followed by 2 hours of incubation with Alexa 488-labelled secondary antibody (1:1,000; Molecular Probes, Eugene, OR, USA). Detailed information for all antibodies is provided in Table 3. The nuclei were stained with DAPI. The images were captured by a confocal microscope.

1.2.11 Cytokine detection

To determine the secretion level of various cytokines, culture supernatants were collected from cells incubated for 24 hours in non-contact or contact conditions. To determinate each concentration, commercial ELISA kits for PGE_2, TGF-β1, IL-6, IL-8 (R&D Systems, Minneapolis, MN, USA) and NO (Cayman Chemical, Ann Arbor, MI, USA) were used according to the manufacturer's protocols.

1.2.12 Mixed leukocyte reaction

To collect culture supernatants (hUCB-MSC conditioned media; UCM), cells were incubated in non-contact or contact conditions for 24 hours and treated for 3 days with celecoxib in RPMI 1640 (Gibco BRL, Grand Island, NY, USA). Then, media were harvested after centrifugation. hMNCs prepared as described above were treated with ConA in collected culture supernatants for 5 days, and hMNC proliferation was determined by cell proliferation ELISA, BrdU kit (Roche, Indianapolis, IN, USA).

1.2.13 Flow cytometric analysis

hUCB-MSCs ($1x10^6$ cells) were stained with FITC- or PE-conjugated antibodies specific for human CD31, CD34, CD44, CD45, CD72 and CD105. Non-specific isotype-matched antibodies used for negative controls. All the antibodies were purchased from BD Bioscience (San Jose, CA, USA), the analysis was performed on a FACS calibur using Cell Quest software (BD Bioscience, San Jose, CA, USA). Detailed information for all antibodies is provided in Table 3.

1.2.14 RNA extraction and RT-PCR

Total RNA was extracted from hUCB-MSCs using 1 ml of Trizol reagent (Invitrogen, Carlsbad, CA, USA) according to the manufacturer's protocol. cDNA was prepared from 1 μg of total RNA by using the Superscript III First-Strand Synthesis System (Invitrogen, Carlsbad, CA, USA). For RT-PCR, the cDNA and primers were combined with a PCR premix (Bioneer, Seongnam, Korea) and the PCR products were separated on a 1.5% agarose gel, visualized, and photographed using a gel documentation system.

1.2.15 Differentiation assay

For adipogenic and osteogenic differentiation, hUCB-MSCs were plated in six-well plate at 70-80% confluence and after stabilization more than 12 hours, cultured with adipogenic differentiation medium (DMEM supplemented with 10% FBS, 1 μM dexamethasone, 10 μM insulin, 200 μM indomethacin and 0.5 mM isobutylmethylxanthine; IBMX) or an osteogenic differentiation medium (DMEM supplemented 10% FBS, 50 μM ascorbic acid, 0.1 μM dexamethasone, 10 mM β-glycerophsphate). DMEM supplemented with 10% FBS was used as a control and media were replaced twice a week. After 2 weeks of induction, adipogenesis of the cells

were determined by staining intracellular lipid accumulation with Oil Red O, osteogenesis were visualized with Alizarin Red staining which is specific for calcium.

For chondrogenic differentiation, $5x10^5$ cells were seeded in 15 ml polypropylene tube and centrifuged to form cell pellets. The pellets were incubated with 1 ml of chondrogenic differentiation medium (Lonza, Allendale, NJ, USA) and the medium replaced twice a week. After 3 weeks, the pellets were fixed, processed, embedded, and sliced into 3 μm sections. The sections were stained with toluidine blue following general procedures.

1.2.16 Statistical analysis

Mean values of all results were expressed as the mean ± SEM. Statistical analyses were conducted using Student's 2-tailed t-test or one-way ANOVA followed by Bonferroni post-hoc test for multigroup comparisons using GraphPad Prism version 5.0 (GraphPad Software, San Diego, CA, USA). Statistical significance is indicated in the figure legends.

1.3 RESULTS

1.3.1 Proliferation of human adult stem cells is decreased by the inhibition of COX-2 or mPGES-1 via G_1 cell cycle arrest

Indomethacin, the inhibitor for both COX-1 and COX-2, interferes with epithelial and tumour cell growth (Noguchi et al., 1991; Zhu et al., 2000). In addition, similar effects were observed when COX-2 was selectively inhibited in other cell types (Leahy et al., 2002; Waskewich et al., 2002). I first investigated whether selective inhibition of COX-2 using celecoxib or inhibition of membrane associated PGE synthase 1 (mPGES-1), a PGE_2 synthesizing enzyme downstream of COX-2 signalling, using cay10526 affected the proliferative phenotype of hUCB-MSCs and hAD-MSCs. Treatment down-regulated the expression of COX-2 or mPGES-1 at the protein level in a dose-dependent manner (Figure 6A) Consistent with the decrease in the protein level, inhibition of PGE_2 producing enzymes resulted in the remarkable dose-dependent decrease in the proliferation of both hUCB-MSCs and hAD-MSCs (Figure 6B). The cumulative proliferative phenotype in MSCs in response to chemical inhibitors was further confirmed by evaluating the cumulative population doubling level (Figure 6C). In addition, I showed that this suppression of self-renewal influenced cell confluency and cellular morphology. Compared with non-treated cells, celecoxib or cay10526-treated cells exhibited flattened or spread out cell bodies with low confluency (Figure 7, marked as ▼). To determine whether these changes in proliferation resulted from the lack of PGE_2, the PGE_2 secretion level was measured by enzyme-linked immunosorbent assay (ELISA). Conditioned media (CM) from COX-2-suppressed hUCB-MSCs contained less than 20% of the PGE_2 concentration of the naïve MSC group (Figure 8A). Inhibition of PGE_2 production led to lower proliferation via G_1 cell cycle arrest. The proportion

of cells in G_1 phase gradually increased dose-dependently, whereas the proportion of cells in S phase decreased (Figure 8B). The apoptotic rate of hUCB-MSCs was not affected by the suppression of PGE_2 synthesis (Figure 8C). I next investigated whether the suppression of COX-2/PGE_2 axis influence the other properties of MSCs. The expression pattern of surface antigens on hUCB-MSCs was not altered after the treatment of celecoxib or cay10526 (Figure 9). Moreover, the expression levels of pluripotency marker genes in hUCB-MSCs were not significantly changed by the inhibition of the COX-2 (Figure 10A). In addition, I found that up-regulation of COX-2/PGE_2 signalling enhanced osteogenesis of hUCB-MSCs, in contrast, suppressed adipogenesis using PCR and specific staining after the induction of differentiation. There was no significant change in chondrogenic differentiation (Figure 10B and C). Taken together, these findings indicate that the COX-2/PGE_2 axis has a critical role in the maintenance of hMSC self-renewal and that down-regulation of this axis leads to cell cycle arrest in G_1 phase without affecting cell apoptosis.

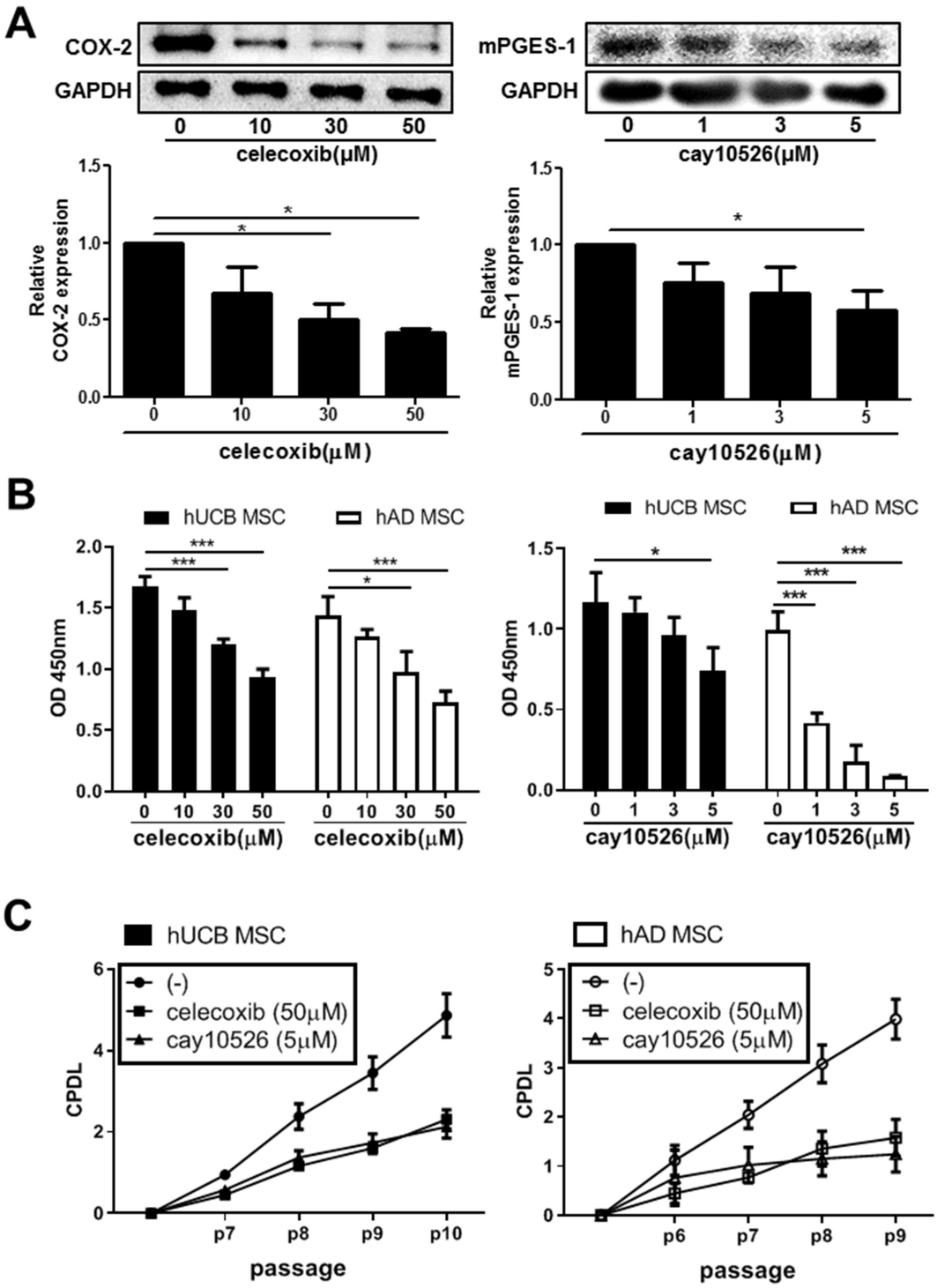
A
COX-2
GAPDH
0 10 30 50
celecoxib(μM)
Relative COX-2 expression
mPGES-1
GAPDH
0 1 3 5
cay10526(μM)
Relative mPGES-1 expression
B
hUCB MSC
hAD MSC
OD 450nm
C
hUCB MSC
hAD MSC
(-)
celecoxib (50μM)
cay10526 (5μM)
CPDL
passage
p6 p7 p8 p9 p10

Figure 6. Inhibition of COX-2/mPGES-1 reduces the cellular growth of hUCB-MSCs and hAD-MSCs.

hUCB-MSCs and hAD-MSCs were treated with celecoxib (selective inhibitor for COX-2) or cay10526 (selective inhibitor for mPGES-1) at indicated concentrations. (A) COX-2 and mPGES-1 protein levels in hUCB-MSCs were examined by Western blot analysis. Cell proliferation was determined by (B) bromodeoxyuridine (BrdU) assay and (C) CPDL. Gel electrophoresis was conducted under the same experimental conditions, and images of blots were cropped. Results show a representative experiment. * $P<0.05$, *** $P<0.001$. Results are shown as the mean ± SEM.

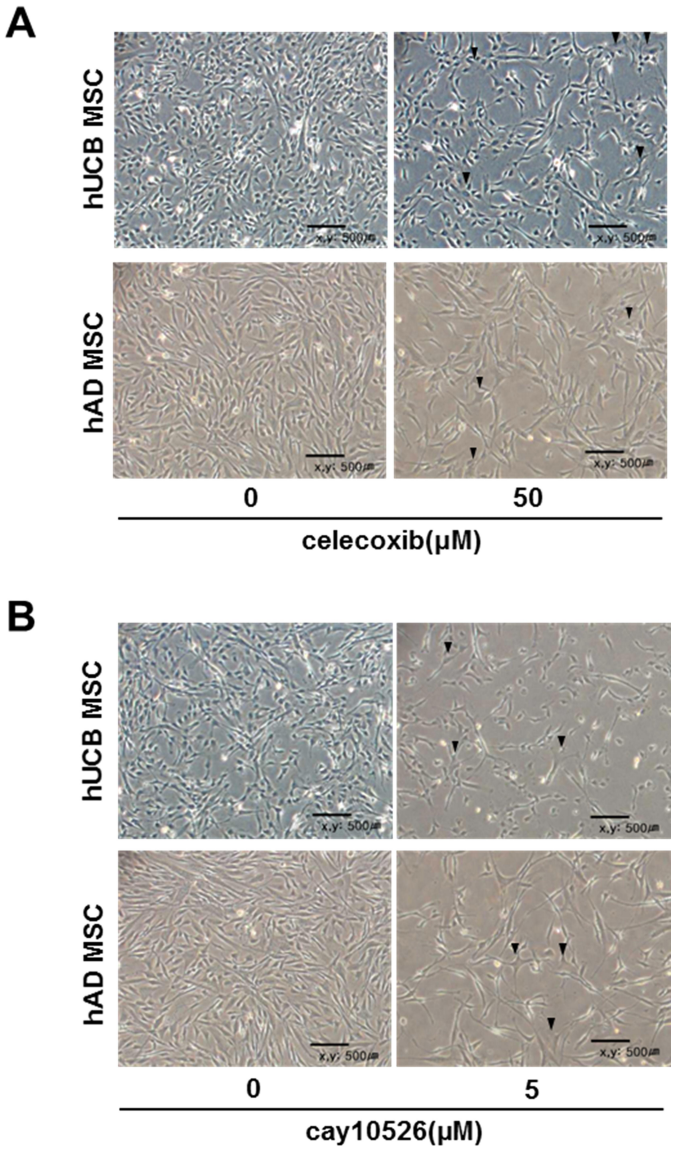

Figure 7. Microscopic images of COX-2 or mPGES-1 inhibited hUCB-MSCs and hAD-MSCs.

hUCB-MSCs and hAD-MSCs were treated with (A) celecoxib (selective inhibitor for COX-2) or (B) cay10526 (selective inhibitor for mPGES-1) at indicated concentrations. Phase-contrast images, bar = 500 μm. Upper panel: hUCB-MSCs. lower panel: hAD-MSCs. ▼; flattened or spread out cell bodies.

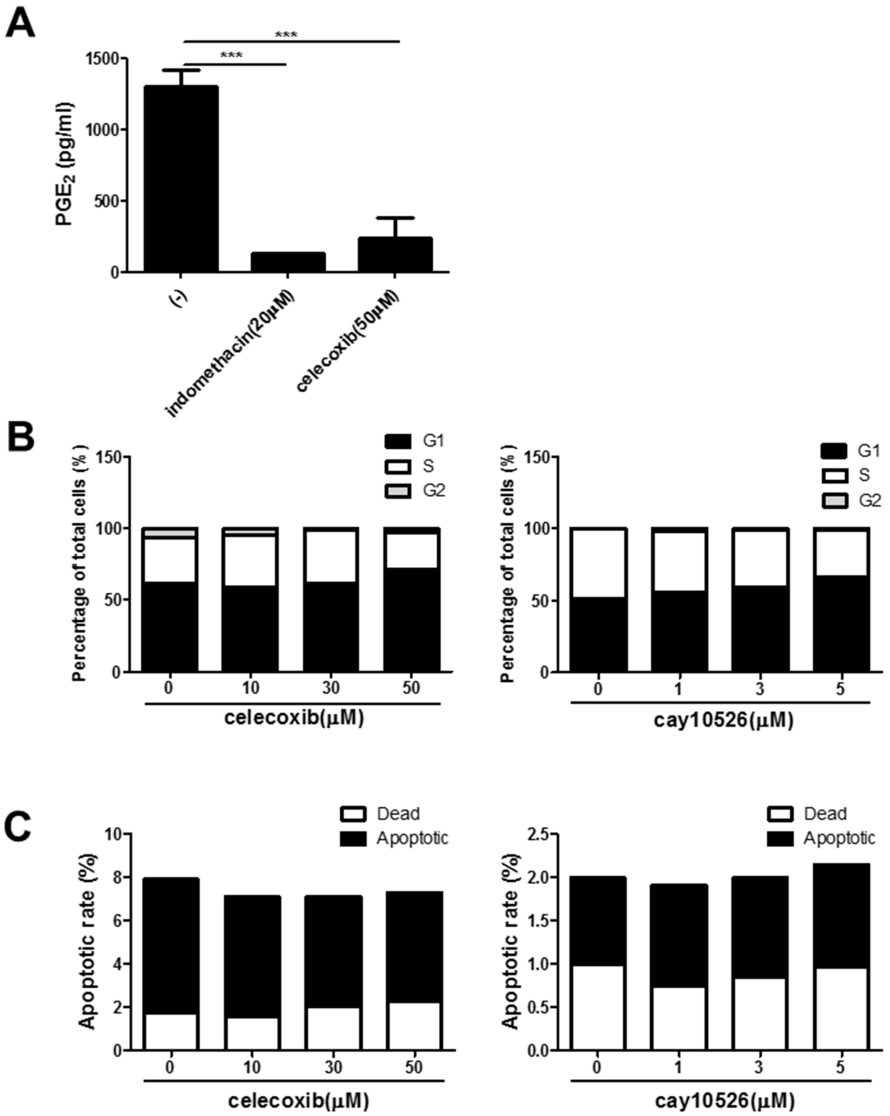

Figure 8. Inhibition of COX-2/mPGES-1 induces G1 cell cycle arrest in hUCB-MSCs and hAD-MSCs.

hUCB-MSCs and hAD-MSCs were treated with celecoxib (selective inhibitor for COX-2) or cay10526 (selective inhibitor for mPGES-1) at indicated concentrations. (A) PGE_2 concentrations of indomethacin or celecoxib-treated cells were measured by ELISA. FACS analysis of (B) cell cycle and (C) apoptosis. Results show a representative experiment. *** $P<0.001$. Results are shown as the mean ± SEM.

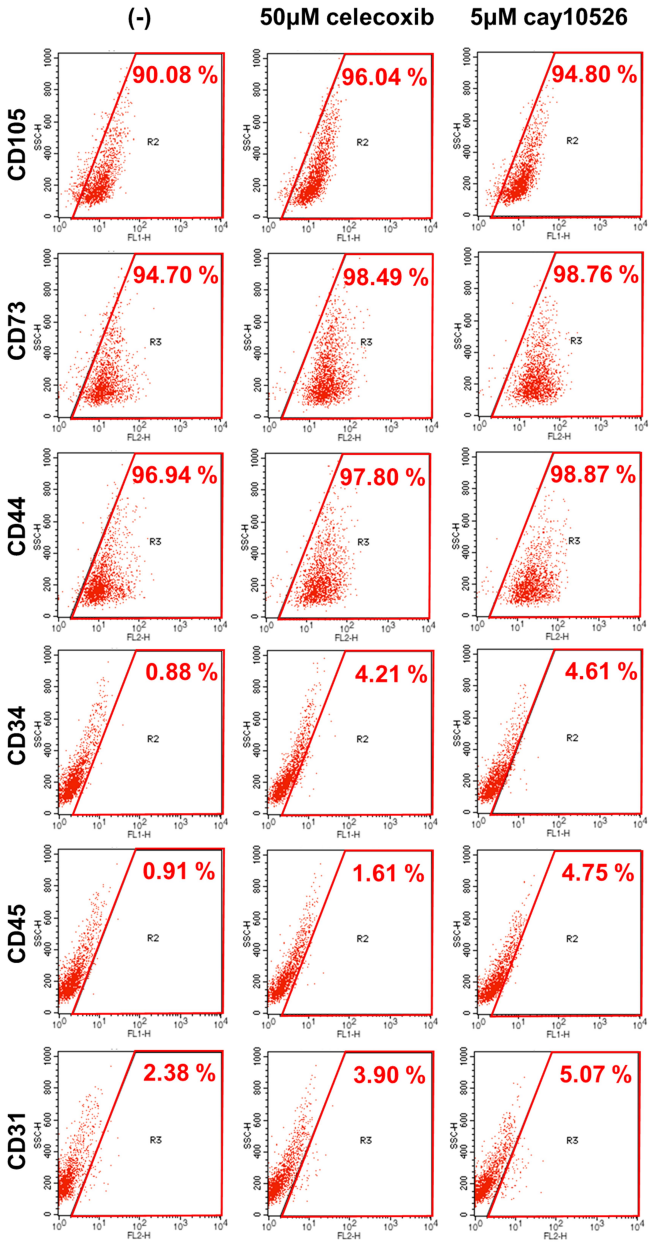

Figure 9. Regulation of COX-2/PGE_2 does not influence the expression profiles of CD markers.

The expression profiles of CD markers in hUCB-MSCs after the treatment of celecoxib or cay10526 were measured by flow cytometric analysis. Positive marker: CD105, CD73 and CD44, Negative marker: CD34, CD45 and CD31. Results show a representative experiment.

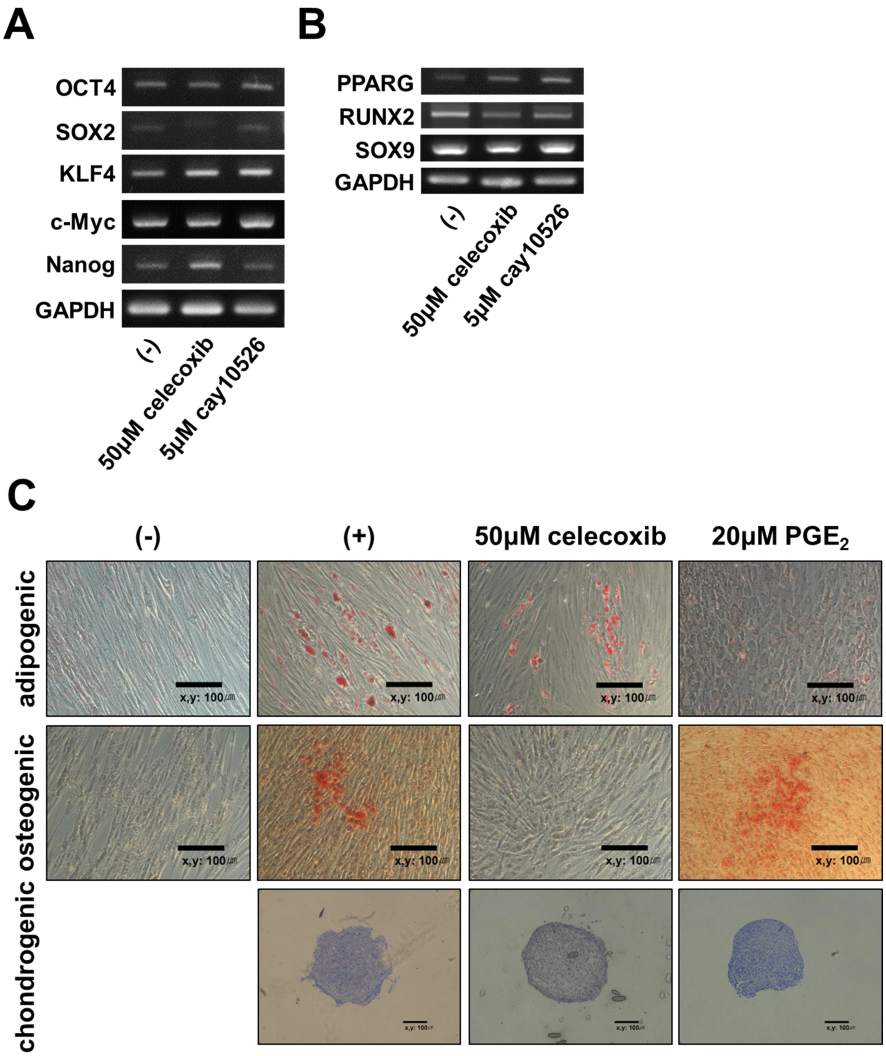

Figure 10. Regulation of COX-2/PGE_2 axis alters the differentiation potential of hUCB-MSCs.

(A-B) mRNA expressions of marker genes for (A) pluripotency and (B) differentiation in hUCB-MSCs were determined after treatment with celecoxib or cay10526 by RT-PCR. (C) hUCB-MSCs were differentiated into adipogenic-, osteogenic- and chondrogenic lineages in the presence of celecoxib and recombinant PGE_2. After 2 weeks of differentiation, the cells were stained with oil-red O for adipogenesis, alizarin S for osteogenesis and toluidine blue for chondrogenesis. Results show a representative experiment.

1.3.2 Decreased cell proliferation by COX-2 inhibition is restored by soluble factors from naive hMSCs

I next examined whether PGE_2 produced by naive hMSCs could restore the proliferation of COX-2-suppressed hMSCs. To determine the effect of soluble factors from naïve hMSCs on COX-2-inhibited cells without cell-to-cell contact, hMSCs were treated with celecoxib for 3 days and subsequently co-cultured with naive cells for 24 hours using the transwell system. Interestingly, co-culture with intact cells rescued the cell growth rate of both celecoxib-treated hUCB-MSCs and hAD-MSCs (Figure 11A). To minimize the influence of the short duration of COX-2 inhibition, COX-2 was further inhibited by siRNA transfection. Specific siRNA for COX-2 (siCOX-2) stably inhibited the expression level of COX-2 until day 3 (Figure 11B). Therefore, I further investigated whether the soluble factor, assumed to be PGE_2, from naïve hMSCs restored the proliferation of COX-2-supressed hMSCs using siCOX-2 to induce relatively persistent inhibition. As expected, soluble factors from intact hUCB-MSCs significantly rescued the proliferation of COX-2-inhibited hUCB-MSCs, whereas secretory factors from siCOX-2-treated hUCB-MSCs did not (Figure 11C). Moreover, direct PGE_2 treatment increased the proliferation of COX-2-inhibited hUCB-MSCs in a dose-dependent manner (Figure 11C). These results suggest that PGE_2 exerts an autocrine regulatory function in the self-renewal of hMSCs.

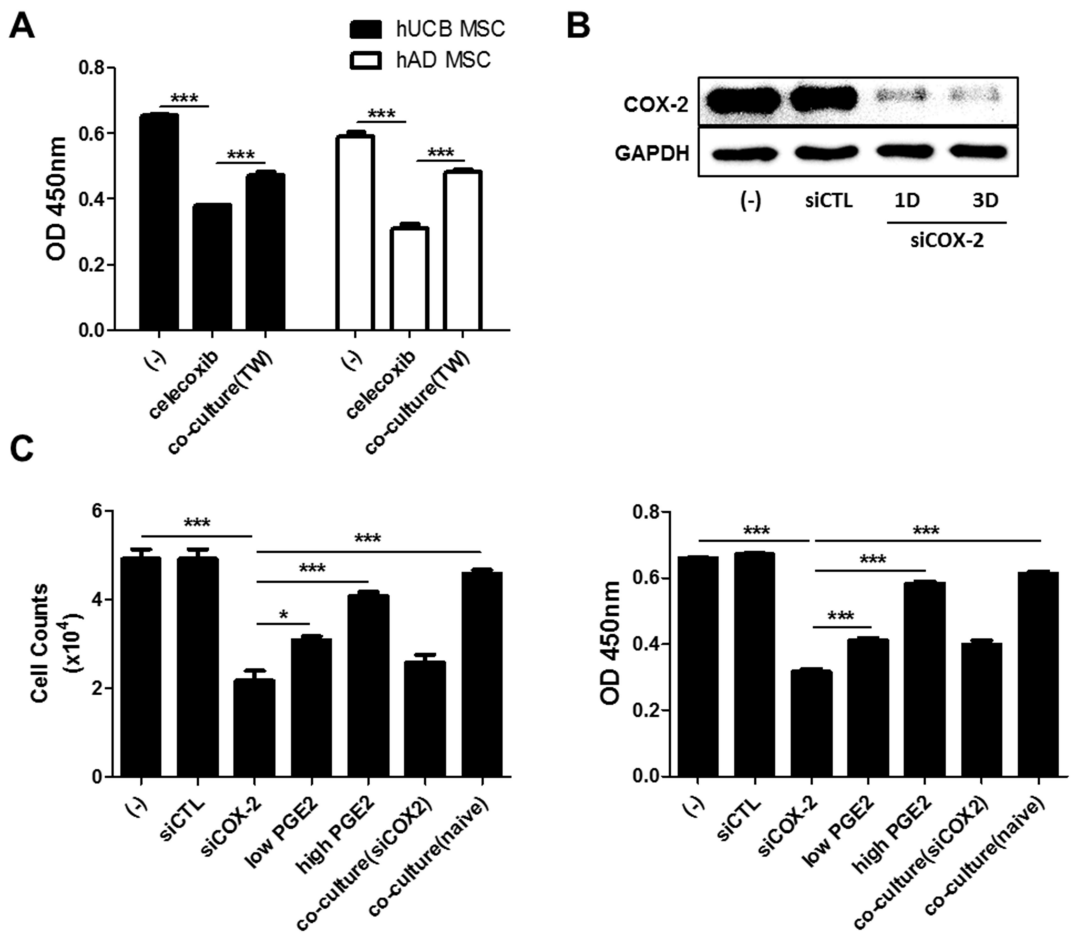

Figure 11. PGE_2 produced by hMSCs restores the COX-2-mediated inhibition of cell proliferation.

(A) COX-2 inhibited cells were co-cultured with naive cells for 24 hours, and the proliferation was determined by BrdU assay. After siRNA transfection, (B) sustained expression levels of COX-2 on day 1 and 3 were detected by Western blot analysis. (C) siCOX-2 transfected cells were treated with PGE_2 or co-cultured with naive and COX-2 suppressed cells, and proliferation was measured by direct cell counts and BrdU assay. Gel electrophoresis was conducted under the same experimental conditions, and images of blots were cropped. * $P<0.05$, *** $P<0.001$. Results are shown as the mean ± SEM.

1.3.3 EP2 receptor is involved in autocrine PGE_2 signalling to regulate hMSC proliferation

PGE_2 has a regulatory role in the self-renewal of hMSCs, and receptor-mediated signalling is involved in this regulation, including through EP receptors (Jang et al., 2012; Kleiveland et al., 2008). Therefore, I examined which receptors are expressed in hMSCs. Because microglia express all EP receptor subtypes, the human microglia cell line HMO6 was used as a positive control. hUCB-MSCs and hAD-MSCs expressed four EP receptor subtypes (Figure 12A). I next explored the crucial receptors involved in PGE_2-mediated cell growth regulation by blocking each receptor with selective antagonists. Remarkably, hUCB-MSC proliferation decreased only when the EP2 receptor was blocked with its antagonist (AH-6809) (Figure 12B and C). The other antagonists did not affect proliferation significantly and EP3 antagonist, L-798106, slightly increased the proliferation (Figure 12B and C). To confirm these findings, hMSCs were treated with butaprost and sulprostone (agonists for EP2 and EP3 receptors) in the presence of celecoxib to determine the effect of specific receptor triggering. While EP2 receptor activation significantly enhanced hUCB-MSC proliferation, EP3 receptor activation did not (Figure 12D). Taken together, these results indicate that the EP2 prostanoid receptor is the pivotal signalling pathway in PGE_2-mediated regulation of hMSC self-renewal.

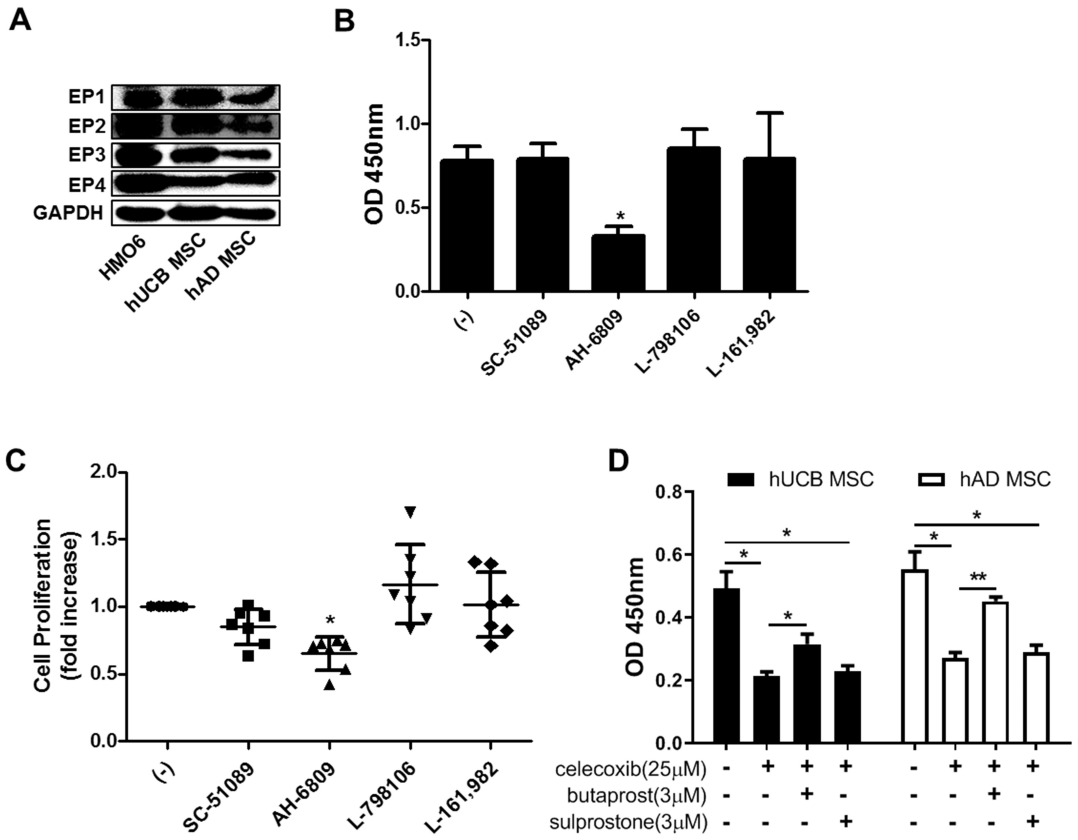

Figure 12. EP2 receptor has a crucial role in hMSC self-renewal.

(A) EP receptor expression in hUCB-MSCs and hAD-MSCs was assessed by Western blot analysis. HMO6, a human microglia cell line, was used as a positive control. In the presence of selective blockers for EPs, (B) cell growth rates were examined by BrdU assay and (C) results of repeated experiments are presented. Selective blockers for EP1: SC-51089, EP2: AH-6809, EP3: L-798106, and EP4: L-161,982. (D) After celecoxib treatment, cells were treated with selective agonists for EP2 or EP3, and proliferation was measured with a BrdU assay kit. Gel electrophoresis was conducted under the same experimental conditions, and images of blots were cropped. Selective agonist for EP2: Butaprost, EP3: Sulprostone. * $P<0.05$, ** $P<0.005$. Results are shown as the mean ± SEM.

1.3.4 PGE_2 secretion by hMSCs is regulated by cell contact

Direct cell-to-cell contact between MSCs and immune cells is crucially involved in regulating the proliferation and activation of immune cells (Duffy et al., 2011; Kim et al., 2013). Although these cell contact-dependent regulatory mechanisms in MSC function have been reported by a number of groups, few mechanistic studies elucidate the effect of cell contact among the hMSCs themselves on their function. Therefore, I investigated whether cell contact among hMSCs can affect COX-2 and mPGES-1 protein expression as well as PGE_2 secretion, which I proved to have a pivotal role in hMSC function. The COX-2 and mPGES-1 expression levels in both hUCB-MSCs and hAD-MSCs drastically decreased when the confluency of the same number of hMSCs was elevated by regulating the attachment area to allow cell-to-cell contact (Figure 13A). These results were visually confirmed by the immunocytochemical staining of COX-2 and mPGES-1 in hUCB-MSCs plated at different confluencies. hUCB-MSCs plated at high density showed reduced expression levels of PGE_2 synthesizing enzymes compared to cells with low density, the non-contact group (Figure 13B). Subsequently, decreased COX-2 and mPGES-1 levels led to lower PGE_2 secretion (Figure 14A).

To determine whether the secretion profile of other soluble factors is affected by cell contact, levels of various cytokines were measured in the hUCB-MSC culture media. In contrast to PGE_2, cell contact increased the production of interleukin (IL)-6 and IL-8, representative cytokines in NF-κB signalling (Figure 14B and C). Secretion of prominent immunomodulatory factors from hMSCs, including transforming growth factor (TGF)-β1, nitric oxide (NO) and indoleamine-2,3-dioxygenase (IDO)-1, was not affected by cell contact (Figure 14D-F). Furthermore, the cell contact status altered the expression pattern of EP receptor subtypes. Western blot analysis showed that hMSCs expressed higher levels of EP2 receptor under non-contact

conditions, whereas EP3 receptor expression increased with cell contact (Figure 15). These findings imply that cell-to-cell contact among hMSCs is important to regulate PGE_2 secretion and EP receptor expression.

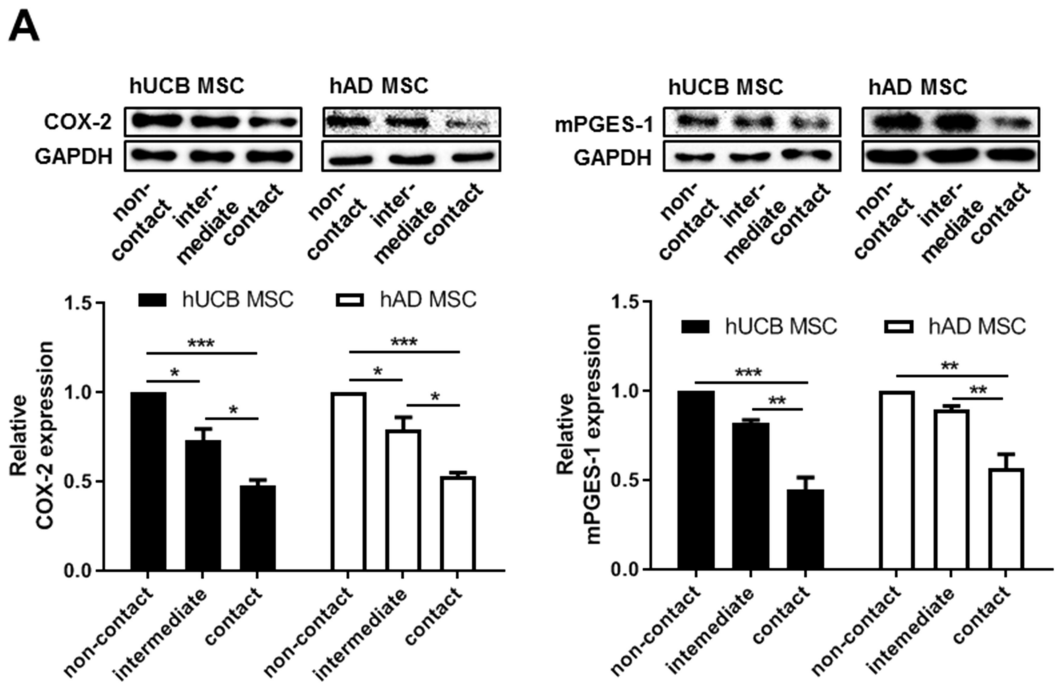
A
hUCB MSC
hAD MSC
COX-2
GAPDH
non-contact
inter-mediate
contact
mPGES-1
Relative COX-2 expression
Relative mPGES-1 expression
1.5
1.0
0.5
0.0
***
**
*
intermediate
intemediate

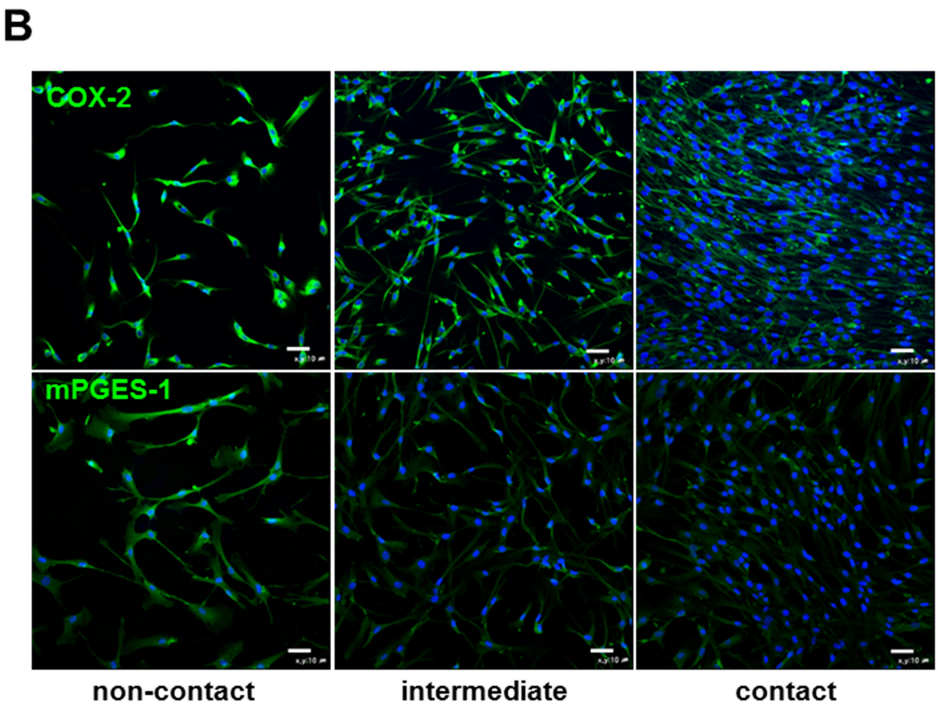
B
COX-2
mPGES-1
non-contact
intermediate
contact

Figure 13. Cell contact downregulates COX-2 expression of hMSCs.
Identical numbers of cells were seeded on culture plates of different widths for 24 hours to achieve different cellular confluencies. COX-2 and mPGES-1 protein levels were examined by (A) Western blot analysis and (B) immunocytochemistry. Bar = 500 μm. Gel electrophoresis was conducted under the same experimental conditions, and images of blots were cropped. * $P<0.05$, ** $P<0.005$, *** $P<0.001$. Results are shown as the mean ± SEM.

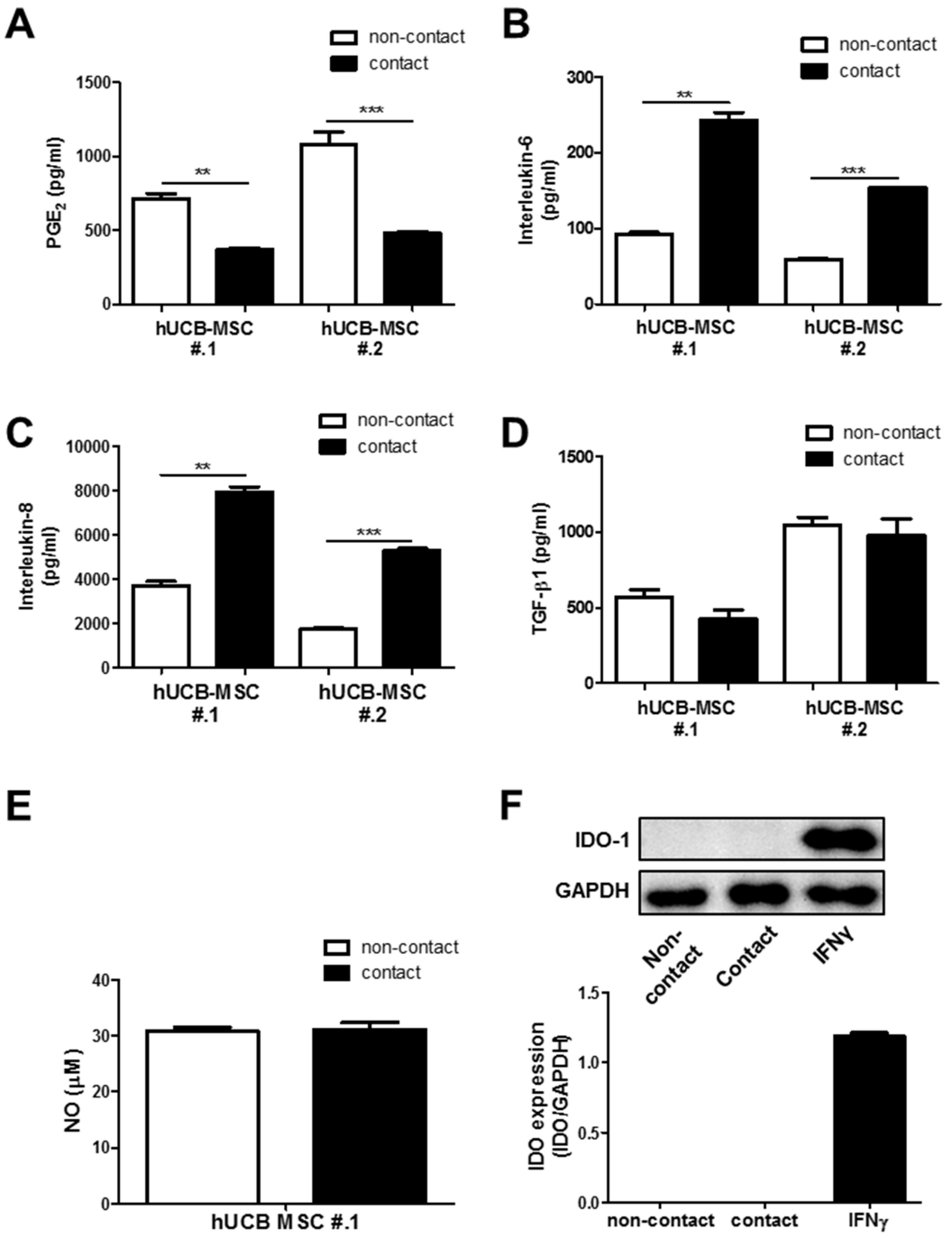
A
non-contact
contact
PGE2 (pg/ml)
1500
1000
500
0
**
***
hUCB-MSC #.1
hUCB-MSC #.2
B
non-contact
contact
Interleukin-6 (pg/ml)
300
200
100
0
**
***
hUCB-MSC #.1
hUCB-MSC #.2
C
non-contact
contact
Interleukin-8 (pg/ml)
10000
8000
6000
4000
2000
0
**
***
hUCB-MSC #.1
hUCB-MSC #.2
D
non-contact
contact
TGF-β1 (pg/ml)
1500
1000
500
0
hUCB-MSC #.1
hUCB-MSC #.2
E
non-contact
contact
NO (μM)
40
30
20
10
0
hUCB MSC #.1
F
IDO-1
GAPDH
Non-contact
Contact
IFNγ
IDO expression (IDO/GAPDH)
1.5
1.0
0.5
0.0
non-contact
contact
IFNγ

Figure 14. Cell-to-cell contact regulates PGE_2 secretion and immune modulatory factors in hMSCs.

Identical numbers of cells were seeded on culture plates of different widths for 24 hours to achieve different cellular confluencies. (A-E) (A) PGE_2, (B) IL-6, (C) IL-8, (D) TGF-β1 and (E) NO levels were determined from culture supernatant by ELISA. (F) The expression level of IDO-1 was determined by Western blotting and IFN-γ treatment group was used as a positive control. Gel electrophoresis was conducted under the same experimental conditions, and images of blots were cropped. ** $P<0.005$, *** $P<0.001$. Results are shown as the mean ± SEM.

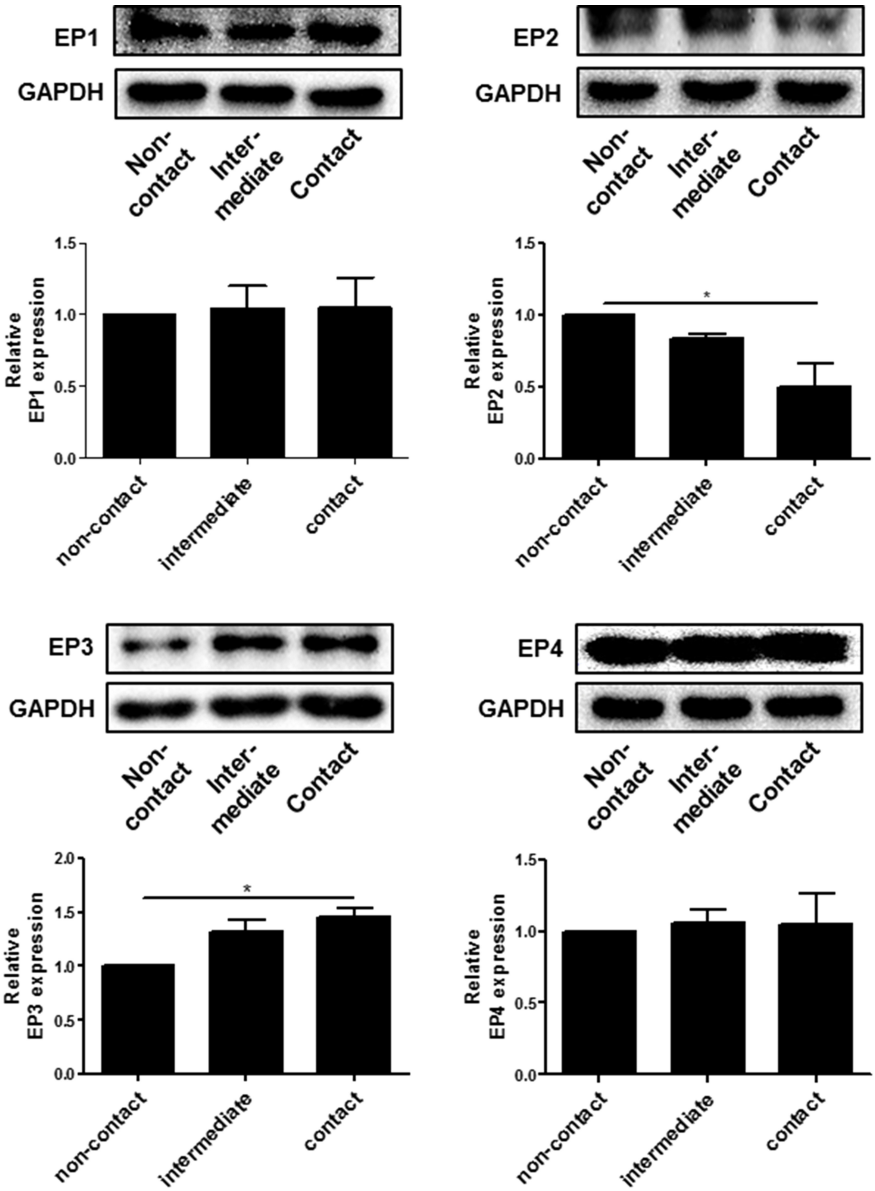

Figure 15. Cell contact status differently regulates the expression of EP receptors in hMSCs.

Identical numbers of cells were seeded on culture plates of different widths for 24 hours to achieve different cellular confluencies. Protein level of EP receptors was measured by Western blot analysis. Gel electrophoresis was conducted under the same experimental conditions, and images of blots were cropped. * $P<0.05$. Results are shown as the mean ± SEM.

1.3.5 Cell contact-dependent COX-2/PGE_2 axis suppression is mediated by gap junction intercellular communication (GJIC)

Gap junctions are formed when cells contact each other, and they regulate cellular function by allowing communication between adjacent cells. Therefore, I investigated whether gap junctions modulate the COX-2/PGE_2 pathway by treating cells with the gap junction decoupler, carbenoxolone (CBX). hMSCs under contact conditions were treated with 100 μM carbenoxolone for 24 hours. Impaired expression of COX-2 and mPGES-1 in hMSCs with cell-to-cell contact was restored after CBX treatment to levels similar to those observed in the non-contact group (Figure 16A and B). The restoration of the protein levels of these synthesis enzymes consequently led to increased PGE_2 secretion (Figure 16C). These findings indicate that PGE_2 production is regulated by gap junction-mediated cell-to-cell interaction.

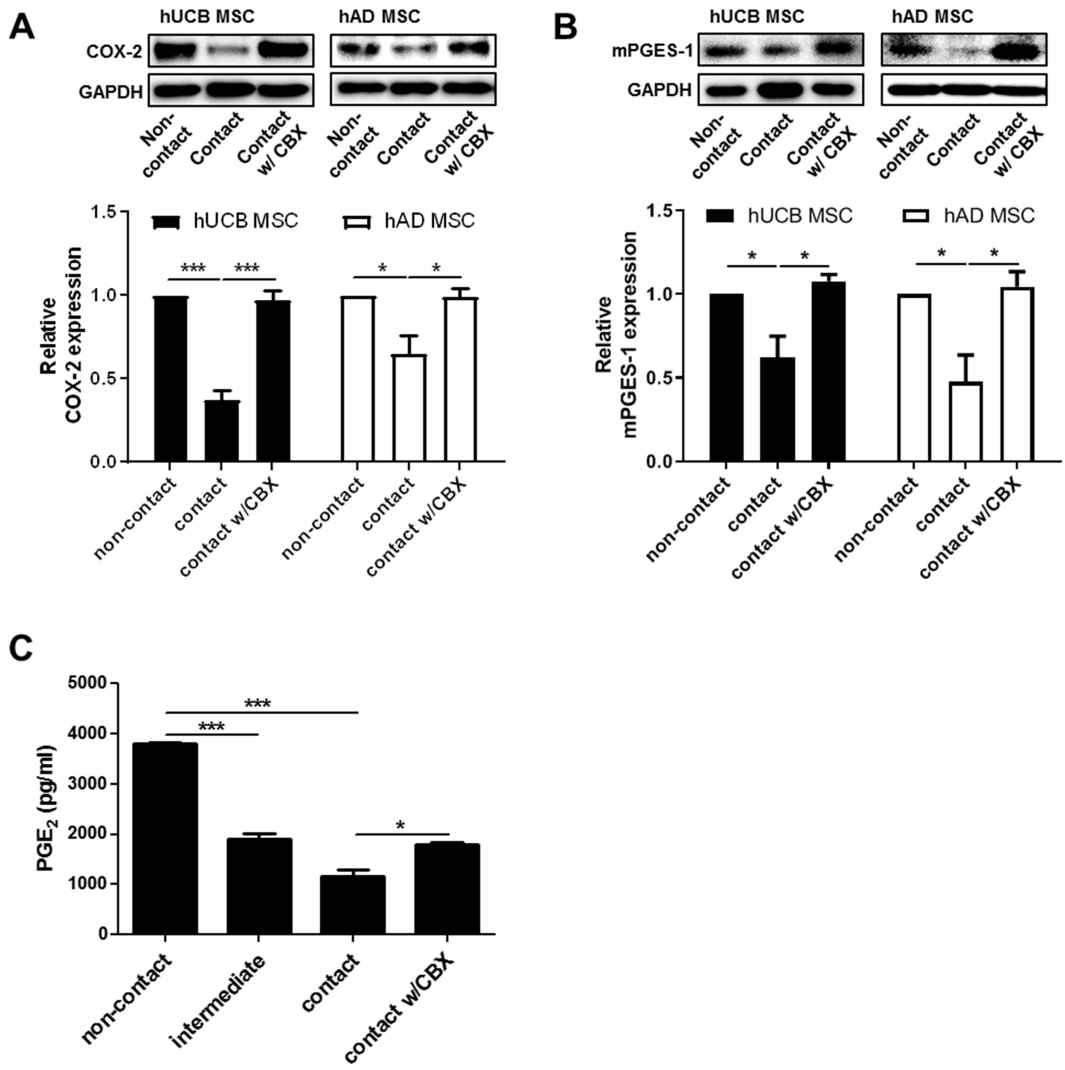

Figure 16. Gap junction intercellular communication is responsible for cell contact-mediated PGE_2 suppression in hMSCs.

hMSCs under cell contact were treated with 100 μM carbenoxolone (CBX), a gap junction decoupler, for 24 hours. Protein expression levels of (A) COX-2 and (B) mPGES-1 were examined by Western blot analysis. (C) PGE_2 concentrations were measured from the cultured media by ELISA. Gel electrophoresis was conducted under the same experimental conditions, and images of blots were cropped. * $P<0.05$, *** $P<0.001$. Results are shown as the mean ± SEM.

1.3.6 PGE_2 production is critical for the immunomodulatory ability of hMSCs, and cell contact-dependent inhibition of PGE_2 release leads to the decline in this ability

In the previous studies, among soluble factors, PGE_2 plays a key molecule for the immunomodulatory function of hMSCs (Kim et al., 2013; Kim et al., 2015). Therefore, I explored the significance of various soluble factors from hUCB-MSCs to inhibit mitogen-induced proliferation of mononuclear cells (MNCs). Mitogen-activated proliferation of MNCs was suppressed when they were co-cultured with hUCB-MSCs, and this inhibitory effect was reduced by the inhibition of COX-2, IDO-1 or IL-10 (Figure 17A). When culture media (CM) from target factor-inhibited hUCB-MSCs was used to culture mitogen-treated MNCs, the inhibition of MNC proliferation in the CM was restored by suppressing COX-2 and IL-10 (Figure 17B). Moreover, COX-2 inhibition in hUCB-MSCs by celecoxib treatment showed a dose-dependent decline in the suppression of MNC proliferation in both co-culture conditions allowing cell-to-cell contact and using CM (Figure 17C and D).

Given that COX-2 signalling is pivotal in the immunomodulatory effect of hUCB-MSCs and that signalling can be altered by cell-to-cell contact, I further assessed whether cell contact status can modulate the immunosuppressive property of hUCB-MSCs. CM from the non-contact group inhibited the proliferation of MNCs to a greater extent than CM from the contact group (Figure 17E). Moreover, the level of IL-10, a prominent anti-inflammatory cytokine, was elevated in the co-culture media, and hUCB-MSCs without cell contact exhibited more potent IL-10 production than cells with cell contact (Figure 17F). Taken together, my findings suggest that PGE_2 plays a crucial role in the immunosuppressive activity of hMSCs and that the cell contact regulation of PGE_2 production in hMSCs correlates with their immune function.

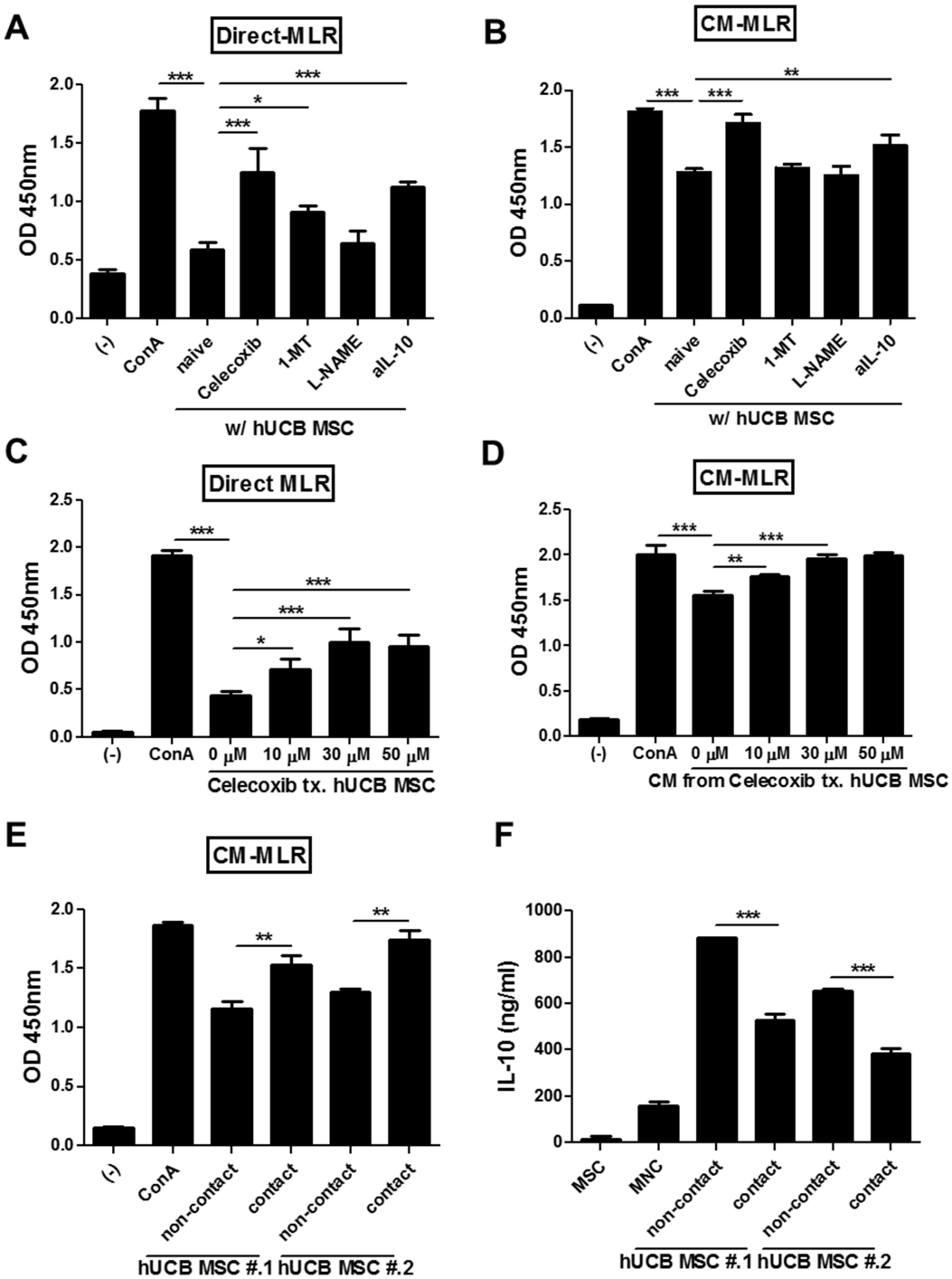
A
Direct-MLR
OD 450nm
2.0
1.5
1.0
0.5
0.0
***
***
*
***
(-)
ConA
naive
Celecoxib
1-MT
L-NAME
aIL-10
w/ hUCB MSC
B
CM-MLR
OD 450nm
**
***
***
(-)
ConA
naive
Celecoxib
1-MT
L-NAME
aIL-10
w/ hUCB MSC
C
Direct MLR
OD 450nm
2.5
2.0
1.5
1.0
0.5
0.0
***
***
***
*
(-)
ConA
0 μM
10 μM
30 μM
50 μM
Celecoxib tx. hUCB MSC
D
CM-MLR
OD 450nm
***
***
**
(-)
ConA
0 μM
10 μM
30 μM
50 μM
CM from Celecoxib tx. hUCB MSC
E
CM-MLR
OD 450nm
**
**
(-)
ConA
non-contact
contact
non-contact
contact
hUCB MSC #.1
hUCB MSC #.2
F
IL-10 (ng/ml)
1000
800
600
400
200
0
***
***
MSC
MNC
non-contact
contact
non-contact
contact
hUCB MSC #.1
hUCB MSC #.2

Figure 17. Cell contact-mediated decrease in the secretion of PGE_2 is followed by the attenuation of the immunosuppressive effects of hMSCs.
(A-E) Proliferation levels of mitogen-activated hMNCs were determined by BrdU, referred to as the MLR (mixed lymphocyte reaction) assay. (A) hMNCs were co-cultured with hUCB-MSCs that were pre-treated with selective inhibitors for various factors (Direct-MLR), or (B) cultured in the presence of conditioned media harvested from hUCB-MSCs (CM-MLR). Celecoxib: selective COX-2 inhibitor, 1-MT: selective IDO inhibitor, L-NAME: selective NOS inhibitor, aIL-10: neutralized with anti-IL-10 antibody. (C) hMNCs were co-culture with hUCB-MSCs treated with various doses of celecoxib, or (D) cultured in the presence of CM from hUCB-MSCs after treatment of various doses of celecoxib. (E) hMNCs were cultured in the presence of CM from the same number of hUCB-MSCs cultured under non-contact or contact condition. (F) IL-10 production in hMNCs cultured with CM from non-contact or contact hUCB-MSCs was measured by ELISA. * $P<0.05$, ** $P<0.005$, *** $P<0.001$. Results are shown as the mean ± SEM.

1.4 DISCUSSION

Although recent studies have demonstrated that a number of autocrine signalling events are involved in the induction or maintenance of MSC functions such as proliferation, differentiation, migration and immunoregulation (Hamidouche et al., 2010; Hemmingsen et al., 2013; Hodgkinson et al., 2013; Jeong et al., 2015; Ke et al., 2014), most of these studies focused on the elucidation of differentiation-related mechanisms. In the present study, I investigated the autocrine effect of PGE_2 on MSCs proliferation, a major characteristic of stem cells that contributes to stemness. A few studies reported that hMSC proliferation is regulated by PGE_2 (Jang et al., 2012; Kleiveland et al., 2008). In these studies, hMSCs derived from bone marrow or umbilical cord blood were treated with various doses of PGE_2. MSC proliferation consistently increased in response to PGE_2 treatment via protein kinase A signalling in both studies. In the present study, I found that PGE_2 produced by hUCB-MSCs and hAD-MSCs plays a crucial role in the maintenance of their proliferative function by regulating COX-2 signalling using chemical inhibitors or siRNA for COX-2. COX-2 inhibition by indomethacin or celecoxib treatment resulted in a consistent decrease in hMSC proliferation. This phenotype might result from the inhibition of potent signalling pathways in hMSCs via COX-2 signalling rather than PGE_2, as COX-2/PGE_2 signalling is involved in the several growth factor signalling pathways, including vascular endothelial growth factor and basic fibroblast growth factor (Baguma-Nibasheka et al., 2007; Wu et al., 2006). I achieved similar effects by suppressing mPGES-1, an enzyme for PGE_2 synthesis downstream of COX-2 signalling. Moreover, PGE_2 treatment of COX-2-inhibited hMSCs rescued their proliferation in a dose-dependent manner. More importantly, I proved that secreted soluble factors from naïve hMSCs restored the proliferation of COX-2-inhibited

hMSCs when they were co-cultured using a transwell system that prevented cell-to-cell contact, indicating that soluble factors from hMSCs themselves can contribute to their proliferation, presumably including PGE_2. The previous study by Jang et al. showed that among the four major sub-types of E-type prostaglandin (EP) receptors, EP2 receptor has a pivotal role in PGE_2-stimulated hUCB-MSC proliferation (Jang et al., 2012). In this study, I demonstrated that only the selective antagonist for EP2 receptor down-regulated basal hMSC proliferation, implying that autocrine stimulation of PGE_2 on hMSC proliferation is mediated by EP2 receptor. In addition, treatment with a selective agonist for EP2 receptor, butaprost, restored the proliferation of celecoxib-treated hMSCs.

Although a number of previous studies have shown that cell-to-cell contact between MSCs and immune cells or cancer cells is an important factor in the immunomodulatory or anti-tumour effect of MSCs, a few groups have focused on the cell-to-cell contacts between MSCs themselves and subsequent alterations in the secretion profile. Schajnovitz et al. reported that MSCs derived from bone marrow (BM-MSCs) possess functional gap junctions, and CXCL12 secretion by BM-MSCs is regulated by cell contact, leading to functional changes in MSCs to maintain the homeostasis of haematopoietic stem cells (Schajnovitz et al., 2011). I show here that PGE_2 secretion from the same number of MSCs was down-regulated when cell-to-cell contact was allowed, whereas production of IL-6 and IL-8 was increased, and TGF-β1 or NO production was not affected by confluent culture conditions that allow cell-to-cell contact. Decreased production of PGE_2 exerted by cell contact was restored by the blockage of cellular communication using CBX, a well-known GJIC inhibitor, indicating that MSCs form functional syncytia via connexin gap junctions, leading to alterations in the secretion profile. In addition, previous studies from the Prockop group reported that compaction of hMSCs into spheroids

self-activates signalling to enhance secretion of anti-inflammatory modulators such as PGE_2, tumour necrosis factor α-induced protein 6 and stanniocalcin 1 (Bartosh et al., 2013; Ylostalo et al., 2012). In these studies, hMSCs cultured as spheres using hanging drop culture produced markedly elevated levels of PGE_2. This discrepancy in PGE_2 regulation by cell contact might result from the differences in culture conditions for MSCs. In the present study, the general plastic adherent 2D culture method was used, and only the plating area was controlled to regulate cell-to-cell contact, whereas the hanging drop method to generate 3D spheroids was used in the studies by Prockop group.

PGE_2 is a potent immunomodulator produced by hMSCs. hMSCs suppress the differentiation and maturation of T lymphocytes and induce the generation of regulatory T cells via COX-2-mediated PGE_2 secretion (Boniface et al., 2009; Duffy et al., 2011; Tatara et al., 2011). Moreover, PGE_2 secretion from MSCs in response to certain inflammatory milieu critically contributes to the immunoregulatory function of MSCs against several immune disorders, including arthritis and colitis (Bouffi et al., 2010; Kim et al., 2013). PGE_2 produced by MSCs exerts anti-inflammatory effects through the regulation of immune cell activation and maturation, including $CD4^+$ helper T cells, B cells, dendritic cells, natural killer cells, monocytes and macrophages (Murphy et al., 2013). In the present study, I have proven that cell contact-dependent regulation of PGE_2 secretion correlates with the functional phenotype of MSCs. Importantly, down-regulation of PGE_2 secretion by cell-to-cell contact led to a decreased immunomodulatory effect of MSCs in a mixed leukocyte reaction. Based on these findings, control of culture conditions regulating cell contact might be a crucial point in the development of therapeutics from MSCs, as a number of studies have been performed and are being conducted to produce therapeutics or cosmetics

using conditioned media from MSCs (Angoulvant et al., 2011; Su et al., 2015; Wei et al., 2009).

Taken together, the present study revealed novel information indicating that PGE_2 secreted from adult stem cells exerts autocrine effects on MSC proliferation by triggering the EP2 receptor, and PGE_2 production is dependent on cell-to-cell contact mediated by GJIC, resulting in a decline in immunoregulatory ability.

CHAPTER Ⅱ

MIS416 enhances therapeutic functions of human umbilical cord blood-derived mesenchymal stem cells against experimental colitis by modulating systemic immune milieu

2.1 INTRODUCTION

Inflammatory bowel diseases (IBDs), including Crohn's disease and ulcerative colitis, are chronic relapsing disorders characterized by excessive intestinal inflammation. Although the precise etiology of IBDs remains unclear, it is known that several causes are involved in the disease onset. The concerted action of genetic susceptibility, environmental risk factors and alterations of the microbiota triggers dysregulated immune responses, resulting in the impairment of mucosal barrier functions. Conventional treatments for IBDs including antibiotics, anti-inflammatory drugs and immunosuppressive medicines have limitations such as drug resistance and low therapeutic responses in certain groups of patients. To overcome these limitations, alternative therapies, such as probiotics, anti-tumor necrosis factor (TNF) therapy and transplantation of mesenchymal stem cells (MSCs) have recently emerged (Ciccocioppo et al., 2011; Danese et al., 2013). Among these remedies, MSCs have been studied for IBD treatment because of their immunomodulatory properties, tissue regenerative capacity and ability to migrate toward damaged areas. Key immunomodulatory functions of MSCs that have been demonstrated both *in vitro* and *in vivo* is their ability to inhibit the excessive proliferation and maturation of immune cells (Le Blanc et al., 2003).

Although the therapeutic use of hUCB-MSCs has been investigated for decades, standardization issues remain to be overcome. For example, reduced productivity of MSCs caused by replicative senescence and donor-to-donor variations make it difficult to maintain consistent therapeutic effects for each recipient (Fehrer and Lepperdinger, 2005). Several strategies have recently been investigated for enhancement of the therapeutic potential of MSCs. Previously, It was reported that NOD2 activation through muramyl dipeptide (MDP) priming upregulated prostaglandin E_2 (PGE_2) secretion from

hUCB-MSCs and increased anti-inflammatory effects in experimental models of IBD (Kim et al., 2013). Similarly, priming of MSCs with growth factors or cytokines has also been reported (Polchert et al., 2008). However, these methods have not been fully verified in regard to safety or optimization. Although many investigations have been performed to elaborate these strategies, other simplified methods are still needed for convenient application.

MIS416 is a novel immunomodulatory microparticle derived from Propionibacterium acnes, which consists of MDP and bacterial DNA. Phagocytic cells, key responders to MIS416, internalize MIS416, resulting in the activation of cytoplasmic receptors, NOD2 and TLR9 (Girvan et al., 2011). NOD2 and TLR9-dependant pathways have been highlighted as therapeutic targets in IBDs, as NOD2 and TLR9 dysfunctions have been shown to play a central role in disease pathophysiology. For example, a frame-shift mutation of NOD2 was associated with the development of Crohn's disease in a study of over 400 unrelated subjects (Ogura et al., 2001), and in experimental colitis, a NOD2 deficiency exacerbated disease severity due to an uncontrolled immune response leading to immune hyper-responsiveness to intestinal antigens mediated by IL-12-producing antigen-presenting cells (Watanabe et al., 2006). In contrast, overexpression of the NOD2 gene rescued mice from peptidoglycan-induced colitis (Yang et al., 2007), and mice deficient in TLR9 and MyD88 no longer demonstrated probiotic-mediated inhibitory effects on intestinal inflammation in experimental colitis (Rachmilewitz et al., 2004). Furthermore, TLR9-induced type I interferon (IFN) resolved intestinal inflammation, and this effect was abolished by type I IFN neutralizing antibodies (Lee et al., 2006). As a NOD2 and TLR9 agonist, MIS416 has the potential to immune modulate IBDs by distinct and complimentary mechanisms. As well as inducing expansion of the peripheral pool of splenic myeloid derived suppressor cells

(MDSCs) (White et al., 2014), MIS416 treatment has been shown to induce innate IFN-γ, nitric oxide (NO) and IL-10 in healthy animal and human studies. As a result of the altered immune milieu, MIS416 treatment also promoted expansion of splenic regulatory T (Treg) cells, and in a model of neuroinflammation, this was associated with suppression of the inflammatory response mediated by T helper (Th) 1, Th2, and Th17 cells (White et al., 2018). As a result of its efficacy in experimental autoimmune encephalomyelitis, MIS416 is currently in clinical trials for multiple sclerosis (White et al., 2014; White et al., 2018).

The mechanisms of action of MSCs in the therapeutic setting include both direct cell-to-cell contact as well as the secretion of soluble factors which modulate diverse immune cell subsets (Corcione et al., 2006; Le Blanc and Mougiakakos, 2012; Yagi et al., 2010; Zappia et al., 2005). hUCB-MSCs were detected in inflamed colons and alleviated the severity in mouse colitis model (Kim et al., 2013; Qiu et al., 2017), suggesting that their immunomodulatory effects occur in the localized environment, and that localization of MSCs at the inflammatory sites is a key factor for their therapeutic effects (De Becker and Van Riet, 2016; Newman et al., 2009). Accordingly, many studies have demonstrated the distribution of injected MSCs at the inflamed colon in experimental colitis model by various methods, such as luciferase, GFP or indocyanine green labeling (Mao et al., 2017; Qiu et al., 2017; Takeyama et al., 2017). Several molecules, such as monocyte chemotactic protein-1 (MCP-1/CCL2), stromal cell-derived factor-1 (SDF-1/CXCL12), integrins and matrix metalloproteinases (MMPs), are involved in the recruitment of MSCs into inflamed tissues (Marquez-Curtis and Janowska-Wieczorek, 2013). Among these factors, MCP-1 is produced by various cells including monocytes/macrophages which are a major source of MCP-1 (Deshmane et al., 2009). It also has been reported that secreted MCP-1 stimulates migration of MSCs to the target region (Dwyer et al.,

2007), and this has been demonstrated in an experimental rat model of stroke, where MCP-1 from ischemically damaged tissue was shown to facilitate migration of the transplanted human MSCs towards the site of injury (Wang et al., 2002).

As MIS416 co-administration might be a novel method for improving hUCB-MSC-based therapies against IBDs, in the present study, I investigated whether MIS416 co-administration could accelerate the therapeutic efficacy of hUCB-MSCs in a DSS-induced colitis model.

2.2 MATERIALS AND METHODS

2.2.1 Mice

All experimental processes were approved by the Seoul National University Institutional Animal Care and Use Committee (IACUC No. SNU-170523-3) in accordance with the guidelines of the committee. C57BL/6J mice (male, 6–8 weeks old) were obtained from Orientbio (Sungnam, Republic of Korea). Mice were housed in a temperature- and humidity-controlled room in the animal facility of Seoul National University. Colitis was experimentally induced by administration of 3% DSS (MP Biochemicals, Solon, OH, USA) in drinking water supplied ad libitum for 7 days unless the application of humane end-point was needed, DSS treatment was replaced by normal drinking water after day 7. MIS416 (Innate Immunotherapeutics, Auckland, New Zealand) was injected into the retro-orbital sinuses on day 1 and day 8. Subsequently, hUCB-MSCs were suspended in PBS (2×10^6 cells/200 μl per head) and infused into mice intraperitoneally on day 1(IRB No. 1707/001-008). Body weight and survival rate were monitored over 12 days. On day 7, the therapeutic potential of the treatments was measured by evaluating the disease activity index (DAI) including body weight loss (0-4), stool consistency (0-4), bleeding (0-4), general activity (0-2) and coat roughness (0-4), with a maximum DAI score of 18 and the humane end-point was established at DAI = 13.5. On day 11, colon, serum and spleen samples were collected from sacrificed mice for further *ex vivo* examinations. To define the systemic influence of MIS416, mice were sacrificed a day after injection (day 2), and colon, serum and spleen samples were collected for analyses.

2.2.2 Histopathological evaluation

The collected colon samples were fixed with 10% formalin. The tissues were embedded in paraffin, cut into 4-μm-thick sections, and stained with hematoxylin and eosin (H&E) as well as picrosirius red (PSR). The histopathological score was obtained by evaluating H&E stained slides based on the following 5 indexes: loss of goblet cells, infiltration of immune cells, crypt abscesses, hyperemia and edema, and loss of epithelium, with a maximum score of 15 (graded from 0-3 for the severity of each index). Generation of fibrotic tissue in the colon was assessed by PSR staining, followed by counterstaining with fast green (Sigma-Aldrich, St. Louis, MO, USA). The ratio of the fibrotic (picrosirius red-positive) area was assessed using ImageJ software version 1.51j8 (National Institutes of Health, Bethesda, MD, USA).

2.2.3 Cytokine detection

IL-6, IL-10, MCP-1, IFN-γ, TNF and IL-12p70 in the serum of mice were measured by flow cytometry using the CBA Mouse Inflammation Kit (BD Bioscience, San Jose, CA, USA). IL-17A and IL-23 in the serum were determined by CBA mouse flex sets (BD Bioscience). IL-6 in hUCB-MSC-cultured medium was measured using the CBA Human Th1/Th2/Th17 Cytokines kit (BD Bioscience) according to the manufacturer's instructions. Briefly, 50 μl of samples or standards were mixed with 50 μl of mixed capture beads and 50 μl of a PE-conjugated detection antibody and incubated for the designated time (2 hrs for mouse, 3 hrs for human samples). Detection was performed with a FACScalibur flow cytometer and evaluated using Cell Quest software (BD Bioscience). To address the level of neutrophil infiltration, Myeloperoxidase (MPO) activity of colon samples was assessed using a Mouse Myeloperoxidase DuoSet kit (R&D Systems, Minneapolis, MN, USA) according to the manufacturer'a instructions.

Briefly, colon segments were homogenized with the protein lysis buffer Pro-prep (Intron Biotechnology Co., Sungnam, Republic of Korea) to a concentration of 10 mg/ml. Appropriately diluted samples and standards were added to wells of 96-well plates pre-coated with a mouse MPO capture antibody and incubated overnight at room temperature. Then, a streptavidin-horseradish peroxidase (HRP)-conjugated detection antibody was added and incubated. After the incubation with streptavidin-HRP, the level of MPO was quantified by reaction with a substrate solution. Absorbance was read at 450 nm using an Infinite200 PRO microplate reader (Tecan, Maennedorf, Switzerland). After indicated treatment to hUCB-MSCs, the level of Nitric Oxide (NO) production was measured by Griess assay (Promega, Fitchburg, WI, USA). And the level of Prostaglandin E_2 (PGE_2) secretion was determined by commercial ELISA kit (R&D Systems, Minneapolis, MN, USA). After enough reaction, the absorbance of the samples was measured at 540nm and 450nm, respectively, using an Infinite200 PRO microplate reader (Tecan).

2.2.4 Isolation and culture of hUCB-MNCs

All experiments using human umbilical cord blood (UCB) or UCB-derived cells were approved by Institutional Review Board (IRB) of the Boramae Hospital and Seoul National University (IRB No. 1707/001-008) with informed maternal consent. Isolation and culture were performed as previously described (1.2 MATERIALS AND METHODS).

2.2.5 Isolation and culture of hUCB-MSCs

hUCB-MSCs were isolated as previously described (1.2 MATERIALS AND METHODS). The cells possessed the characteristics of MSCs (Kang et al., 2018; Lee et al., 2016) and were verified by expression

of surface markers by flow cytometric analysis. I used the cells at passage 8 for *in vivo* experiments and passage 8 to 10 for *in vitro* experiments.

2.2.6 Cell migration assay

hUCB-MSCs were suspended in culture medium, and 500 μl of the cell suspension (1×10^4 cells/mL) was added to transwell inserts (8 μm pore size). Subsequently, 500 μl of MSC conditioned medium was added to the lower chambers. After 24 hours of incubation, hUCB-MSCs that migrated to the underside of the membrane were fixed, and the remaining cells in the upper chamber were carefully swiped with a cotton swab. The membranes of the transwell were stained with DAPI and sealed on slides. A confocal microscope (Nikon, Eclipse TE200, Japan) was used to count the number of cells on the underside of the insert for each group.

2.2.7 Cell cycle assay

Cell cycle assay was conducted as previously described (1.2 MATERIALS AND METHODS).

2.2.8 Quantitative PCR

Quantitative PCR was conducted as previously described (1.2 MATERIALS AND METHODS).

2.2.9 Flow cytometric analysis

To confirm the expression of cell surface markers, isolated primary cells were stained with a fluorochrome-conjugated antibody and analyzed. After cell surface staining, the cells were stained with antibodies against intracellular protein, as necessary. For intracellular staining, I used transcription factor buffer set (BD Biosciences, #562725) according to manufacturer's instruction. Briefly, the cells were fixed by 1x Fix/Perm

Buffer, and permeabilized by 1x Perm/Wash Buffer. Detailed information for all antibodies is provided in Table 4. Fluorescence was detected with a FACScalibur flow cytometer and evaluated using Cell Quest software (BD Biosciences).

2.2.10 Western blot analysis

Western blot analysis was conducted as previously described (1.2 MATERIALS AND METHODS). Detailed information for all antibodies is provided in Table 4.

2.2.11 Immunohistochemistry

4-μm-thick paraffin-embedded sections of colon were deparaffinised and rehydrated. For permeabilization, the samples were incubated with 0.05% Triton X-100 solution at room temperature for 10 min and blocked with 5% normal goat serum (NGS) at room temperature for 1 hour. Then, the cells were stained with FITC-rat anti-mouse Foxp3 monoclonal antibody (eBioscience, San Diego, CA, USA). Before imaging, nuclei were counterstained with DAPI. The images were captured by a confocal microscope (Nikon). Detailed information for all antibodies is provided in Table 4.

2.2.12 Cell proliferation assay

Proliferation of hUCB-MSCs and hUCB-MNCs was determined after treatment with MIS416 (IRB No. 1707/001-008). In addition, to identify the suppression ability of hUCB-MSCs, isolated $CD4^+$ T cells were co-cultured with MIS416-pre-treated hUCB-MSCs, followed by a proliferation assay. Cell proliferation was measured using a bromodeoxyuridine (BrdU) ELISA kit (Roche, Indianapolis, IN, USA). After the indicated treatment, BrdU labeling solution (100 μM) was added into the culture medium in 96-well plates.

Table 4. Antibody information

	Primary antibody	Dilution	Source	Cat. #
Western blotting	Rabbit anti-COX-2	1:1000	Abcam, Cambridge, MA, USA	ab15191
	Mouse anti-iNOS	1:100	Santa Cruz Biotechnology, Santa Cruz, CA, USA	sc-7271
	Mouse anti-IDO-1	1:500	Merck-Millipore, Darmstadt, Germany	MAB5412
	Rabbit anti-RIP2	1:1000	Abcam, Cambridge, MA, USA	ab8428
	Rabbit anti-MyD88	1:1000	Merck-Millipore, Darmstadt, Germany	AB16527
	Rabbit anti-IKK alpha	1:1000	Cell Signaling Technology, Beverly, MA, US	2682s
	Rabbit anti-Phospho NFkB p65	1:1000	Cell Signaling Technology, Beverly, MA, US	3033s
	Rabbit anti-Total NFkB p65	1:1000	Cell Signaling Technology, Beverly, MA, US	8242s
	Rabbit anti-IkB alpha	1:1000	Cell Signaling Technology, Beverly, MA, US	9242s
	Rabbit anti-Phospho JNK	1:1000	Cell Signaling Technology, Beverly, MA, US	9251s
	Rabbit anti-JNK	1:1000	Cell Signaling Technology, Beverly, MA, US	9252s
	Rabbit anti-Phospho p38	1:1000	Cell Signaling Technology, Beverly, MA, US	4511s
	Mouse anti-Total p38	1:500	Merck-Millipore, Darmstadt, Germany	MABS1754
	Rabbit anti-Phospho ERK	1:1000	Cell Signaling Technology, Beverly, MA, US	9101s
	Rabbit anti-Total ERK	1:1000	Cell Signaling Technology, Beverly, MA, US	4695s
FACS	FITC Mouse anti-Human CD4	1:50	BD Bioscience, San Jose, CA, USA	555346
	APC Mouse anti-Human IFN-γ	1:50	BD Bioscience, San Jose, CA, USA	554702
	PE Mouse anti-Human IL-4	1:50	BD Bioscience, San Jose, CA, USA	554516
	PE Mouse anti-Human FoxP3	1:50	BD Bioscience, San Jose, CA, USA	560046
	PE Mouse anti-Human IL-17A	1:50	BD Bioscience, San Jose, CA, USA	560438
	APC Rat anti-mouse CD4	0.125 μg/test	eBioscience, San Diego, CA, USA	17-0042-82
	PE Rat anti-mouse CD25	0.125 μg/test	eBioscience, San Diego, CA, USA	12-0251-82
	FITC Rat anti-mouse FoxP3	1 μg/test	eBioscience, San Diego, CA, USA	11-5773-82
	FITC Mouse Anti-Human CD45	1:50	BD Bioscience, San Jose, CA, USA	555482
	PE Mouse Anti-Human HLA-DR	1:50	BD Bioscience, San Jose, CA, USA	555812
	FITC Mouse anti-Human CD105 (Endoglin)	1:50	BD Bioscience, San Jose, CA, USA	561443
	APC Mouse anti-Human CD73	1:50	BD Bioscience, San Jose, CA, USA	560847
	APC Mouse Anti-Human CD29	1:50	BD Bioscience, San Jose, CA, USA	559883
	FITC Mouse Anti-Human CD44	1:50	BD Bioscience, San Jose, CA, USA	555478
	PE Mouse Anti-Human CD36	1:50	BD Bioscience, San Jose, CA, USA	555455
	PE Mouse Anti-Human CD34	1:50	BD Bioscience, San Jose, CA, USA	555822
IHC	FOXP3 Monoclonal Antibody	1:200	eBioscience, San Diego, CA, USA	14-5773-80

The culture medium containing BrdU solution was removed after overnight incubation at 37 °C, and the cells were fixed with FixDenat solution for 30 min at room temperature. The cells were then incubated with an anti-BrdU-POD working solution for 90 min at room temperature. Following three rinses with washing solution, a substrate solution was added to the cells and incubated for 5~30 min at room temperature. After sufficient color development, the OD values were read at 450 nm on a microplate reader (TECAN).

2.2.13 *In vivo* cell tracking

For *in vivo* cell trafficking, hUCB-MSCs were transduced with a green fluorescent protein (GFP)-encoding retroviral vector. For retrovirus preparation, the pMX-GFP vector and retrovirus packaging vectors were co-transfected into 293FT cell (Invitrogen) using FuGENE 6 transfection reagent (Promega). Viral supernatants were collected at 48 hours post-transfection, filtered through a 0.45 μm PVDF membrane filter and then directly used to infect hUCB-MSCs. Transduction efficiency was monitored by fluorescence microscopy and flow cytometric analysis. These cells (2×10^6 cells/head) were intraperitoneally injected into mice on day 1. On day 2 and day 11, mice were sacrificed, and colon samples were collected. The distribution of hUCB-MSCs was imaged by confocal imaging (Nikon, Eclipse TE200, Japan) using 4-μm-thick paraffin-embedded sections. Further, colon samples were chopped and filtered to obtain a single-cell suspension, on day 2 and day 11. Then, samples were stained with antibody of hUCB-MSCs surface markers, anti-human CD29, and fluorescence was detected by flow cytometric analysis.

2.2.14 Statistical analysis

The mean values of all data are expressed as the means ±SEM. Statistical analysis was performed using GraphPad Prism version 7.0 (GraphPad Software, San Diego, CA, USA). Data were assessed for normality using the D'Agostino and Pearson normality test. Where data were normally distributed, the significance of the data was determined by using Student's t tests for comparison of two groups or one-way ANOVA coupled to Bonferroni's test for multiple groups. Where data were not normally distributed, Mann–Whitney U test or Kruskal-Wallis method coupled to Dunn's multiple comparison test were used. For analysis of survival data, Kaplan-Meier test and Mantel-Cox post-test were used. Nonparametric tests were conducted by Kruskal-Wallis method coupled to Dunn's multiple comparison test. P-values less than 0.05 were considered to be statistically significant and are indicated in the text.

2.3 RESULTS

2.3.1 MIS416 enhances the therapeutic effect of hUCB-MSCs against DSS-induced colitis in mice

The ligands of pattern-recognition receptors (PRRs), as components of innate immune systems, affect the diverse functions of hUCB-MSCs including immunomodulation, migration, proliferation, differentiation and cytokine secretion (Kim et al., 2010; Le Blanc and Mougiakakos, 2012; Opitz et al., 2009; Pevsner-Fischer et al., 2007; Tomchuck et al., 2008). To investigate whether MIS416, a microparticle comprising NOD2 and TLR9 agonists, could enhance the therapeutic effects of hUCB-MSCs, I co-injected hUCB-MSCs and MIS416 in DSS-induced colitis mice as described at Figure 18A. The survival rate was further increased by co-treatment compared to hUCB-MSC or MIS416 single treatments (Figure 18B) ((+) vs U+M p= 0.003; U vs U+M p=0.04; M vs U+M p=0.006). The therapeutic effects were also determined by attenuation of body weight loss-the body weight in the co-treatment group was markedly increased compared with hUCB-MSC- or MIS416-treated groups (Figure 18C) ((+) vs U+M p<0.0001; U vs U+M p=0.0444; M vs U+M p=0.0050). By assessment of DAI on day 7, it was confirmed that the severity of DSS-induced colitis was further attenuated by co-administration of MIS416 and hUCB-MSCs compared to each single treatment (Figure 18D) ((+) vs U+M p<0.0001; U vs U+M p=0.0025; M vs U+M p= 0.0025). I next measured the length of colon on day 11, and the colon lengths were significantly increased in co-treated group compared to each single treated groups (Figure 18E) ((+) vs U+M p=0.0003; U vs U+M p=0.0294; M vs U+M p= 0.0275). Taken together, these results suggest that co-treatment with MIS416 enhances the therapeutic efficacy of hUCB-MSCs against DSS-induced colitis.

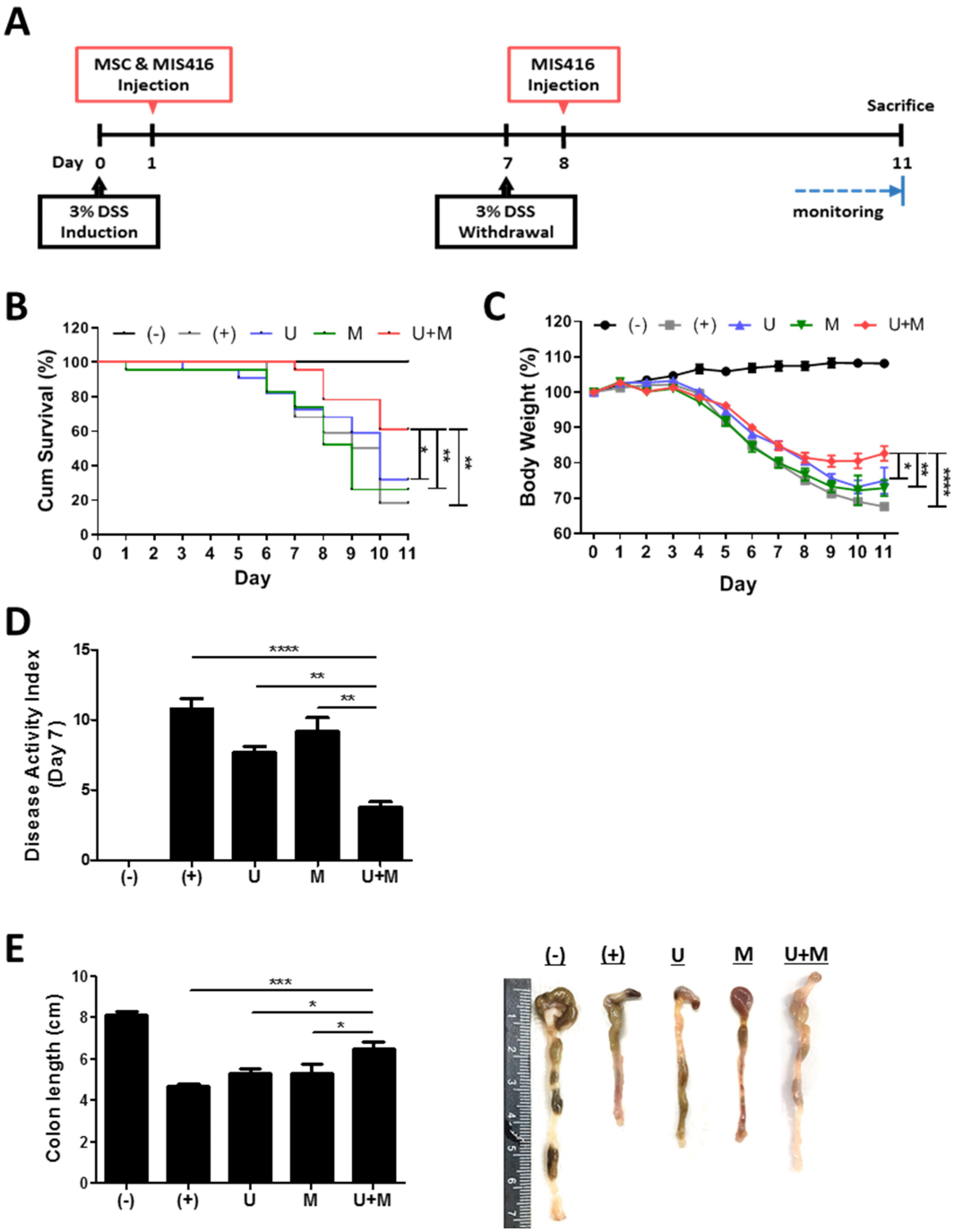
A
MSC & MIS416 Injection
MIS416 Injection
Sacrifice
Day 0 1 7 8 11
3% DSS Induction
3% DSS Withdrawal
monitoring
B
Cum Survival (%)
(-) (+) U M U+M
Day
C
Body Weight (%)
(-) (+) U M U+M
Day
D
Disease Activity Index (Day 7)
(-) (+) U M U+M
E
Colon length (cm)
(-) (+) U M U+M

Figure 18. Co-administration of MIS416 and hUCB-MSCs enhances the therapeutic effects of the cells against experimental colitis.

Mice were exposed to 3% DSS in their drinking water for 7 days and injected intraperitoneally hUCB-MSCs at day 1, and MIS416 at day 1 and 8 through retro-orbital route. (A) Scheme for the experimental design. (B) Survival rates of the mice were monitored. (C) Changes in body weights were measured daily. (D) DAI for colitis severity. (E) On day 11, colon length of mice was measured by gross examination. n=10-22 mice per group, three independent animal experiments were performed. (-): Negative control group, (+): DSS administered group, U: hUCB-MSCs treated group, M: MIS416 treated group, U+M: hUCB-MSCs and MIS416 co-treated group. *P<0.05, **P<0.01, ***P<0.001, ****P<0.0001. Results are shown as the mean ± SEM.

2.3.2 MIS416 improves the anti-inflammatory function and tissue regenerative capacity of hUCB-MSCs in the colon

I next examined H&E-stained colon samples to investigate the histopathological changes in the colons of DSS colitis mice on day 11. In the same context as previous results, colonic inflammation was more effectively resolved by co-treatment with MIS416 and hUCB-MSCs than each single treatment (Figure 19A) ((+) vs U+M $p<0.0001$; U vs U+M $p=0.0051$; M vs U+M $p=0.0103$). In addition, fibrosis-associated mucosal and submucosal collagen depositions were quantified by PSR staining. Treatment of hUCB-MSCs or MIS416 alone did not show significant changes, on the other hand, only co-treatment markedly decreased fibrosis and enhanced tissue regeneration (Figure 19B) ((+) vs U $p=0.2537$; (+) vs U+M $p=0.0011$; U vs U+M $p>0.9999$; M vs U+M $p=0.0254$). Levels of proinflammatory cytokines, such as TNF, IFN-γ, IL-6, IL-12, IL-17A and IL-23 were elevated in the serum of DSS-induced colitis mice. The levels of TNF were decreased in both hUCB-MSC- and co-treated mice serum, but significant change was not detected between two groups ((+) vs U $p=0.0234$; (+) vs U+M $p=0.0177$; U vs U+M $p>0.9999$; M vs U+M $p>0.9999$). With IFN-γ and IL-6, although significant change was not detected between hUCB-MSC treatment and co-treatment, mice administered both MIS416 and hUCB-MSCs showed a greater significant decrease compared to positive control group (for IFN-γ, (+) vs U $p=0.0401$; (+) vs U+M $p=0.0003$; U vs U+M $p=0.5635$; M vs U+M $p=0.0034$/ for IL-6, (+) vs U $p>0.9999$; (+) vs U+M $p=0.0245$; U vs U+M $p>0.9999$; M vs U+M $p=0.0082$). The levels of IL-12, IL-17A and IL-23 were also further decreased in the co-administration group compared with each single treatment groups, respectively (Figure 20A) (for IL-12, (+) vs U+M $p<0.0001$; U vs U+M $p=0.0066$; M vs U+M $p<0.0001$/ for IL-17A, (+) vs U+M $p=0.0119$; U vs U+M $p=0.0019$; M vs U+M $p=0.0483$/ for IL-23, (+)

vs U+M $p<0.0001$; U vs U+M $p=0.0192$; M vs U+M $p=0.0086$). I next measured MPO activity to evaluate the infiltration of immune cells, particularly neutrophils. DSS-induced increases in MPO activity were rescued by injection of hUCB-MSCs, and co-administration with MIS416 significantly improved this rescue (Figure 20B) ((+) vs U $p<0.0001$; (+) vs U+M $p<0.0001$; U vs U+M $p=0.0172$; M vs U+M $p=0.0011$). These findings demonstrate that MIS416 facilitates hUCB-MSCs to reduce secretion of proinflammatory cytokines and diminish tissue degeneration more effectively in the DSS-induced colitis model.

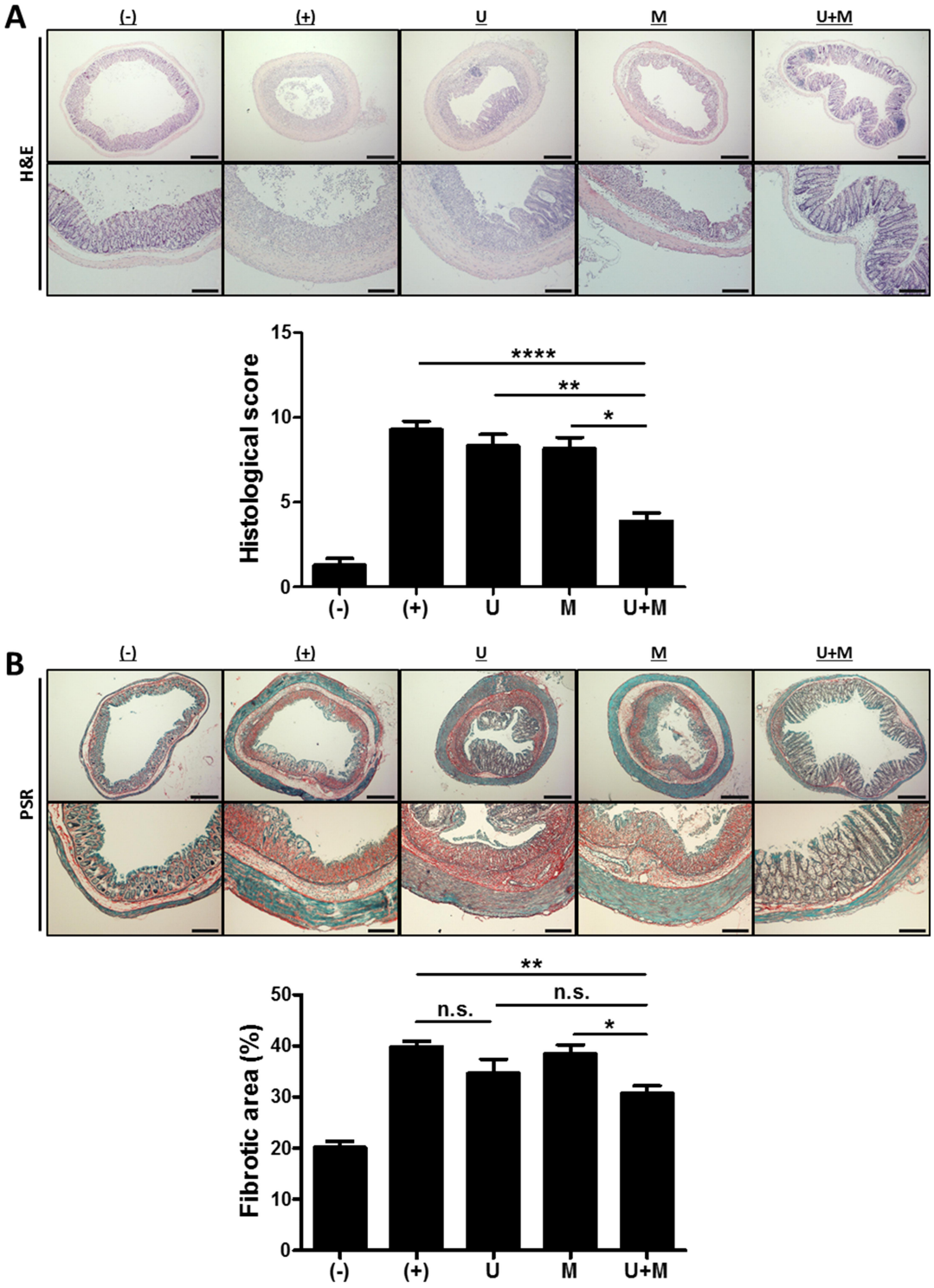
A
(-)
(+)
U
M
U+M
H&E
Histological score
15
10
5
0
****
**
*
(-)
(+)
U
M
U+M
B
(-)
(+)
U
M
U+M
PSR
Fibrotic area (%)
50
40
30
20
10
0
**
n.s.
n.s.
*
(-)
(+)
U
M
U+M

Figure 19. Co-administration of MIS416 and hUCB-MSCs attenuates inflammation and fibrosis in mice.

(A) Representative images of H&E-stained sections, bar = 500 μm (upper), 200 μm (lower). Histopathological scoring was performed based on the evaluation criteria. (B) Representative images of PSR-stained sections, bar = 500 μm (upper), 200 μm (lower). The fibrotic areas were quantified. n=10-22 mice per group, three independent animal experiments were performed. (-): Negative control group, (+): DSS administered group, U: hUCB-MSCs treated group, M: MIS416 treated group, U+M: hUCB-MSCs and MIS416 co-treated group. *P<0.05, **P<0.01, ****P<0.0001. Results are shown as the mean ± SEM.

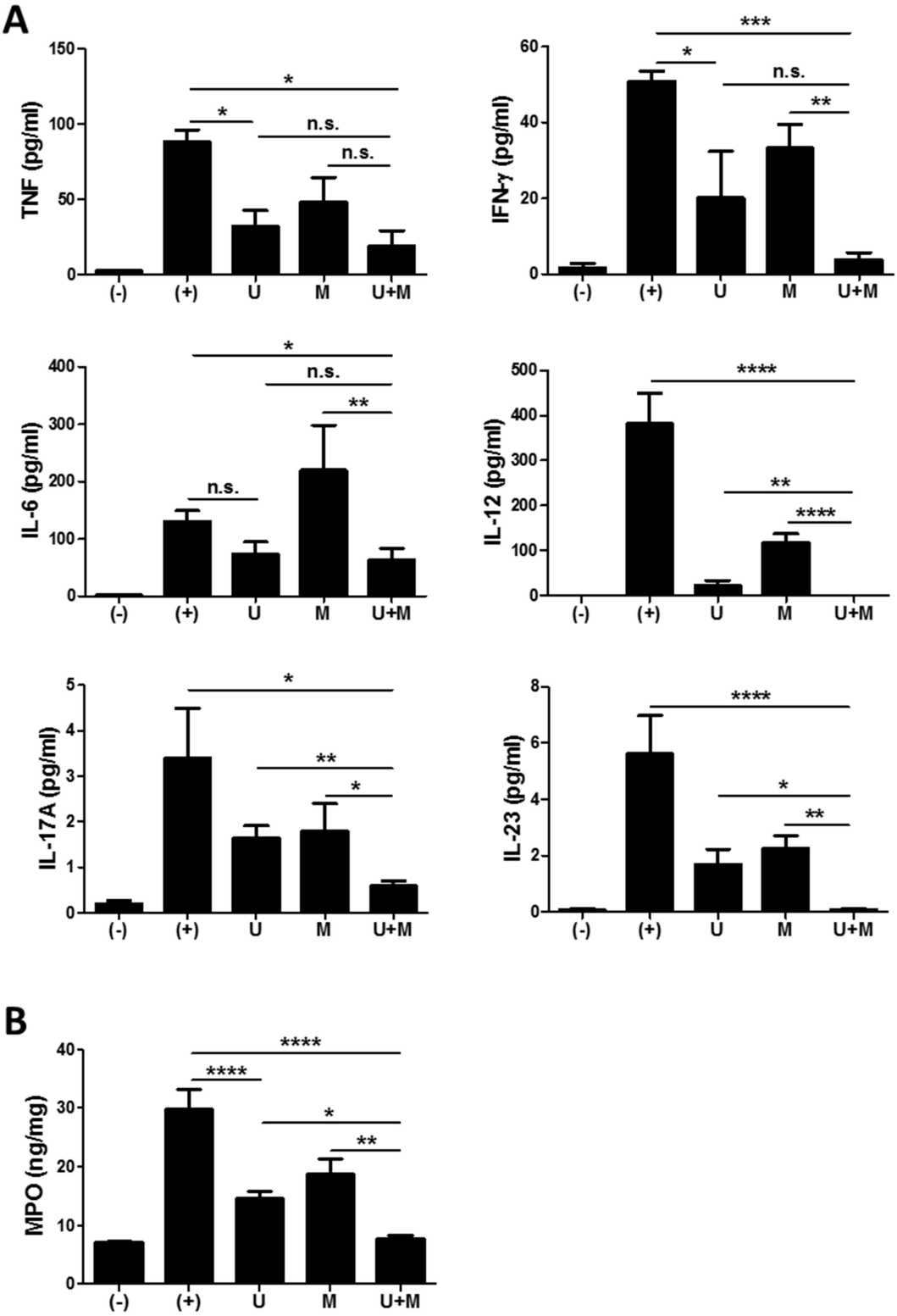
A
TNF (pg/ml)
IFN-γ (pg/ml)
IL-6 (pg/ml)
IL-12 (pg/ml)
IL-17A (pg/ml)
IL-23 (pg/ml)
(-)
(+)
U
M
U+M
n.s.
B
MPO (ng/mg)

Figure 20. Co-administration of MIS416 and hUCB-MSCs decreases secretion of pro-inflammatory cytokines.

(A) The levels of TNF, IFN-γ, IL-6, IL-12, IL-17A and IL-23 in the serum of mice were evaluated on day 11 by CBA. (B) MPO activity of colon was measured as an indicator for neutrophil infiltration. n=10-22 mice per group, three independent animal experiments were performed. (-): Negative control group, (+): DSS administered group, U: hUCB-MSCs treated group, M: MIS416 treated group, U+M: hUCB-MSCs and MIS416 co-treated group. *P<0.05, **P<0.01, ***P<0.001, ****P<0.0001. Results are shown as the mean ± SEM.

2.3.3 MIS416 does not directly affect the proliferation and immunomodulatory functions of hUCB-MSCs

I next investigated whether MIS416 priming could affect the therapeutic properties of hUCB-MSCs. hUCB-MSCs were treated with the indicated concentrations of MIS416. MIS416 treatment did not cause any significant change in the morphology of the cells (Figure 21A). To investigate alterations in the proliferative capacity, the BrdU assay was performed. MIS416 treatment did not change the proliferation of hUCB-MSCs (Figure 21B) ((-) vs MIS416 5 μg /ml p=0.9978; (-) vs MIS416 50 μg/ml p=0.9807). In the same context with the proliferation, MIS416 administration did not influence on the cell cycle profile of hUCB-MSCs (Figure 21C) ((-) vs MIS416 5 μg/ml p>0.9999; (-) vs MIS416 50 μg/ml p=0.9469).

To examine whether MIS416 could regulate the immunomodulatory ability of hUCB-MSCs, I evaluated the expression levels of COX-2, iNOS and IDO-1, which are enzymes related to immunomodulation by hMSCs (Chen et al., 2010; Meisel et al., 2004; Sato et al., 2007). Western blot analysis revealed that MIS416 treatment had no significant effect on the expressions of COX-2, iNOS, and IDO-1 (Figure 21D) (for COX-2, (-) vs MIS416 5 μg/ml p=0.9817; (-) vs MIS416 50 μg/ml p=0.7894/ for iNOS, (-) vs MIS416 5 μg/ml p=0.7031; (-) vs MIS416 50 μg/ml p=0.5383/ for IDO-1, (-) vs MIS416 5 μg/ml p=0.3366; (-) vs MIS416 50 μg/ml p=0.7858). Consistently, levels of PGE_2 and NO secretion into the culture medium were not altered by MIS416 priming (Figure 21E) (for PGE_2, (-) vs MIS416 50 μg/ml p=0.7294/ for NO, (-) vs MIS416 50 μg/ml p=0.7412). The level of IL-6 secretion also did not exhibit any significant change (Figure 21E) ((-) vs MIS416 50 μg/ml p=0.7679). In addition, key downstream adaptor molecules, RIP2 for NOD2 and MyD88 for TLR9 were not changed by MIS416 treatment. The phosphorylation levels of signaling

cascades, NF-κB and mitogen-activated protein kinase (MAPK) were also not altered (Figure 22A). Consistent with previous studies (Kim et al., 2013; Lee et al., 2016), the proliferation of hMNCs co-cultured with hUCB-MSCs was markedly inhibited. However, hUCB-MSCs primed with MIS416 did not show a significant difference from unstimulated cells (Figure 22B) ((+) vs U $p<0.0001$; (+) vs U+M $p<0.0001$; U vs U+M $p>0.9999$). I next evaluated the migratory ability of hUCB-MSCs primed with MIS416 *in vitro*. The number of migrated cells remained unchanged after MIS416 treatment (Figure 22C) (U vs U+M $p=0.9489$). Overall, these findings suggest that MIS416 augments the therapeutic abilities of hUCB-MSCs by indirect mechanism, but not by direct influence on the cells.

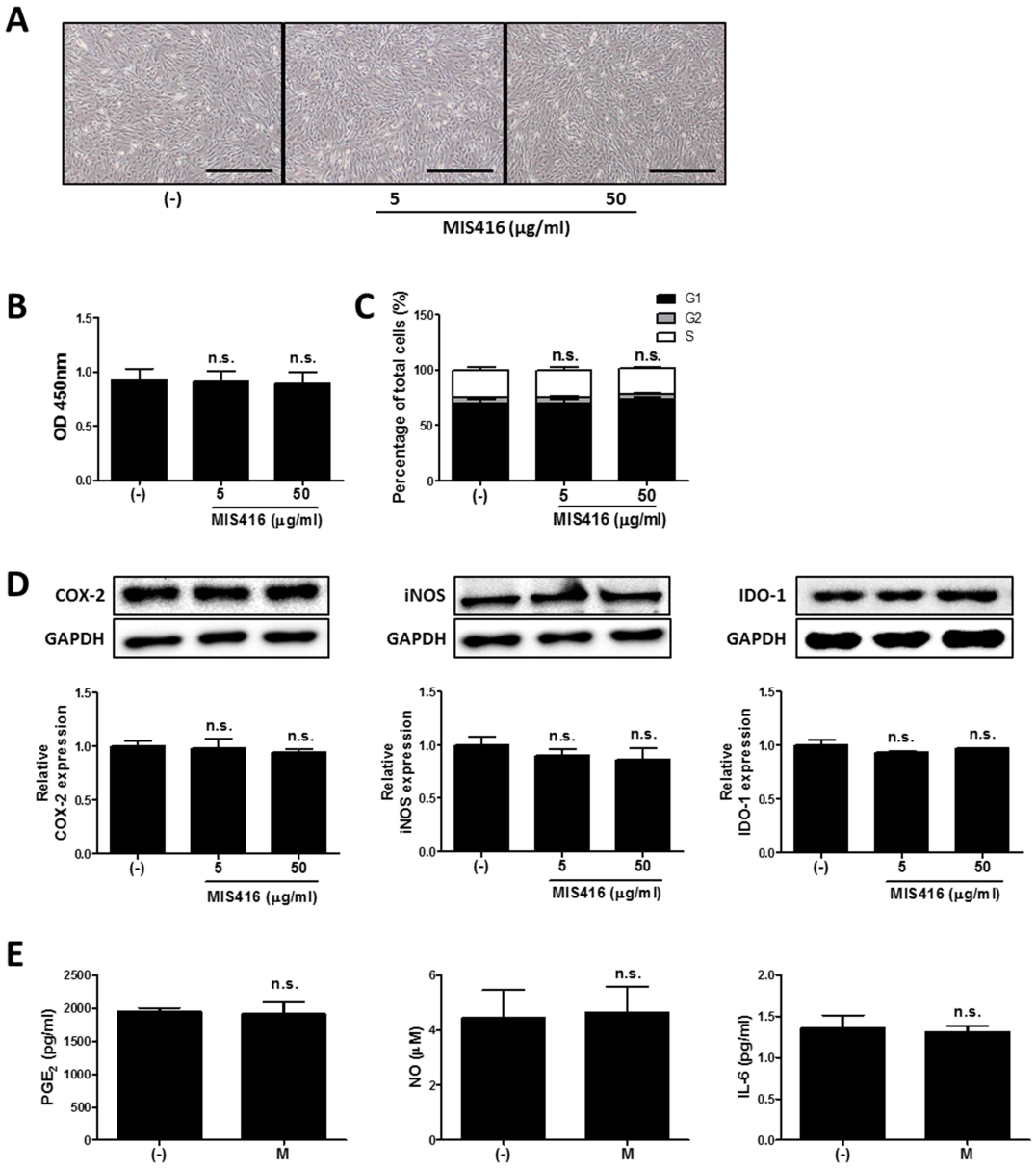
A
(-)
5
50
MIS416 (μg/ml)
B
OD 450nm
n.s.
n.s.
(-)
5
50
MIS416 (μg/ml)
C
Percentage of total cells (%)
G1
G2
S
n.s.
n.s.
(-)
5
50
MIS416 (μg/ml)
D
COX-2
GAPDH
iNOS
GAPDH
IDO-1
GAPDH
Relative COX-2 expression
Relative iNOS expression
Relative IDO-1 expression
n.s.
n.s.
(-)
5
50
MIS416 (μg/ml)
E
PGE2 (pg/ml)
NO (μM)
IL-6 (pg/ml)
n.s.
(-)
M

Figure 21. MIS416 does not have direct effect on the properties of hUCB-MSCs including immunomodulatory functions *in vitro*.

hUCB-MSCs were treated with indicated concentrations of MIS416 for 24 hours and further analyses were conducted. (A) Representative of bright-field microscopy images of hUCB-MSCs, bar = 500 μm. (B) Proliferation of hUCB-MSCs was determined by BrdU assay. (C) Cell cycle assay. (D) The relative expression levels of COX-2, iNOS and IDO-1 in hUCB-MSCs were analyzed by immunoblotting analysis. (E) Secretion levels of PGE_2, NO and IL-6 were measured by ELISA. Gel electrophoresis was conducted under the same experimental conditions, and images of blots were cropped. Experiments were performed in triplicate. (-): Negative control group, (+): ConA activated group, U: hUCB-MSCs, U+M: MIS416 treated hUCB-MSCs. Results are shown as the mean ± SEM.

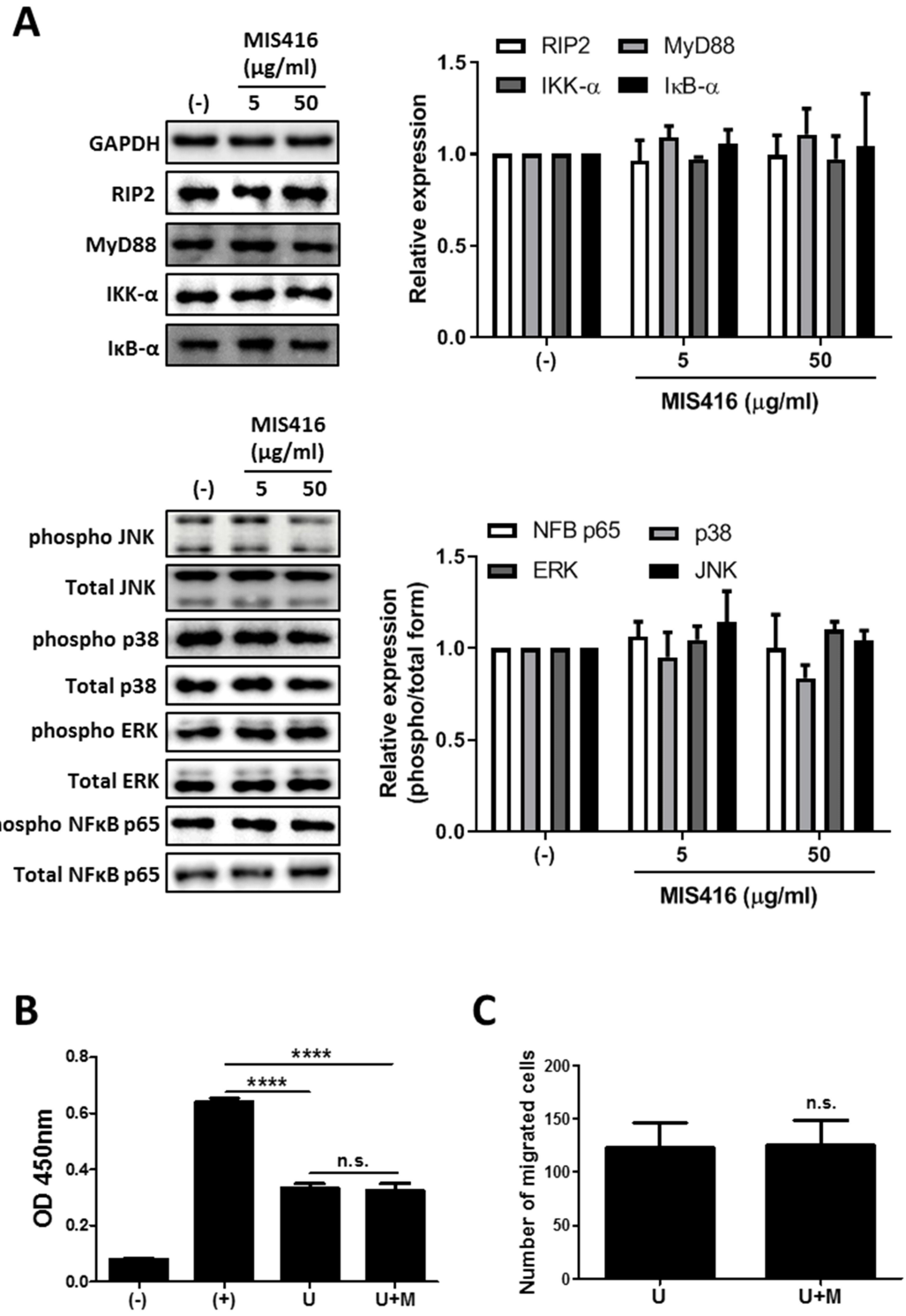
A
MIS416 (μg/ml)
(-)
5
50
GAPDH
RIP2
MyD88
IKK-α
IκB-α
RIP2
MyD88
IKK-α
IκB-α
Relative expression
1.5
1.0
0.5
0.0
(-)
5
50
MIS416 (μg/ml)
MIS416 (μg/ml)
(-)
5
50
phospho JNK
Total JNK
phospho p38
Total p38
phospho ERK
Total ERK
phospho NFκB p65
Total NFκB p65
NFB p65
p38
ERK
JNK
Relative expression (phospho/total form)
1.5
1.0
0.5
0.0
(-)
5
50
MIS416 (μg/ml)
B
OD 450nm
0.8
0.6
0.4
0.2
0.0
****
****
n.s.
(-)
(+)
U
U+M
C
Number of migrated cells
200
150
100
50
0
n.s.
U
U+M

Figure 22. MIS416 does not modify NOD2 and TLR9 related signaling pathways and immune cell suppression in hUCB-MSCs.

hUCB-MSCs were treated with indicated concentrations of MIS416 for 24 hours and further analyses were conducted. (A) (Upper) Expression levels of RIP2, MyD88, IKK-α and IκB-α/ (Lower) Phosphorylation levels of NF-κB p65, p38 MAPK, ERK and JNK were determined by western blot analysis and qunatified. (B) Mixed Lymphocytes Reaction (MLR) assay of hUCB-MSCs. (C) Transwell migration assay was performed and migrated cells were quantified. Gel electrophoresis was conducted under the same experimental conditions, and images of blots were cropped. Experiments were performed in triplicate. (-): Negative control group, (+): ConA activated group, U: hUCB-MSCs, U+M: MIS416 treated hUCB-MSCs. ****P<0.0001. Results are shown as the mean ± SEM.

2.3.4 Exposure to MIS416 causes increases in the number of immune cells via activation of innate immune cells such as $CD14^+$ macrophages

I observed that co-treatment with hUCB-MSCs and MIS416 was better than either treatment alone in DSS-induced colitis, although MIS416 had no direct effect on hUCB-MSCs. Thus, I hypothesized that MIS416 would indirectly upregulate the therapeutic effects of hUCB-MSCs by targeting NOD2 or TLR9 on other cells. I investigated changes in the spleen, the largest secondary lymphoid organ which contains various immune cells, after systemic administration of MIS416 on day 11. Significant enlargement of the spleen was identified in both mice treated with MIS416 alone and co-treated with hUCB-MSCs (Figure 23A). The length and weight of the spleen were considerably increased in MIS416-treated groups (Figure 23B and C) (for length, (+) vs M p=0.0109; (+) vs U+M p=0.0254/ for weight, (+) vs M p=0.0002; (+) vs U+M p=0.0049). To determine whether MIS416 elicited a detectable splenic response at an earlier time point, I investigated the spleen of mice a day after MIS416 treatment (on day 2). Although there was no significant change in the length (Figure 23D and E), the weight of the spleen was increased (Figure 23F) (for length, (+) vs M p>0.9999/ for weight, (+) vs M p=0.0458). I mimicked this phenomenon *in vitro* by treating hUCB-MNCs with MIS416 and observed that cell proliferation was dose-dependently elevated (Figure 24A and B) ((-) vs MIS416 0.5 μg/ml p=0.0419; (-) vs MIS416 5 μg/ml p=0.0062; (-) vs MIS416 50 μg/ml p=0.0041). Furthermore, isolated $CD4^+$ T cells did not proliferate in the presence of MIS416 (Figure 24C). By contrast, proliferation of $CD14^+$ cells was increased in response to MIS416 (Figure 24D) ((-) vs MIS416 0.5 μg/ml p<0.0001; (-) vs MIS416 5 μg/ml p<0.0001; (-) vs MIS416 50 μg/ml p=0.0035), and depletion of $CD14^+$ cells led to decreased proliferation of hUCB-MNCs (Figure 24E) (Naive vs $CD14^-$ cells, at MIS416 0.5 μg/ml p=0.0131; at MIS416 5 μg/ml p=0.0011; at 50 μg/ml

p=0.3409). These findings suggest that MIS416 systemically stimulates the immune environment and increases the number of activated immune cells through activation of innate immune cells, such as $CD14^+$ macrophages.

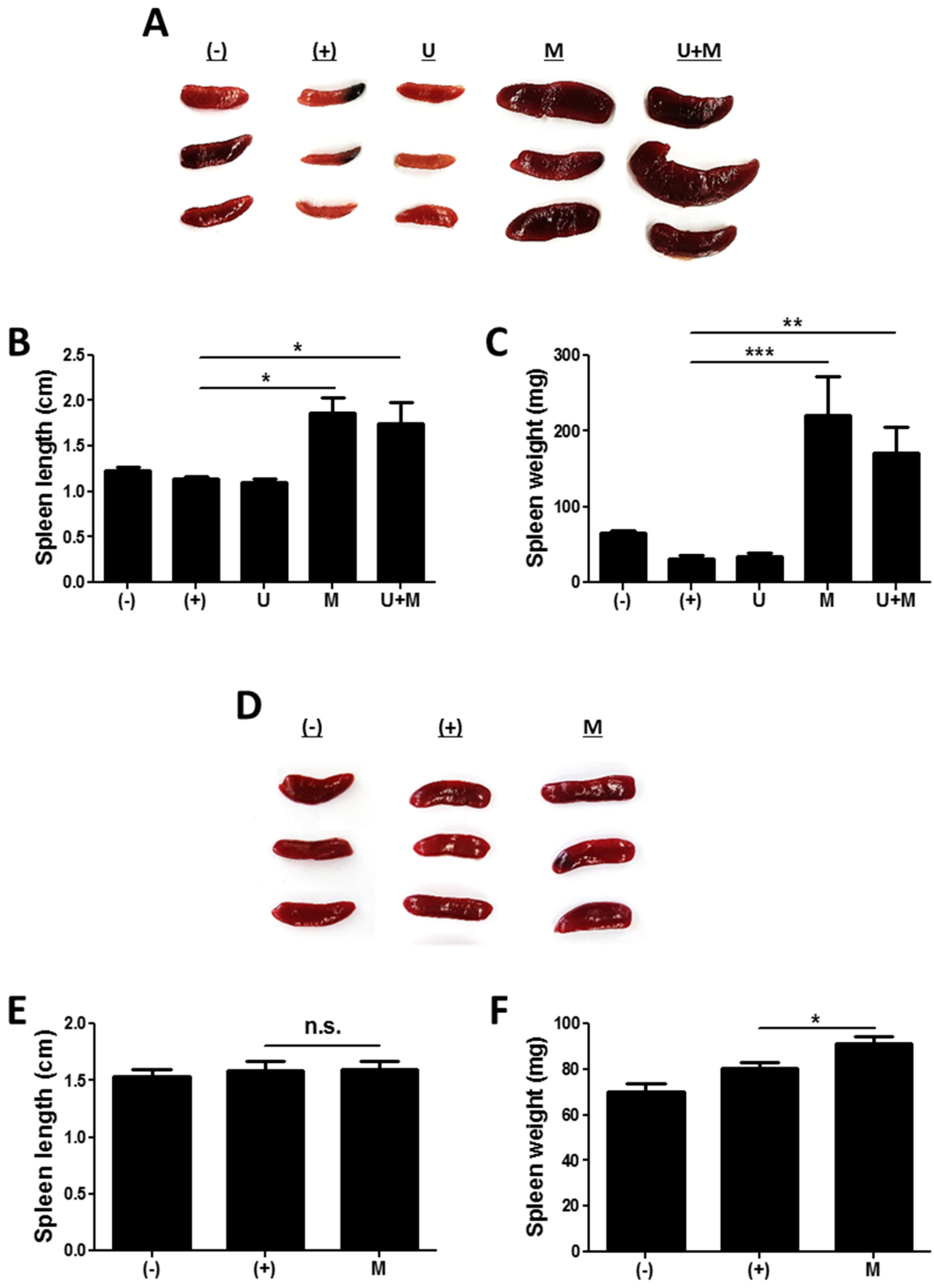
A
(-)
(+)
U
M
U+M
B
Spleen length (cm)
2.5
2.0
1.5
1.0
0.5
0.0
*
*
(-)
(+)
U
M
U+M
C
Spleen weight (mg)
300
200
100
0
**
***
(-)
(+)
U
M
U+M
D
(-)
(+)
M
E
Spleen length (cm)
2.0
1.5
1.0
0.5
0.0
n.s.
(-)
(+)
M
F
Spleen weight (mg)
100
80
60
40
20
0
*
(-)
(+)
M

Figure 23. Injection of MIS416 alters systemic immune milieu of DSS colitis mice.

(A-C) Each group of mice were sacrificed on day 11. (A) Gross examination of spleen. (B) Length and (C) weight of spleens were measured. (D-F) Each group of mice were sacrificed a day after MIS416 administration (day 2). (D) Gross examination of spleen. (E) Length and (F) weight of spleens were measured. n=5-9 mice per group, two independent animal experiments were performed. (-): Negative control group, (+): DSS administered group, U: hUCB-MSCs treated group, M: MIS416 treated group, U+M: hUCB-MSCs and MIS416 co-treated group. *P<0.05, **P<0.01, ***P<0.001. Results are shown as the mean ± SEM.

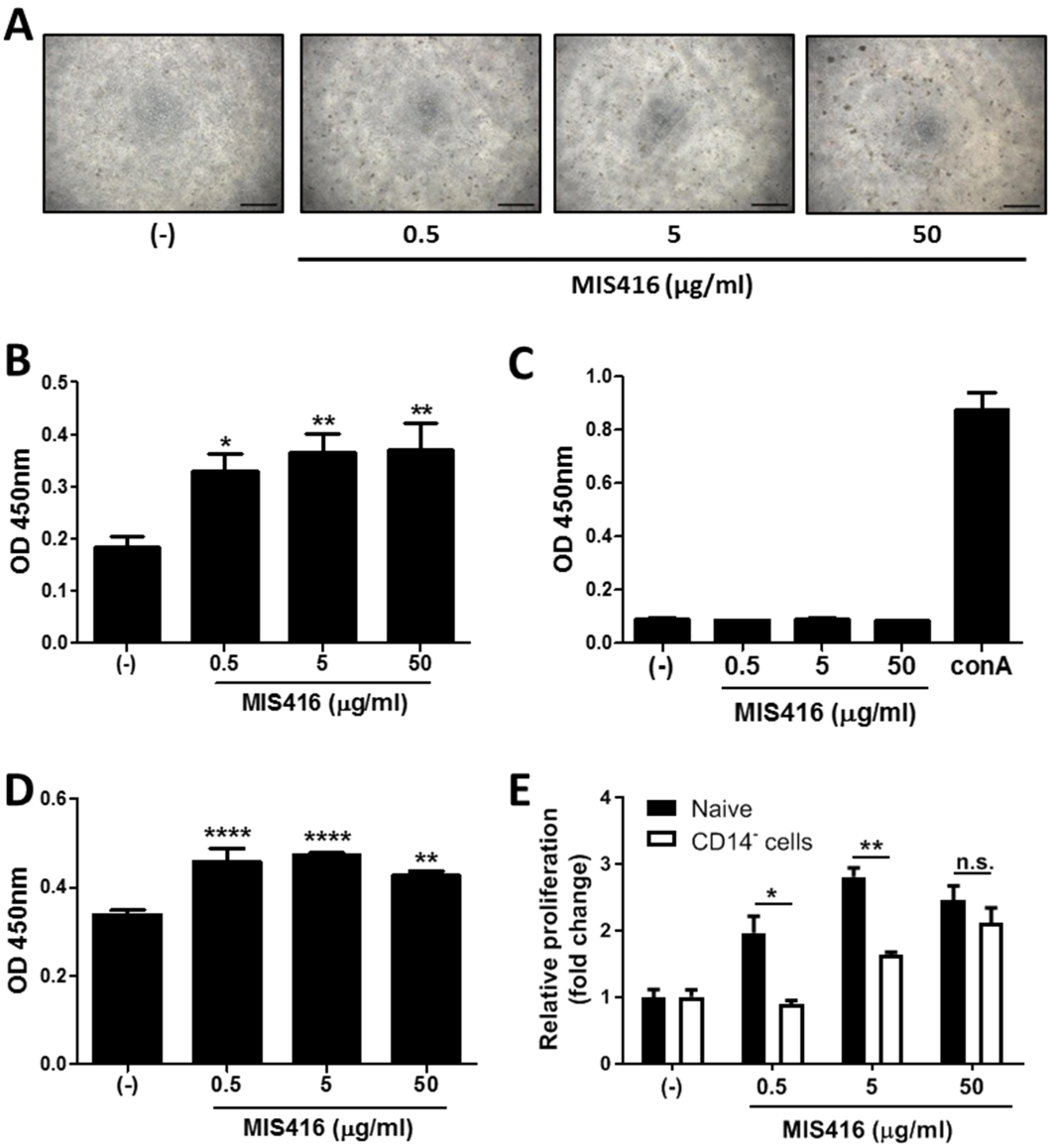
A
(-)
0.5
5
50
MIS416 (μg/ml)
B
OD 450nm
0.0
0.1
0.2
0.3
0.4
0.5
*
**
**
(-)
0.5
5
50
MIS416 (μg/ml)
C
OD 450nm
0.0
0.2
0.4
0.6
0.8
1.0
(-)
0.5
5
50
conA
MIS416 (μg/ml)
D
OD 450nm
0.0
0.2
0.4
0.6
****
****
**
(-)
0.5
5
50
MIS416 (μg/ml)
E
Relative proliferation (fold change)
Naive
CD14- cells
*
**
n.s.
0
1
2
3
4
(-)
0.5
5
50
MIS416 (μg/ml)

Figure 24. MIS416 promotes proliferation of hUCB-MNCs via innate immune cell such as $CD14^+$ cells.

hUCB-MNCs or -derived immune cells were treated with indicated concentrations of MIS416 for 3 days. (A) Representative of bright-field microscopy images of hUCB-MNCs, bar = 100 μm. (B) Proliferation of hUCB-MNCs was determined by BrdU assay. Proliferation of (C) isolated $CD4^+$ T cells and (D) isolated $CD14^+$ macrophage-like cells, and relative proliferations of (E) naive and $CD14^+$ cell-depleted hUCB-MNCs were measured by BrdU ELISA kit. *In vitro* experiments were performed in triplicate. *P<0.05, **P<0.01, ****P<0.0001. Results are shown as the mean ± SEM.

2.3.5 MIS416 and hUCB-MSCs collaborate in the modulation of intestinal immune balance by regulating polarization of T helper cell lineages

I further investigated whether MIS416 treatment altered the proportions of immune cells in hUCB-MNCs using flow cytometric analysis. Consistent with previous studies (Girvan et al., 2011; White et al., 2018), the proportion of proinflammatory effector cells, including $CD3^+$, $CD4^+$ and $CD8^+$ cells, were decreased whereas $CD19^+$ cells were increased (Figure 25) (for $CD3^+$ cells, (-) vs M $p=0.0023$/ for $CD4^+$ cells, (-) vs M $p<0.0001$/ for $CD8^+$ cells, (-) vs M $p=0.0021$/ for $CD19^+$ cells, (-) vs M $p=0.0142$). Next, I sought to explore the systemic effects of MIS416 on cell fate decisions in the T helper cell lineages. Treatment with MIS416 reduced the populations of $CD4^+IFN\text{-}\gamma^+$ Th1 cells (Figure 26A) and increased the proportions of $CD4^+IL\text{-}4^+$ Th2 cells in hUCB-MNCs (Figure 26B) (for $CD4^+IFN\text{-}\gamma^+$ Th1 cells, (-) vs M $p=0.0354$/ for $CD4^+IL\text{-}4^+$ Th2 cells, (-) vs M $p=0.0142$). The proportion of $CD4^+IL\text{-}17A^+$ cells was decreased in the presence of MIS416 (Figure 26C) ((-) vs M $p=0.0002$). In addition, I determined that treatment with MIS416 augmented the proportion of $CD4^+FoxP3^+$ Treg cells in hUCB-MNCs (Figure 26D) ((-) vs M $p<0.0001$). I also confirmed increased Treg cells *in vivo*, detecting higher numbers of $CD4^+CD25^+FoxP3^+$ Treg cells in the colons of MIS416-treated mice than DSS-induced mice on day 2 (Figure 27A and B) ((+) vs M $p=0.0050$). I next determined the level of IL-10, which can act as both an inducer and effector cytokine of regulatory T cells. On day 2, the expression level of IL-10 was altered by MIS416 injection (Figure 27C) ((+) vs M $p=0.0131$). By day 11, MIS416-treated mice showed slightly increased levels of IL-10, whereas robust serum IL-10 expression was identified in mice co-treated with MIS416 and hUCB-MSCs (Figure 27D) ((+) vs U+M $p<0.0001$; U vs U+M $p=0.0284$; M vs U+M $p=0.0069$). In the same context, the colonic infiltration of $Foxp3^+$ Treg cells was significantly increased in the colons of mice treated with MIS416 and

hUCB-MSCs than with either MIS416 or hUCB-MSCs alone (Figure 27 E and F) ((+) vs U+M p=0.0001; U vs U+M p=0.0313; M vs U+M p=0.0006). These findings indicate that MIS416 alters the immune cell composition by suppressing effector cells and promoting regulatory cells, which are remarkably augmented by co-administration of MIS416 and hUCB-MSCs.

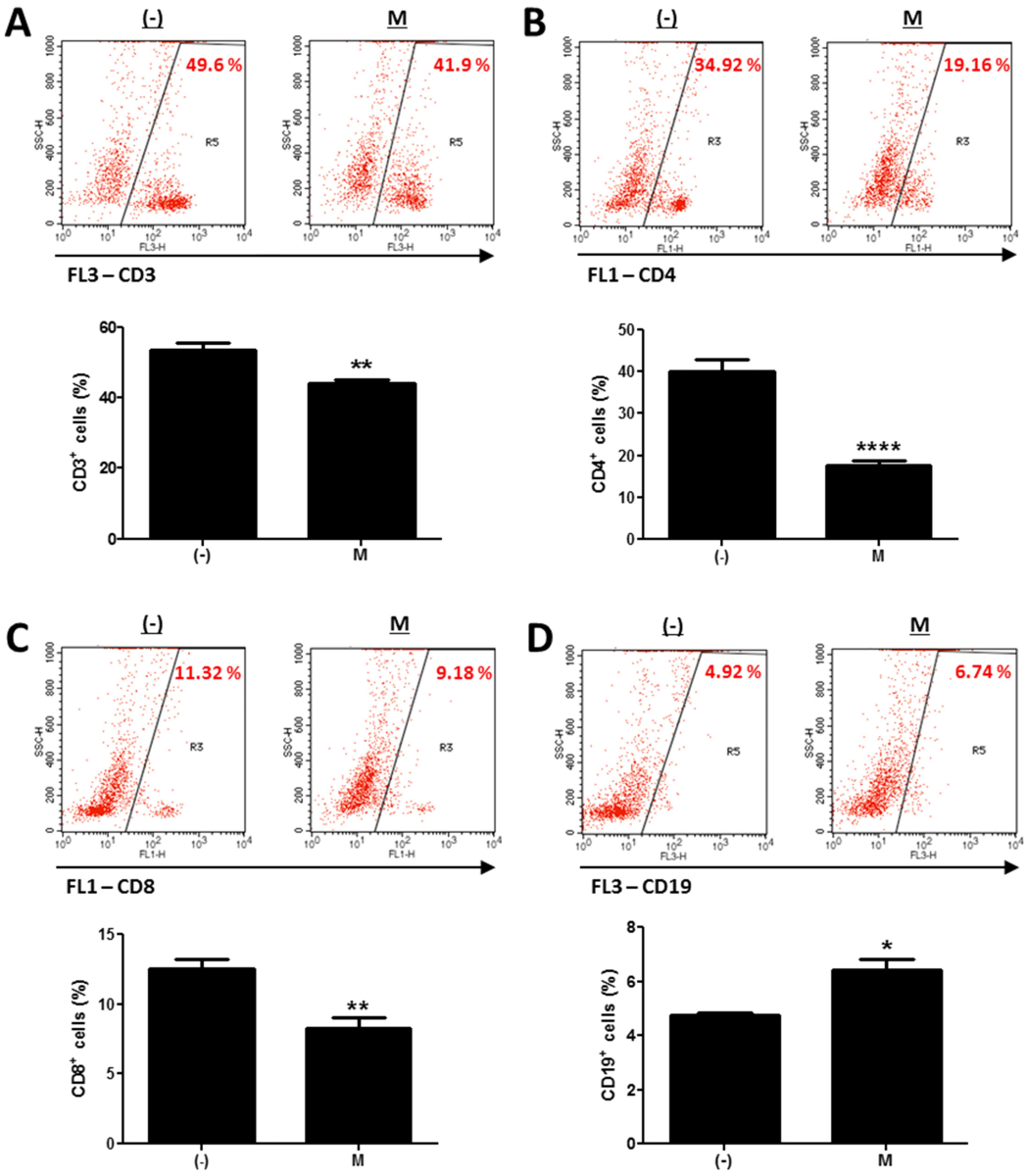

Figure 25. MIS416 alters the proportion of lineage-specific immune cells. hUCB-MNCs were treated with MIS416 (50 μg/ml) for 3 days, and (A) CD3, (B) CD4, (C) CD8 and (D) CD19 expressing cells were analyzed by flow cytometric analysis. (-): Negative control group, M: MIS416 treated group. *P<0.05, **P<0.01, ****P<0.0001. Results are presented as means ± SEM from three independent experiments.

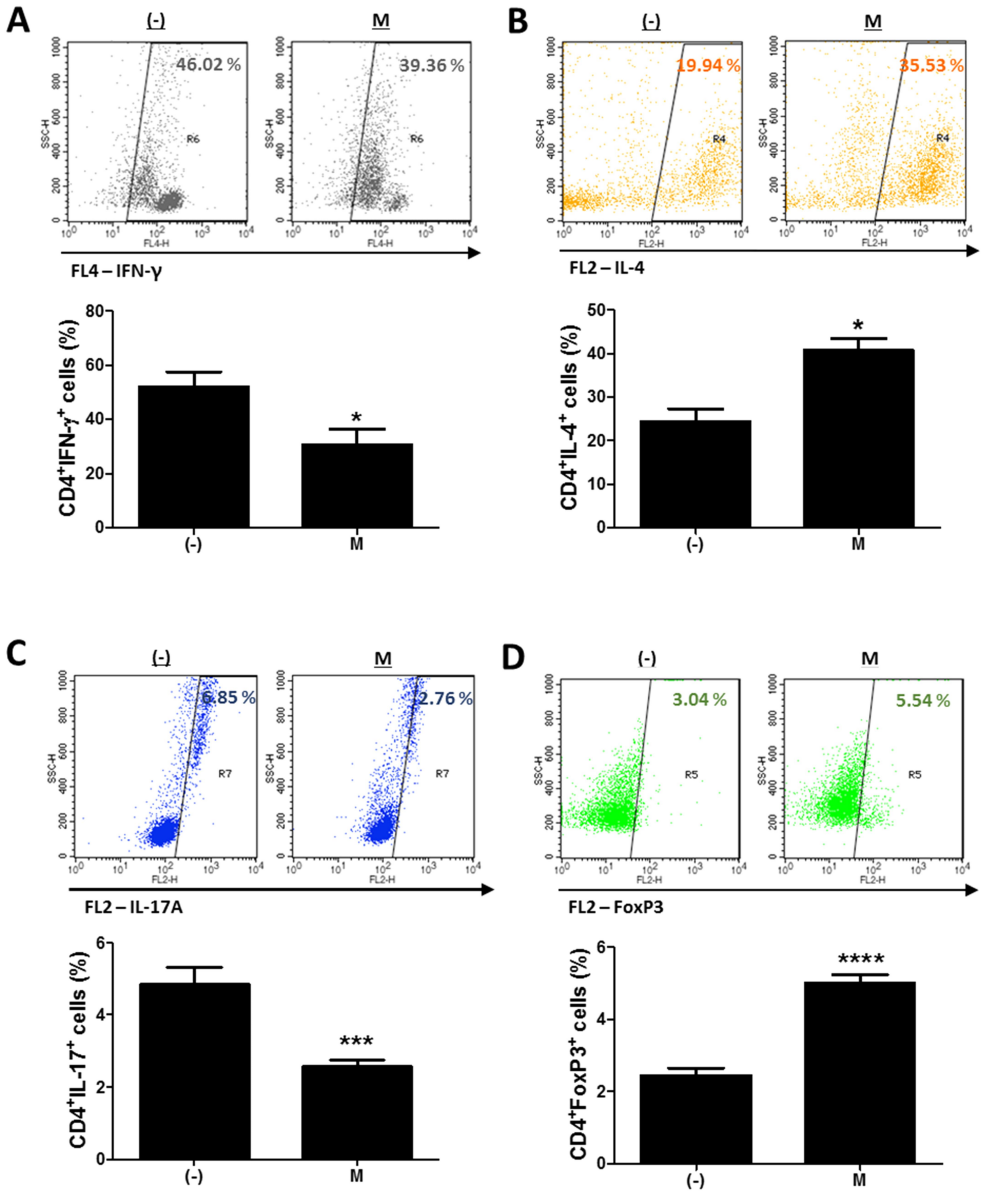

Figure 26. MIS416 alters immune cell profile in hUCB-MSCs.

hUCB-MNCs were cultured with MIS416 for 3 days and analysed for each population of T helper lineages by flow cytometric analysis. Populations of (A) $CD4^+IFN\text{-}\gamma^+$ cells for Th1, (B) $CD4^+IL\text{-}4^+$ cells for Th2, (C) $CD4^+IL\text{-}17A^+$ cells for Th17 and (D) $CD4^+FoxP3^+$ cells for Treg were determined. *In vitro* experiments were performed in triplicate. *P<0.05, ***P<0.001, ****P<0.0001. Results are shown as the mean ± SEM.

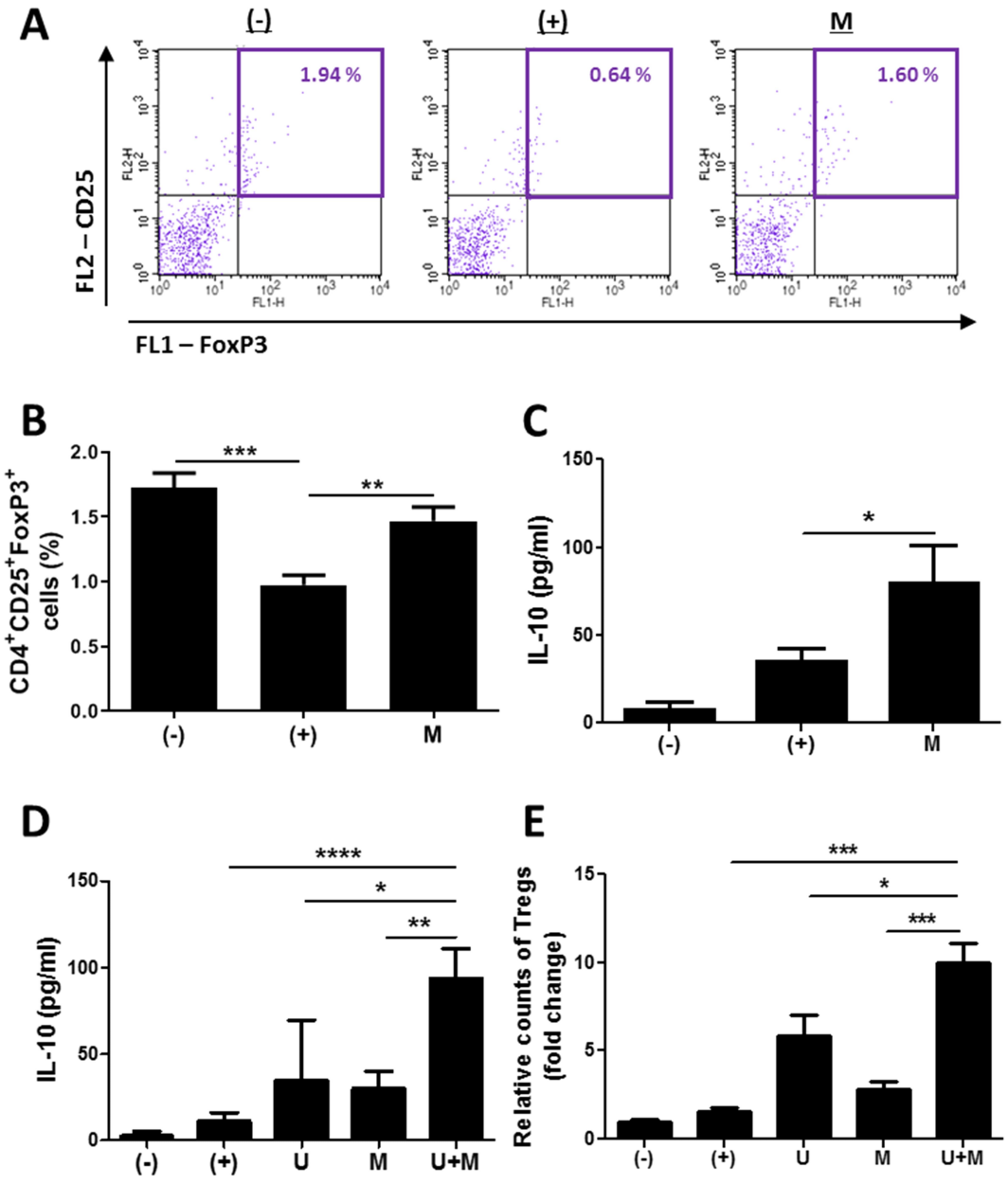
A
(-)
(+)
M
1.94 %
0.64 %
1.60 %
FL2 – CD25
FL1 – FoxP3
FL2-H
FL1-H
B
CD4+CD25+FoxP3+ cells (%)
***
**
(-)
(+)
M
C
IL-10 (pg/ml)
*
(-)
(+)
M
D
IL-10 (pg/ml)
****
*
**
(-)
(+)
U
M
U+M
E
Relative counts of Tregs (fold change)
***
*
***
(-)
(+)
U
M
U+M

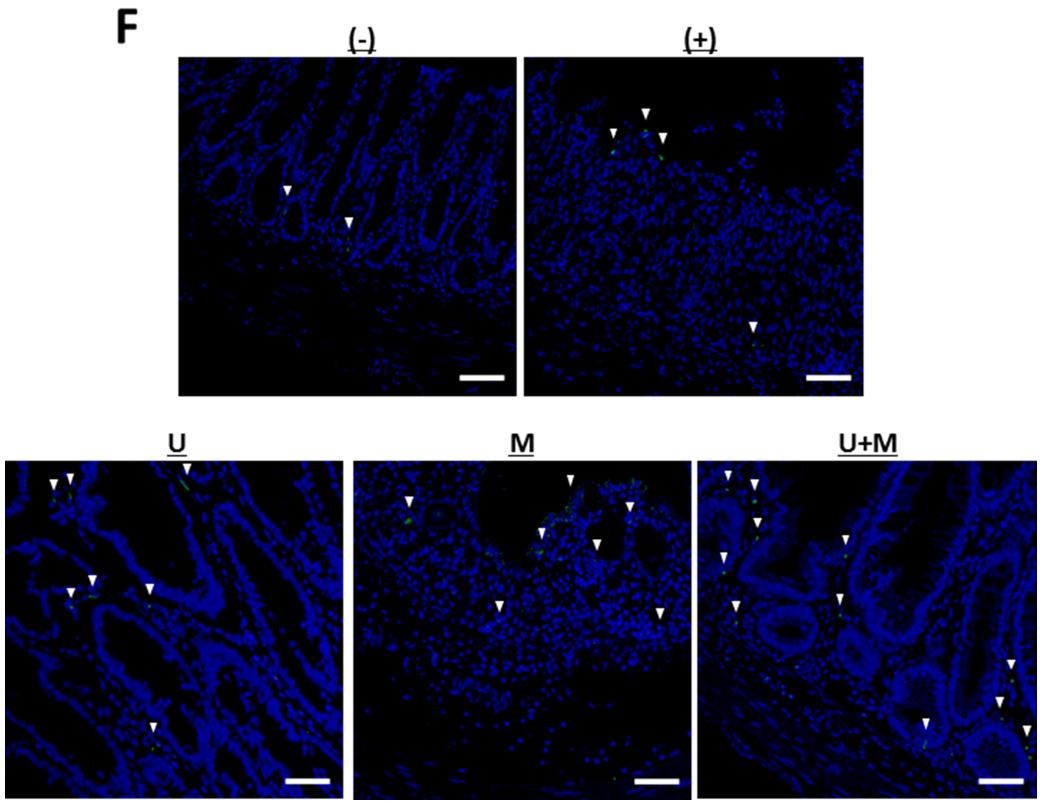

Figure 27. MIS416 and hUCB-MSCs cooperate in immune homeostasis by regulating polarization of T helper cells.

(A-C) Each group of mice were sacrificed a day after MIS416 administration (day 2). (A) Populations of $CD4^{+}CD25^{+}FoxP3^{+}$ cells in spleen were analysed by flow cytometric analysis and (B) quantification. (C) The levels of IL-10 in serum were detected by CBA analysis. (D-F) Each group of mice were sacrificed on day 11. (D) The levels of IL-10 in serum were measured by CBA. (E) Quantification of FoxP3-expressing cells in colon and (F) representative images, bar = 100 μm, and the ▼; $FoxP3^{+}$ cells. n=7-8 mice per group, two independent animal experiments were performed. (-): Negative control group, (+): DSS administered group, U: hUCB-MSCs treated group, M: MIS416 treated group, U+M: hUCB-MSCs and MIS416 co-treated group. *P<0.05, **P<0.01, ***P<0.001, ****P<0.0001. Results are shown as the mean ± SEM.

2.3.6 Alteration of the immune environment by MIS416 improves the immunosuppressive effect of hUCB-MSCs

The immune system in the peritoneal cavity dynamically interacts with both the lymphatic system and general circulation by exchange of the fluids and cells, and intraperitoneally infused hMSCs remain in peritoneal cavity whilst interacting with the peritoneal immune system (Bazhanov et al., 2016; Rojas-Cartagena et al., 2005). To address whether MIS416-mediated immune change affected immunomodulation of hUCB-MSCs, I analyzed the cytokine profiles in the serum of MIS416-treated mice on day 2. Although the level of TNF was not significantly elevated, it was observed that secretion of IFN-γ, IL-6 and IL-12 was markedly increased by MIS416 infusion on day 2 (Figure 28A) (for TNF, (+) vs M $p>0.9999$/ for IFN-γ, (+) vs M $p<0.0001$/ for IL-6, (+) vs M $p=0.0311$/ for IL-12, (+) vs M $p=0.0354$). Based on these results, MIS416-mediated immune cell stimulation altered secretory profile of cytokines in the serum of mice. These cytokines are reported to activate the immunomodulatory functions of MSCs (Djouad et al., 2007; Krampera et al., 2006; Marigo and Dazzi, 2011; Polchert et al., 2008; Sheng et al., 2008). To investigate whether these cytokines could promote therapeutic potential of hUCB-MSCs, the cells were cultured with IL-6, IL-12, and IFN-γ for 24 hours. Combination of these cytokines did not show any effects on the proliferation or viability of hUCB-MSCs (Figure 28B-D) (for CCK-8 assay, (-) vs stimulated $p=0.5121$/ for MTT assay, (-) vs stimulated $p=0.8722$). However, expression levels of COX-2 and IDO-1 were increased by treatment of cytokine cocktail; by contrast, iNOS expression was not changed (Figure 29A-C) (for COX-2, (-) vs stimulated $p=0.0099$/ for iNOS, (-) vs stimulated $p=0.7819$/ for IDO-1, (-) vs stimulated $p=0.0494$). Consistently, secretion of PGE_2 was increased, whereas the level of NO in the culture medium was not altered by cytokine cocktail (Figure 29D and E) (for PGE_2, (-) vs stimulated $p=0.0022$/ for NO,

(-) vs stimulated p=0.100). To define the inhibitory effects of stimulated hUCB-MSCs on immune cells, proliferation of hUCB-MNCs was analyzed. As a result, proliferation of hUCB-MNCs was shown to be decreased by hUCB-MSCs (Figure 2.7G) ((+) vs U p=0.0071). Importantly, the suppression was enhanced by treatment with a cytokine cocktail (Figure 29F) ((+) vs U stimulated p<0.0001; U vs U stimulated p=0.0020). Taken together, I have demonstrated that MIS416-mediated increases of secreted cytokines IL-6, IL-12, and IFN-γ enhance the immunosuppression of hUCB-MSCs.

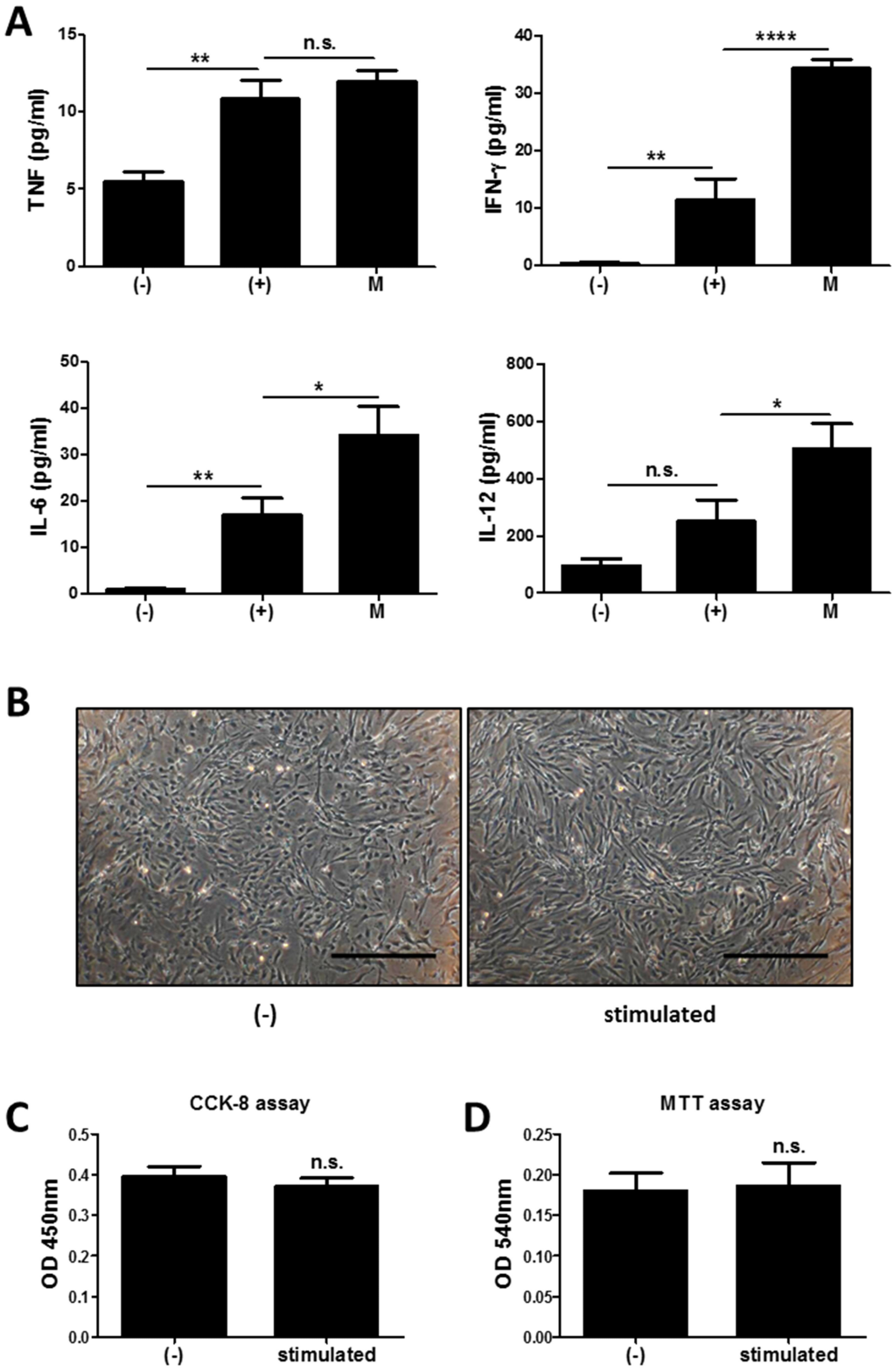
A
TNF (pg/ml)
IFN-γ (pg/ml)
IL-6 (pg/ml)
IL-12 (pg/ml)
(-)
(+)
M
n.s.
B
(-)
stimulated
C
CCK-8 assay
OD 450nm
D
MTT assay
OD 540nm

Figure 28. MIS416 mediates increase in cytokines.

(A) The levels of TNF, IFN-γ, IL-6 and IL-12 in serum of mice were evaluated a day after MIS416 administration (day 2) by CBA analysis. (B-D) Combination of cytokines, IL-6 (25 ng/ml), IL-12 (20 ng/ml) and IFN-γ (20 ng/ml), were used to treat hUCB-MSCs for 24 hours. (B) Representative of bright-field microscopy images of hUCB-MSCs, bar = 500 μm. Proliferation and cell viability of hUCB-MSCs were determined by (C) CCK-8 assay and (D) MTT assay. n=7-8 mice per group, two independent animal experiments were performed. *In vitro* experiments were performed in triplicate. (-): Negative control group, (+): Positive control group, M: MIS416 treated group, U: hUCB-MSCs, stimulated: cytokine cocktail-treated hUCB-MSCs. *P<0.05, **P<0.01, ****P<0.0001. Results are shown as the mean ± SEM.

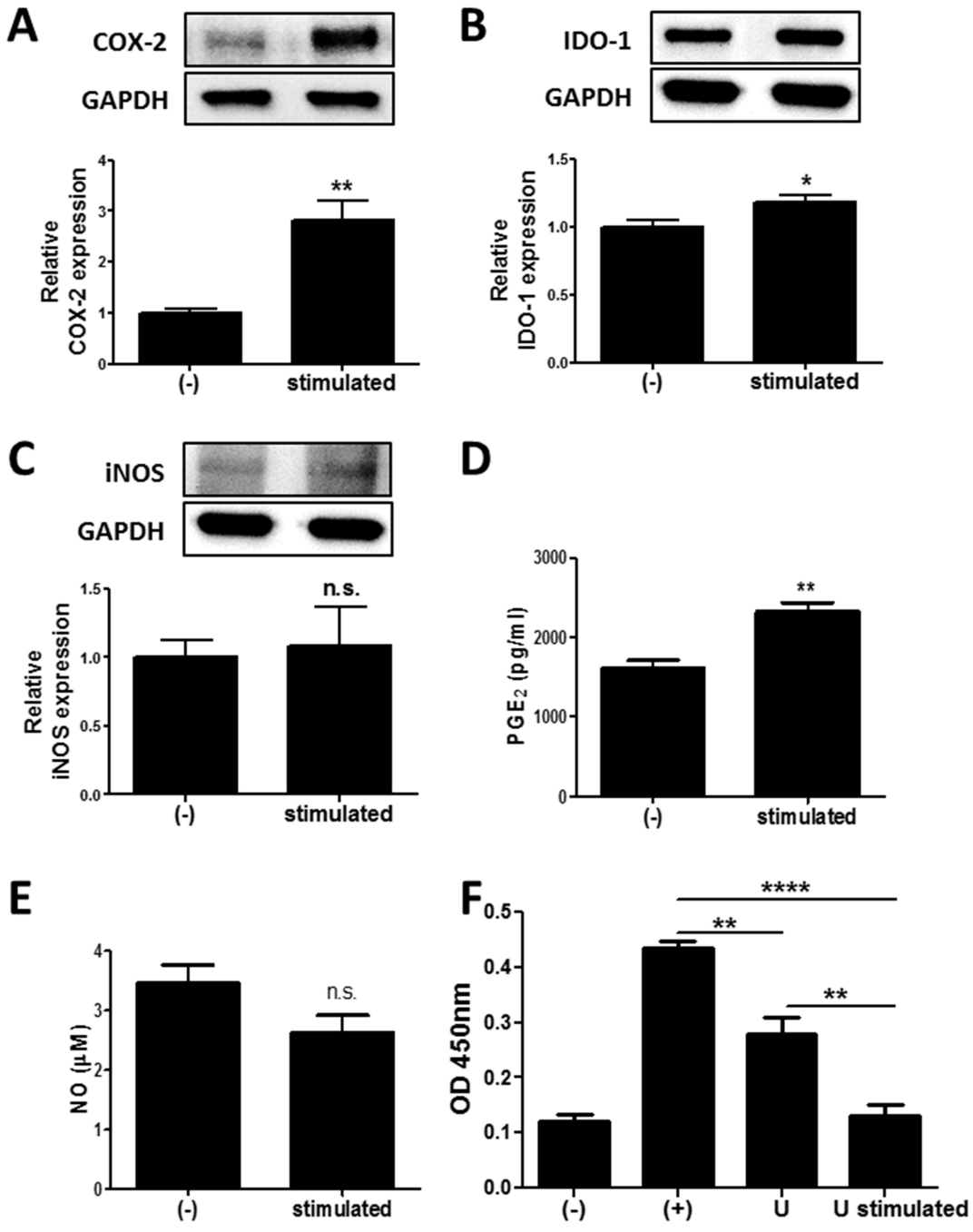
A
COX-2
GAPDH
Relative COX-2 expression
**
(-)
stimulated
B
IDO-1
GAPDH
Relative IDO-1 expression
*
(-)
stimulated
C
iNOS
GAPDH
Relative iNOS expression
n.s.
(-)
stimulated
D
PGE2 (pg/ml)
**
(-)
stimulated
E
NO (μM)
n.s.
(-)
stimulated
F
OD 450nm
****
**
**
(-)
(+)
U
U stimulated

Figure 29. MIS416-mediated increase of cytokines upregulate immune modulative function of hUCB-MSCs.

(A-C) The expression levels of (A) COX-2, (B) iNOS and (C) IDO-1 in hUCB-MSCs were analyzed using western blot analysis. (D-E) Secretion levels of (D) PGE_2 and (E) NO were measured by ELISA. (F) hUCB-MNCs were co-cultured with hUCB-MSCs stimulated with the cytokines directly and their proliferation was determined by BrdU ELISA assay. *In vitro* experiments were performed in triplicate. Gel electrophoresis was conducted under the same experimental conditions, and images of blots were cropped. (-): Negative control group, (+): Positive control group, M: MIS416 treated group, U: hUCB-MSCs, stimulated/U stimulated: cytokine cocktail-treated hUCB-MSCs. *P<0.05, **P<0.01, ****P<0.0001. Results are shown as the mean ± SEM.

2.3.7 MIS416-induced secretion of MCP-1 promotes the migration of hUCB-MSCs

The engraftment to inflamed sites is crucial for therapeutic potential of hUCB-MSCs (Mao et al., 2017; Qiu et al., 2017; Takeyama et al., 2017). Therefore, I investigated whether MIS416 administration could upregulate the mobilization of hUCB-MSCs into inflamed colon. DSS-colitis mice were intraperitoneally injected with GFP positive hUCB-MSCs in the presence or absence of MIS416. On day 2, GFP-positive hUCB-MSCs were detected in inflamed colon by immunohistochemistry (Figure 30A) ((-) vs U p=0.0083). hUCB-MSCs were more frequently detected in colon of co-treated mice than hUCB-MSCs treated mice (Figure 2.8A) (U vs U+M p=0.0001). However, hUCB-MSCs were not detected in the colon of the mice on day 11. The presence of hUCB-MSCs was also confirmed by flow cytometric analysis (Figure 30B) ((-) vs U p=0.0207; U vs U+M p=0.0083). I next investigated which molecules affected the migratory ability of hUCB-MSCs in the presence of MIS416. MCP-1 is known to stimulate migration of MSCs to the target region (Dwyer et al., 2007). To confirm whether MIS416 caused an increase of MCP-1, the sera of each group were collected on day 2. As a result, the mice injected with MIS416 showed markedly increased level of MCP-1 on day 2 (Figure 31A) ((+) vs M p<0.0001). The elevated level of MCP-1 were also detected in the serum of MIS416 treated group on day 11. Although MIS416-mediated MCP-1 secretion was decreased in the co-treated group, the level of MCP-1 remained significantly higher than in the mice treated with hUCB-MSCs alone (Figure 31B) ((+) vs M p<0.0001; (+) vs U+M p>0.9999; U vs U+M p=0.0047; M vs U+M p<0.0001). To address the potential for MCP-1 to stimulate the migratory capacity of hUCB-MSCs, an *in vitro* migration assay was conducted, where MCP-1-primed hUCB-MSCs showed increased migratory capacity (Figure 31C) (U vs U+MCP-1 p=0.0033). These data

suggest that MIS416-mediated enhanced MCP-1 secretion may be important for the improved migration of hUCB-MSCs to inflamed colon.

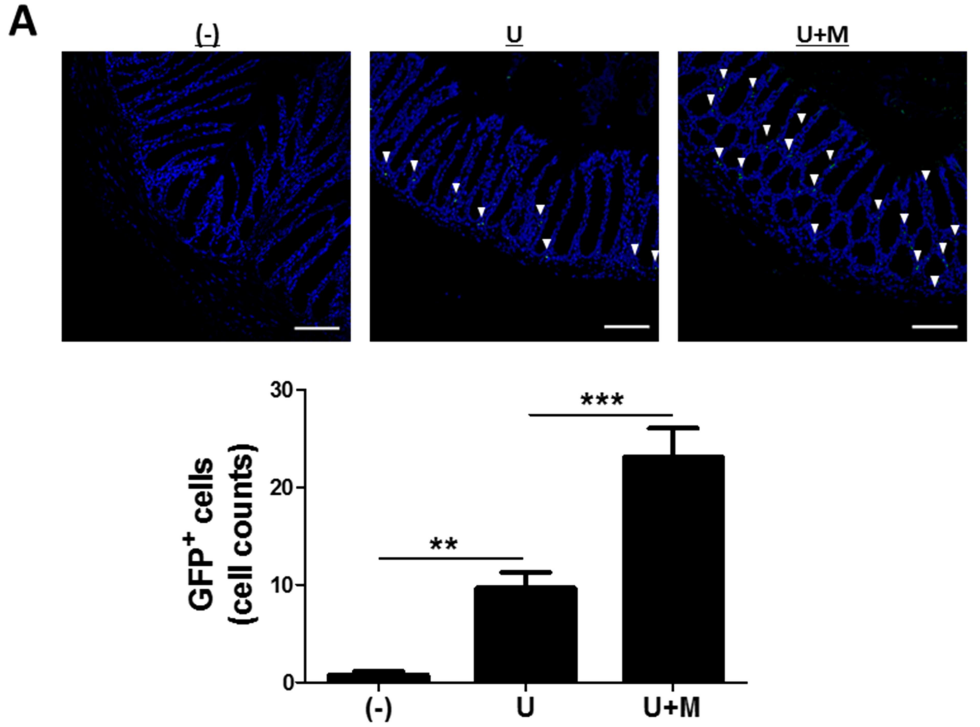
A
(-)
U
U+M
GFP+ cells (cell counts)
30
20
10
0
**
***
(-)
U
U+M

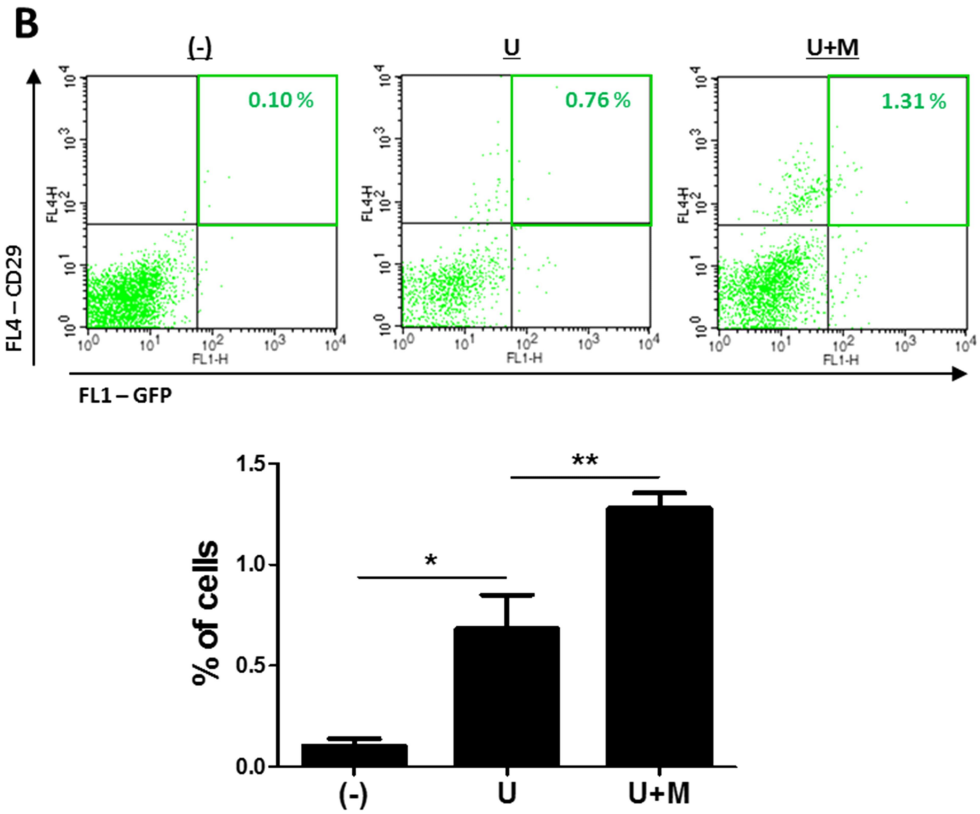
B
(-)
U
U+M
0.10 %
0.76 %
1.31 %
FL4 – CD29
FL1 – GFP
FL4-H
FL1-H
% of cells
1.5
1.0
0.5
0.0
*
**
(-)
U
U+M

Figure 30. MIS416 increases the colonic infiltration of hUCB-MSCs.
GFP expressing hUCB-MSCs were injected intraperitoneally into DSS-induced colitis mice. The colon sections were examined for green fluorescent cells using a confocal microscope and flow cytometer a day after injection (day 2). (A) Representative images of colons by confocal microscopy, bar = 100 μm, and the quantification. ▼; eGFP positive cells. (B) Populations of GFP positive hUCB-MSCs were analyzed by flow cytometric analysis. n=8-11 mice per group, three independent animal experiments were performed. (-): Negative control group, U: hUCB-MSCs treated group, U+M: hUCB-MSCs and MIS416 co-treated group. *P<0.05, **P<0.01, ***P<0.001. Results are shown as the mean ± SEM.

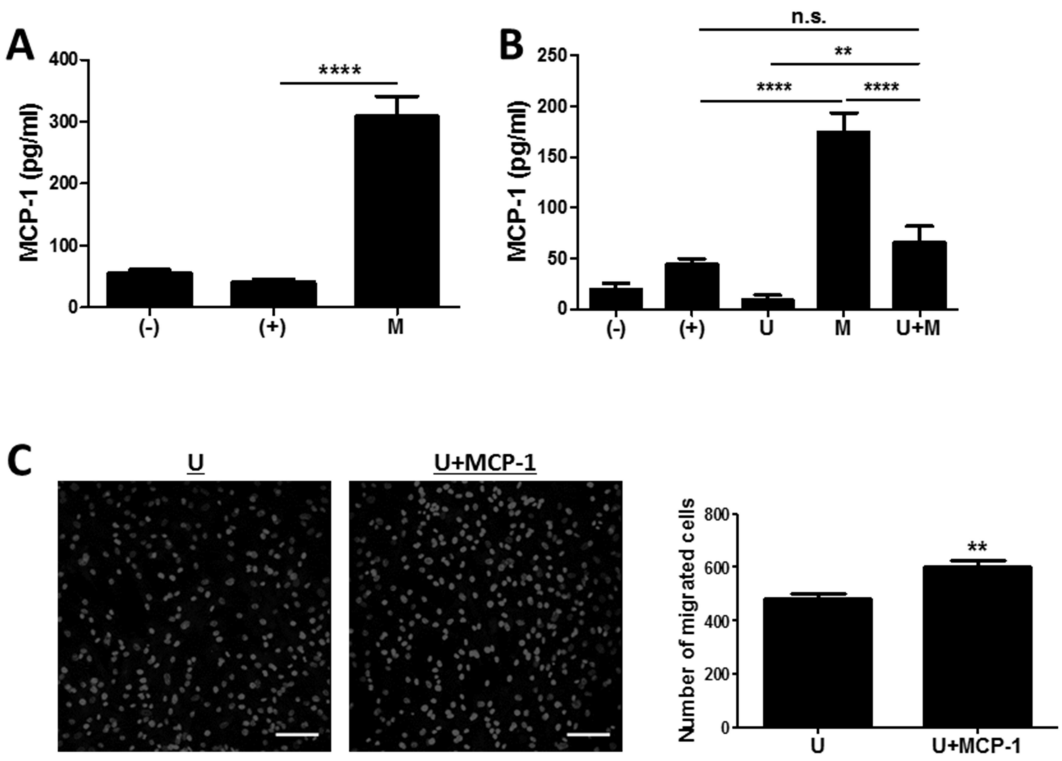

Figure 31. MIS416 increases the systemic level of MCP-1 which promotes migration of hUCB-MSCs toward the lesion.

(A-B) Levels of MCP-1 in serum were evaluated by CBA. Each group of mice were sacrificed on (A) day 2 and (B) day 11. (C) hUCB-MSCs were incubated with MCP-1 for 24 hours. *In vitro* migration ability of hUCB-MSCs was determined using Trans-well migration assay. Representative of confocal microscopy images of migrated hUCB-MSCs, bar = 100 μm, and the quantification. n=8-11 mice per group, three independent animal experiments were performed. *In vitro* experiments were performed in triplicate. (-): Negative control group, (+): DSS administered group, U: hUCB-MSCs treated group, M: MIS416 treated group, U+M: hUCB-MSCs and MIS416 co-treated group. **P<0.01, ****P<0.0001. Results are shown as the mean ± SEM.

2.4 DISCUSSION

In the present study, I have proposed co-administration of MIS416 and MSCs as an enhancement strategy for cell therapy. This strategy may be more convenient for clinical application compared to previous methods (Cho et al., 2012; Sheng et al., 2008; Wang et al., 2009) that require additional preparatory steps, such as cell priming or genetic manipulation. Also, this approach could reduce the associated risks with such additional manipulations, which include tumor formation and contamination of a heterogeneous population. Through gross, histologic and serologic assessments, I demonstrated that administration of MIS416 distinctly increased the therapeutic effects of hUCB-MSCs in experimental colitis model.

Of note, the improved therapeutic efficiency was not likely mediated by direct interaction between MIS416 and hUCB-MSCs, as I demonstrated that MIS416 treatment could not alter the proliferative, immune cell suppressive and migratory capacity of hUCB-MSCs. In fact, this finding is not unexpected, due to the physical properties of MIS416, which restrict cell uptake and subsequent sensing of MIS416 ligands to phagocytic innate immune cells such as plasmacytoid dendritic cells, myeloid dendritic cells and macrophages (Girvan et al., 2011; White et al., 2018). Consistent with hUCB-MSCs, $CD4^+$ T cells were not directly influenced by MIS416. And MIS416-mediated expansion of immune cells was observed only when innate immune cells were present (Girvan et al., 2011; White et al., 2018). In the present study, I also demonstrated that MIS416-mediated increased proliferation of hUCB-MNCs was relatively impeded when $CD14^+$ macrophage-like cells were depleted.

I showed that application of MIS416 microparticle contributed to increased numbers of immune cells in the spleen. In addition, I examined

the effects of MIS416 on the composition of splenic immune cells. Interestingly, proinflammatory cells, including Th1 cells and Th17 cells, were suppressed, and conversely, the proportions of Th2 cells, B cells and Treg cells were increased. Stimulation of innate immune receptors and their downstream signaling pathways modulated the balance between various immune cells (Klaschik et al., 2010; Uhlig et al., 2006). The innate ligands within MIS416 each have well documented immune regulatory activities. NOD2 ligand has been shown to regulate Th1 responses and simultaneously, play a crucial role in the induction of Th2 immune responses and Treg cells (Macho Fernandez et al., 2011; Pulendran et al., 2010; Watanabe et al., 2004). In addition to this, TLR9 stimulation drives maturation and proliferation of B cells (He et al., 2004; Leadbetter et al., 2002). Based on these results, it may be delineated that MIS416 favors the development of regulatory immune cell subsets, although MIS416 induced increases in the quantity of both pro- and anti-inflammatory immune cells. The DSS-induced increase of proinflammatory cytokines, except for IL-6 was attenuated in the serum of MIS416 treated mice on day 11. This suggests that alternative immune cells induced by MIS416 treatment are preferentially able to suppress inflammation and gradually restore immunologic balance in the body.

Imbalance between Th1/Th17 cells and Treg cells in intestine leads to dysregulated inflammation and consequently onset of IBDs (Hu et al., 2016; Li et al., 2007). MIS416 is known to promote myeloid cell activity and increase the innate IFN-γ to modify disease activity in an auto-immune model (White et al., 2014; White et al., 2018). In the same context with the previous article (Girvan et al., 2011), the level of IFN-γ was elevated in the serum of MIS416-infused mice. In agreement, Girvan et al. and White et al. have reported that MIS416-mediated innate IFN increased the secretion of TGF-β1 and IL-10, MIS416 also increased the expression of PDL-1 on

myeloid cells known to induce the formation of Treg cells (Girvan et al., 2011; White et al., 2018). Moreover, the type I IFN induced by TLR9 activation suppressed the differentiation of Th1 and Th17 cells, whereas the expansion of Treg cells was promoted (Guo et al., 2008; Katakura et al., 2005; Lee et al., 2006; Moschen et al., 2008). Consistent with these reports, I observed that treatment with MIS416 decreased the proportion of Th17 cells in hUCB-MNCs and the levels of IL-17A and IL-23 in the serum of mice. In addition, MIS416 increased the colonic infiltration of Treg cells by upregulating IL-10 secretion. Importantly, the levels of IL-17A and IL-23 were most reduced in hUCB-MSCs and MIS416 co-treated mice, and the infiltration of Treg cells and IL-10 secretion were notably augmented by co-treatment. These findings indicate that MIS416 and hUCB-MSCs cooperated to resolve an intestinal inflammation and attenuate the severity of experimental colitis by controlling the balance in Th1, Th17 and Treg cells.

In addition to IFN-γ, the level of IL-6 and IL-12 secretion in the serum of mice was also elevated by MIS416 treatment. Reciprocal interaction between peritoneal immune system and general immune system is accomplished by exchanging the fluids and cells. In addition, peritoneal immune response affects the functions of infused hMSCs, which attached to specific peritoneal sites such as mesentery and omentum (Bazhanov et al., 2016; Rojas-Cartagena et al., 2005). The combination of these cytokines enhanced the immunosuppressive ability of hUCB-MSCs by upregulating the COX-2- and IDO-1-related pathways (Ciccocioppo et al., 2015; Kim et al., 2013). Although MIS416 has been reported to increase the level of NO in the serum (White et al., 2018), MIS416-induced cytokines could not alter NO production by hUCB-MSCs. Based on these data, it seems that upregulation of these cytokines plays a role in increased immunomodulation and tissue regeneration by hUCB-MSCs *in vivo*.

MSCs suppress activated immune cells through direct cell-to-cell contact inhibition as well as environmental change mediated by soluble factors (Yagi et al., 2010; Yousefi et al., 2013). Thus, mobilization of MSCs into inflamed sites is important for suppression of activated immune cells placed in the adjacent lesion. Consistent with previous studies (Mao et al., 2017; Qiu et al., 2017; Takeyama et al., 2017), hUCB-MSCs migrated to inflamed colon of mice. More interestingly, the present study showed that systemic infusion of MIS416 immediately generated robust production of MCP-1. MCP-1 is known to induce the migration of various types of cells involved in the recovery process, including MSCs (Dwyer et al., 2007; Wang et al., 2002; Widera et al., 2004). MIS416-induced MCP-1 enhanced the migratory capacity of hUCB-MSCs *in vitro* and *in vivo*; thus, many more hUCB-MSCs mobilized to the inflamed colon in response to MCP-1.

Through these findings, I reveal that application of MIS416 ameliorated DSS-induced colitis compared to a single application of hUCB-MSCs and that this effect was mediated through 3 different ways. Firstly, by inhibition of Th1 and Th17 cells, polarization of Th2 cells and enhancement of Treg and B cells. In particular, MIS416 and hUCB-MSCs cooperated to shift the balance from Th1/Th17 to the Treg directed responses. Second, MIS416-mediated changes in immune milieu facilitated the increase of cytokines such as IFN-γ, IL-6 and IL-12. The hUCB-MSCs stimulated by these cytokines subsequently suppress proinflammatory cells in the inflamed colon. Lastly, MIS416-induced MCP-1 enhanced the migratory capacity of hUCB-MSCs, resulting in an increase in colonic infiltration. In summary, MIS416 enhances the therapeutic efficacy of hUCB-MSCs against experimental colitis by improving the immunosuppressive capacity of the cells and regulating immune homeostasis in the gut.

GENERAL DISCUSSION

Many researchers and clinicians are claiming the necessity of standardization to avoid controversial and disappointing results from clinical trials using adult stem cells. However, I would rather advocate 'Customized Clinical Strategy', which is specific to the implanted cells and disease-related environment to overcome the current obstacles to hMSC-based therapy and subsequently achieve improved therapeutic outcomes. As the part of those tailored tactics, the time point of cell administration can be adduced. It is reported that MSCs recognized and responded to the immune system of recipients (Ankrum et al., 2014) and would be influenced by resident immune cells after a cell transplantation (Giuliani et al., 2014). Hence, disease-specific immune status of a patient is very important for determining the time for delivery of hMSCs. Although the hypothesis needs to be further verified, immunomodulatory ability of MSCs is mediated by inflammatory milieu and the responsiveness of MSC could be maximized when infused at the peak of inflammation (Wei et al., 2013). Indeed, hMSC showed a more protective role in GVHD patients when injected 3 or 7 days after transplantation, compared to 15 minutes before transplantation (Shi et al., 2010). On the other hand, in this study, I presented that MIS416 caused an increase in secretion of several proinflammatory cytokines and it might be subsequently connected to the deterioration of the disease. Therefore, in the case of co-administration with immune stimulators to chronic relapsing disease such as IBDs, fine-tuning of the delivery time point is needed

The crosstalk between particular disease risk factors such as robust activation of effector immune cells and MSCs plays a pivotal role for identifying therapeutic mechanism of hMSCs and developing disease-specific stem cell therapy (Ravanidis et al., 2017). For example, Th2 cell, B cell and mast cell play a pivotal role in the pathogenesis of atopic dermatitis as

key effector cells in hypersensitivity and allergic reactions (Kawakami et al., 2009). Among the secretory molecules, histamine is reported to activate BM-MSC, upregulating the secretion level of IL-6 (Nemeth et al., 2012). Pre-exposure to these molecules are expected to boost the therapeutic function of hMSC when the cells encounter the molecules again *in vivo*. Therefore, it would be proposed priming with substances of the effector cells, instead of typical proinflammatory cytokine including IFN-γ and TNF-α, as an enhancement strategy for MSC-based therapy aimed at reducing allergic responses and chronic inflammation in AD. This approach may be applied to other diseases by analyzing the key effector molecules in the disease pathogenesis and expected to provide customized MSCs suited to treat the target diseases.

To date, MSCs have been utilized in preclinical studies and clinical trials for many years. However, several results of preclinical studies and clinical applications using these cells have been controversial. This discrepancy could be caused by an incomplete verification by using inadequate or insufficient disease models. In line with disease-specific preconditioning, the better understanding of the target disease is needed. Researchers have developed animal models by mimicking particular pathogenesis of the diseases or simply reproducing the symptoms. In case of tumors, even with the same diagnosis, the property of individual tumors are totally different depending on the lesion, the origin of the cells and ratio of mutations (Johnson and Fleet, 2013). Thus, the animal through single chemical injection or genetic modification could not completely represent the specific disease and fully reflect the pathophysiology. To overcome this limitation, researchers achieved replicable results from various model supporting diverse disease mechanism. Nevertheless, species barriers should be still considered. In addition, with growing demands, animal experimentation have been gradually reduced and replaced. Recently, 3D

organoids have emerged as an alternative disease model for typical 2D cell culture and animal experiments. The *in vitro* 3D culture system facilitate a better understanding of organogenesis and stem cell behavior *ex vivo*. Furthermore, because the organoid could be generated by using adult stem cells of patients with a genetic disease, the culture system has an advantage in the investigation on a pathogenesis or drug screening (Huch and Koo, 2015). It is reported that various organoids, including brain and intestine, has been established (Clevers, 2016) and the development is expanding on the other organs.

Another strongly suggested problem is the individual difference in MSCs based on the variable backgrounds from donor to donor (Siegel et al., 2013). To overcome the limitation, several improvement methods have been employed. Among the studies, Kang et al. revealed that hUCB-MSCs have donor-dependent individual differences and hypoxic preconditioning, a promising tool for hMSC targeting cardiovascular diseases, was applied to improve the therapeutic function of those cells to ischemic diseases (Kang et al., 2018). As a result, hUCB-MSCs isolated from different donors do not show the same response to hypoxic conditioning. Based on genome-wide gene expression analysis, it illustrated that hypoxic-preconditioned hUCB-MSC possessed distinctive expression patterns of specific genes and the expression pattern represents the pro-angiogenic property of hUCB-MSCs, suggesting general indicators to guarantee successful stem cell therapy. Accordingly, the development of disease-specific screening criteria and selection based on the criteria are still needed for actual implantation of hMSC, even the enhancement methods would be applied. Furthermore, strategies for improvement of the consistency and efficacy of MSCs have to be qualified whether the method is really effective for the specific disease and cells.

In the present study, I proposed two different complementary

methods for improving the therapeutic efficacy of hMSCs. Each method targets different steps in cell preparation, hence these findings might contribute to establishing comprehensive enhancement strategies with the other developed methods. For example, hMSCs cultured under non-contact status are inserted to biocompatible scaffold and the complex implanted to the damaged joint with TNF-α inhibitor to treat degenerative arthritis. In addition, biomedical technologies at the cutting edge such as a gene therapy or monoclonal antibody medicines are considered for combinatorial treatment with hMSCs. Gene therapy means the delivery of targeted genes into cells of patients with genetic defects to cure the defect-mediated disorders (Kaji and Leiden, 2001). Since the first attempt to transfer human DNA in 1990, numerous clinical trials have been conducted (Ginn et al., 2013). Recently, advanced technology using clustered regularly interspaced short palindromic repeat (CRISPR)/Cas9 RNA-based nucleases facilitate more detailed genetic editing at desired sites (Hsu et al., 2014). MSCs can support the therapeutic process using CRISPR/cas9 by regenerating damaged tissues. In addition, with this technology, hMSCs could be genetically engineered to suppress the expression of MHC-I complex, which is known for immunogen of the cells (Soland et al., 2010). To treat cancers, Immunotherapy with chimeric antigen receptor (CAR) T cells, which involves genetic modification of autologous T cells, were merged (Androulla and Lefkothea, 2018). MSCs are also used to control adverse effects of CAR T cell immunotherapy including suppression of unwanted immune cells, with its own immunoregulatory function. Moreover, Development of monoclonal antibody reagents enables more deliberate and definite disease treatments. Given these therapeutic potentials, several monoclonal antibodies were approved by US FDA as commercial drugs (Cai, 2016). Dupilumab developed as Th2 immune-related disorders were reported to be able to treat atopic dermatitis and asthma by inhibiting IL-4 receptors (Beck et al., 2014; Wenzel et al., 2013). However, hMSCs

are known to suppress excessive activation of mast cell and B cells as well as Th2 cells (Franquesa et al., 2015; Kim et al., 2015). Accordingly, it could be inferred that hMSCs cooperate with dupilumab to suppress IL-4 mediated inflammatory responses and augment the therapeutic efficacy by suppressing another type of immune cells or regenerating tissue damages.

In the present study, I demonstrated that cell-to-cell contact between the cells induced impairment in the immunomodulatory ability of hMSCs and its conditioned medium. Therefore, full confluency of hMSC in the preparation step has to be prevented to avoid the loss of therapeutic functions. In addition, activation of EP2 receptor or inhibition of GJIC might be applied to cell culture method to achieve improved yield and immunoregulatory function of hMSCs (Figure 32). In the second part of this study, I revealed that MIS416 induced a systemic change in immune circumstance to suppress the Th1/17 type immune response and recruit counterpart proportion of immune cells such as B, Th2 and Treg cells. Infused hUCB-MSCs responded to the immediate change in cytokine milieu mediated by MIS416 and immunoregulatory ability of hUCB-MSCs was improved. Furthermore, I showed that increased *in vivo* level of MCP-1 played a crucial role in engraftment of transplanted cells. Through these mechanisms, MIS416 improves the therapeutic efficacy of hUCB-MSCs against experimental colitis (Figure 33). Accordingly, I anticipate that these findings could bring the expansion of knowledge about the mechanisms of hMSCs-based therapy and provide unique enhancement strategies in the clinical field.

In conclusion, despite of its known limitations, hMSCs still hold a considerable promise as an alternative therapeutic reagent for various incurable diseases due to their unique biomedical potential. Therefore, further researches on the disease-specific status and conditions are needed and hMSC-based therapy has to be modified suitable for each targeted disease.

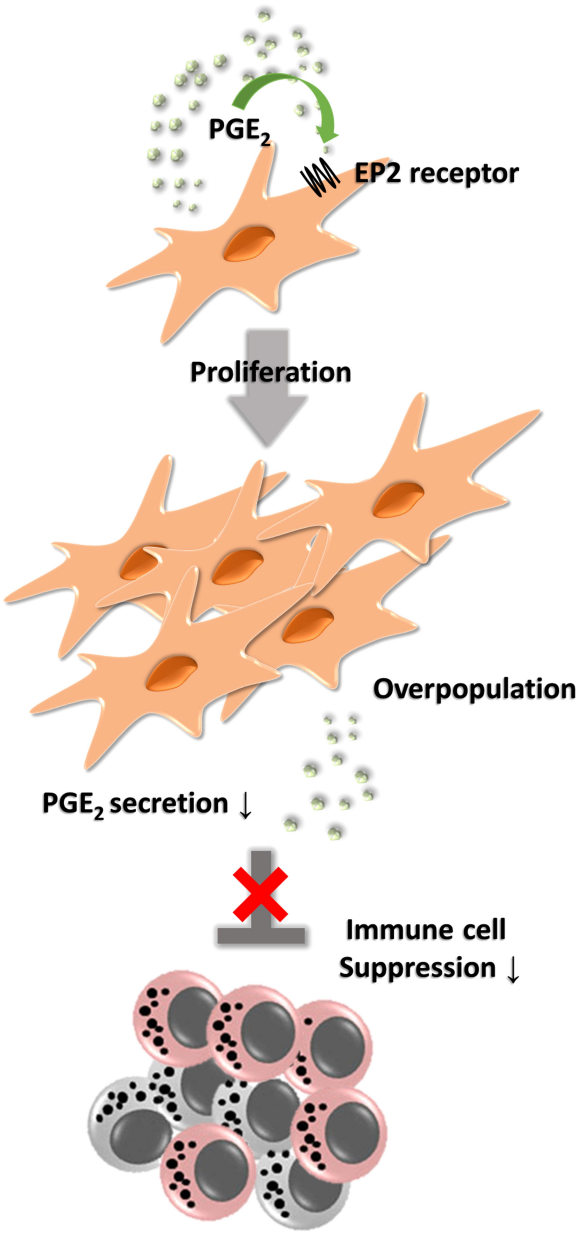

Figure 32. Regulation of autocrine PGE_2, EP2 receptor and immune modulatory function by cell-to-cell contact.

Full confluency of hMSC in the preparation step has to be prevented to avoid the loss of therapeutic function. Furthermore, activation of EP2 receptor or inhibition of GJIC might be applied to cell culture method to achieve improved yield and immunoregulatory function of hMSCs.

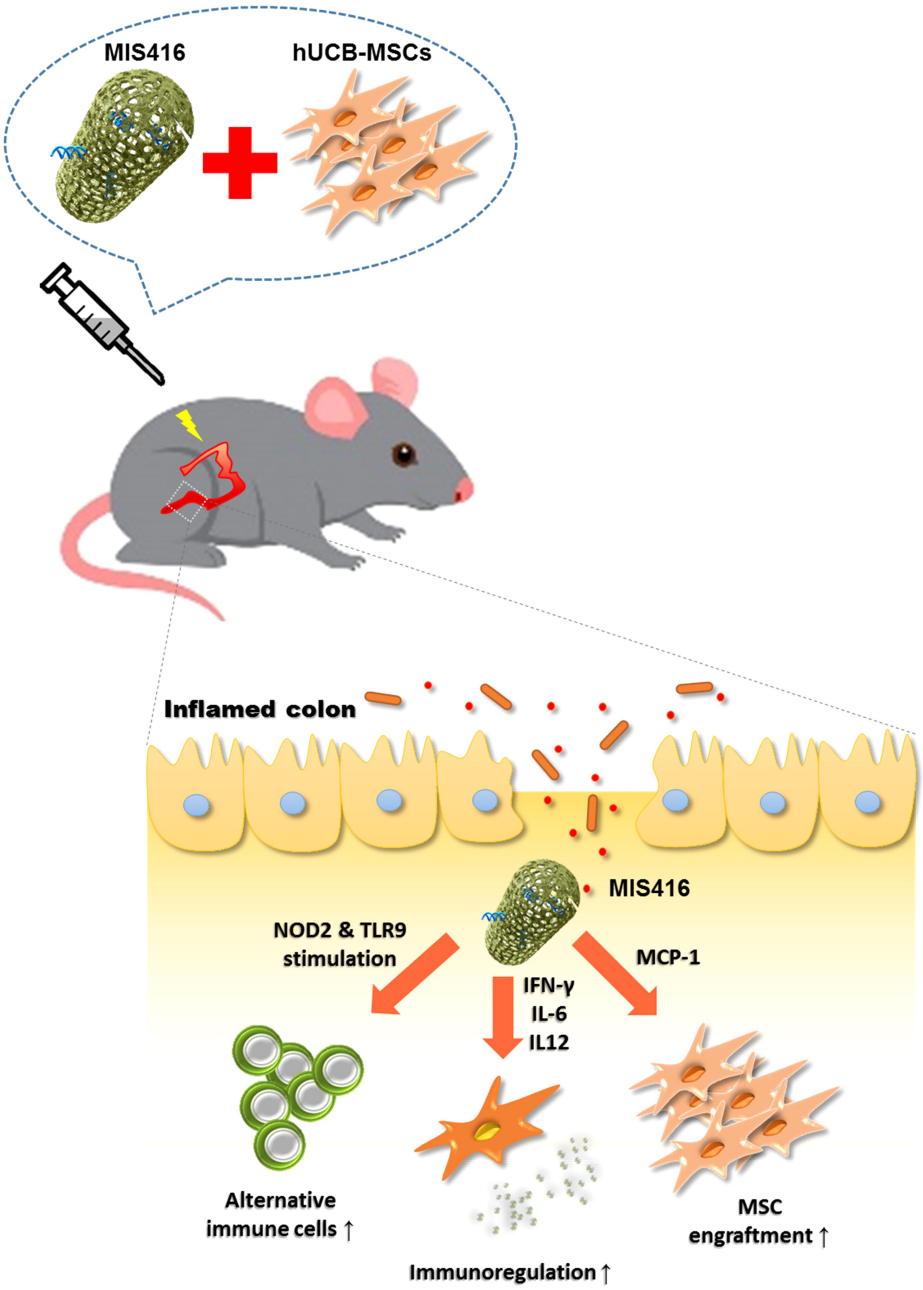

Figure 33. The role of infused MIS416 in fuctional enhancement of hUCB-MSCs.

MIS416 improves the therapeutic efficacy of hUCB-MSCs against experimental colitis by modifying immune environment in the gut and thus, enhances the immunosuppressive ability of the cells

Moreover, development of hMSCs for cell-based therapy need a comprehensive management to achieve improved therapeutic outcomes from an isolation to actual application (Figure 34).

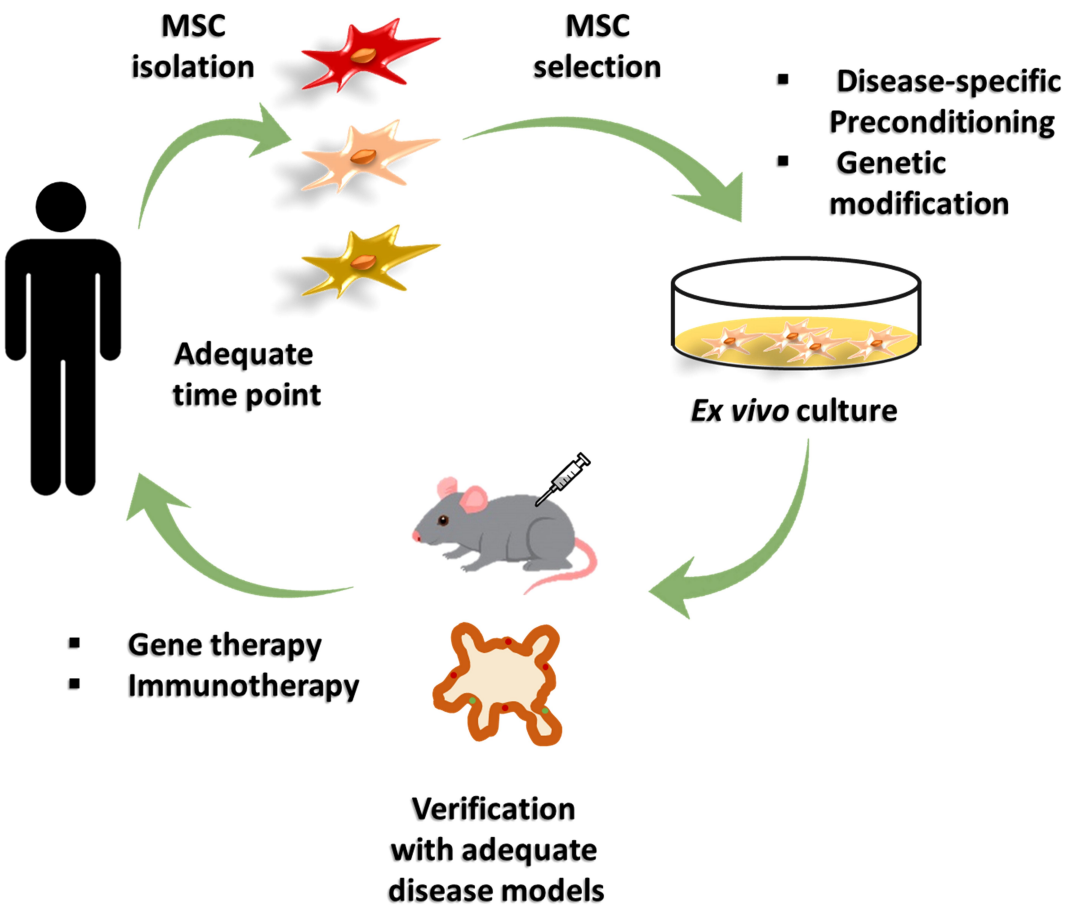

Figure 34. Comprehensive management of production of hMSCs for transplantation.

Isolated hMSCs should be selected based on the disease-specific analysis. Selected MSCs are cultured with key molecules in a pathogenesis of the target disease and during the period, the property of the selected cells has to be maintained. In addition, the therapeutic function is repeatedly validated with proper disease models. To improve the therapeutic outcomes, the adequate time point is important and hMSCs are able to be applied with advanced medical technologies.

REFERENCES

Akiyama, K., Chen, C., Wang, D., Xu, X., Qu, C., Yamaza, T., Cai, T., Chen, W., Sun, L., and Shi, S. 2012. Mesenchymal-stem-cell- induced immunoregulation involves FAS-ligand-/FAS-mediated T cell apoptosis. Cell Stem Cell, 10, 544-555.

An, Y., Liu, W.J., Xue, P., Ma, Y., Zhang, L.Q., Zhu, B., Qi, M., Li, L.Y., Zhang, Y.J., Wang, Q.T., and Jin, Y. 2018. Autophagy promotes MSC-mediated vascularization in cutaneous wound healing via regulation of VEGF secretion. Cell Death Dis, 9, 58.

Androulla, M.N., and Lefkothea, P.C. 2018. CAR T-cell Therapy: A new era in cancer immunotherapy. Curr Pharm Biotechnol, 19, 5-18.

Angoulvant, D., Ivanes, F., Ferrera, R., Matthews, P.G., Nataf, S., and Ovize, M. 2011. Mesenchymal stem cell conditioned media attenuates *in vitro* and *ex vivo* myocardial reperfusion injury. J Heart Lung Transplant, 30, 95-102.

Ankrum, J.A., Ong, J.F., and Karp, J.M. 2014. Mesenchymal stem cells: immune evasive, not immune privileged. Nat biotechnol, 32, 252.

Annabi, B., Lee, Y.T., Turcotte, S., Naud, E., Desrosiers, R.R., Champagne, M., Eliopoulos, N., Galipeau, J., and Béliveau, R. 2003. Hypoxia promotes murine bone marrow derived stromal cell migration and tube formation. Stem Cells, 21, 337-347.

Atashi, F., Modarressi, A., and Pepper, M.S. 2015. The role of reactive oxygen species in mesenchymal stem cell adipogenic and osteogenic differentiation: a

review. Stem Cells Dev, 24, 1150-1163.

Baguma-Nibasheka, M., Barclay, C., Li, A.W., Geldenhuys, L., Porter, G.A., Blay, J., Casson, A.G., and Murphy, P.R. 2007. Selective cyclooxygenase-2 inhibition suppresses basic fibroblast growth factor expression in human esophageal adenocarcinoma. Mol Carcinog, 46, 971-980.

Baksh, D., Yao, R., and Tuan, R.S. 2007. Comparison of proliferative and multilineage differentiation potential of human mesenchymal stem cells derived from umbilical cord and bone marrow. Stem Cells, 25, 1384-1392.

Bartosh, T.J., Ylostalo, J.H., Bazhanov, N., Kuhlman, J., and Prockop, D.J. 2013. Dynamic compaction of human mesenchymal stem/precursor cells into spheres self-activates caspase-dependent IL1 signaling to enhance secretion of modulators of inflammation and immunity (PGE_2, TSG6, and STC1). Stem Cells, 31, 2443-2456.

Bartosh, T.J., Ylöstalo, J.H., Mohammadipoor, A., Bazhanov, N., Coble, K., Claypool, K., Lee, R.H., Choi, H., and Prockop, D.J. 2010. Aggregation of human mesenchymal stromal cells (MSCs) into 3D spheroids enhances their anti-inflammatory properties. Proc Natl Acad Sci USA, 107, 13724-13729.

Bazhanov, N., Ylostalo, J.H., Bartosh, T.J., Tiblow, A., Mohammadipoor, A., Foskett, A., and Prockop, D.J. 2016. Intraperitoneally infused human mesenchymal stem cells form aggregates with mouse immune cells and attach to peritoneal organs. Stem Cell Res Ther, 7, 27.

Beck, L.A., Thaçi, D., Hamilton, J.D., Graham, N.M., Bieber, T., Rocklin, R., Ming, J.E., Ren, H., Kao, R., and Simpson, E. 2014. Dupilumab treatment in

adults with moderate-to-severe atopic dermatitis. N Engl J Med, 371, 130-139.

Bernstein, I.D., and Delaney, C. 2012. Engineering stem cell expansion. Cell Stem Cell, 10, 113-114.

Bhang, S.H., Lee, S., Shin, J.Y., Lee, T.J., Jang, H.K., and Kim, B.S. 2014. Efficacious and clinically relevant conditioned medium of human adipose-derived stem cells for therapeutic angiogenesis. Mol Ther, 22, 862-872.

Bianco, P., Cao, X., Frenette, P.S., Mao, J.J., Robey, P.G., Simmons, P.J., and Wang, C.Y. 2013. The meaning, the sense and the significance: translating the science of mesenchymal stem cells into medicine. Nat Med, 19, 35-42.

Block, G.J., Ohkouchi, S., Fung, F., Frenkel, J., Gregory, C., Pochampally, R., DiMattia, G., Sullivan, D.E., and Prockop, D.J. 2009. Multipotent stromal cells are activated to reduce apoptosis in part by upregulation and secretion of stanniocalcin 1. Stem Cells, 27, 670-681.

Boniface, K., Bak-Jensen, K.S., Li, Y., Blumenschein, W.M., McGeachy, M.J., McClanahan, T.K., McKenzie, B.S., Kastelein, R.A., Cua, D.J., and de Waal Malefyt, R. 2009. Prostaglandin E_2 regulates Th17 cell differentiation and function through cyclic AMP and EP2/EP4 receptor signaling. J Exp Med, 206, 535-548.

Boomsma, R.A., and Geenen, D.L. 2012. Mesenchymal stem cells secrete multiple cytokines that promote angiogenesis and have contrasting effects on chemotaxis and apoptosis. PloS One, 7, e35685.

Bouffi, C., Bony, C., Courties, G., Jorgensen, C., and Noel, D. 2010.

IL-6-dependent PGE_2 secretion by mesenchymal stem cells inhibits local inflammation in experimental arthritis. PLoS One, 5, e14247.

Boyette, L.B., Creasey, O.A., Guzik, L., Lozito, T., and Tuan, R.S. 2014. Human bone marrow derived mesenchymal stem cells display enhanced clonogenicity but impaired differentiation with hypoxic preconditioning. Stem Cells Transl Med, 3, 241-254.

Cai, H.H. 2016. Therapeutic monoclonal antibodies approved by FDA in 2015. MOJ Immunol, 3, 87.

Caliari, S.R., and Harley, B.A. 2014. Collagen-GAG scaffold biophysical properties bias MSC lineage choice in the presence of mixed soluble signals. Tissue Eng Part A, 20, 2463-2472.

Carrion, F., Nova, E., Ruiz, C., Diaz, F., Inostroza, C., Rojo, D., Mönckeberg, G., and Figueroa, F. 2010. Autologous mesenchymal stem cell treatment increased T regulatory cells with no effect on disease activity in two systemic lupus erythematosus patients. Lupus, 19, 317-322.

Castellone, M.D., Teramoto, H., Williams, B.O., Druey, K.M., and Gutkind, J.S. 2005. Prostaglandin E_2 promotes colon cancer cell growth through a Gs-axin-β -catenin signaling axis. Science, 310, 1504-1510.

Chen, K., Wang, D., Du, W.T., Han, Z.-B., Ren, H., Chi, Y., Yang, S.G., Zhu, D., Bayard, F., and Han, Z.C. 2010. Human umbilical cord mesenchymal stem cells exert immunosuppressive activities through a PGE_2-dependent mechanism. Clin immunol, 135, 448-458.

Chen, L.B., Jiang, X.B., and Yang, L. 2004. Differentiation of rat marrow mesenchymal stem cells into pancreatic islet β-cells. World J Gastroenterol, 10, 3016.

Chen, L., Tredget, E.E., Wu, P.Y., and Wu, Y. 2008. Paracrine factors of mesenchymal stem cells recruit macrophages and endothelial lineage cells and enhance wound healing. PloS One, 3, e1886.

Cherian, P.P., Cheng, B., Gu, S., Sprague, E., Bonewald, L.F., and Jiang, J.X. 2003. Effects of mechanical strain on the function of Gap junctions in osteocytes are mediated through the prostaglandin EP2 receptor. J Biol Chem, 278, 43146-43156.

Cho, Y.H., Cha, M.J., Song, B.W., Kim, I.K., Song, H., Chang, W., Lim, S., Ham, O., Lee, S.Y., Choi, E., Kwon, H.M., and Hwang, K.C. 2012. Enhancement of MSC adhesion and therapeutic efficiency in ischemic heart using lentivirus delivery with periostin. Biomaterials, 33, 1376-1385.

Choi, J.J., Yoo, S.A., Park, S.J., Kang, Y.J., Kim, W.U., Oh, I.H., and Cho, C.S. 2008. Mesenchymal stem cells overexpressing interleukin 10 attenuate collagen induced arthritis in mice. Clin Exp Immunol, 153, 269-276.

Ciccocioppo, R., Bernardo, M.E., Sgarella, A., Maccario, R., Avanzini, M.A., Ubezio, C., Minelli, A., Alvisi, C., Vanoli, A., and Calliada, F. 2011. Autologous bone marrow-derived mesenchymal stromal cells in the treatment of fistulising Crohn's disease. Gut, 60, 788-798.

Ciccocioppo, R., Cangemi, G.C., Kruzliak, P., Gallia, A., Betti, E., Badulli, C., Martinetti, M., Cervio, M., Pecci, A., Bozzi, V., Dionigi, P., Visai, L., Gurrado,

A., Alvisi, C., Picone, C., Monti, M., Bernardo, M.E., Gobbi, P., and Corazza, G.R. 2015. *Ex vivo* immunosuppressive effects of mesenchymal stem cells on Crohn's disease mucosal T cells are largely dependent on indoleamine-2,3-dioxygenase activity and cell-cell contact. Stem Cell Res Ther, 6, 137.

Clevers, H. 2016. Modeling development and disease with organoids. Cell, 165, 1586-1597.

Corcione, A., Benvenuto, F., Ferretti, E., Giunti, D., Cappiello, V., Cazzanti, F., Risso, M., Gualandi, F., Mancardi, G.L., Pistoia, V., and Uccelli, A. 2006. Human mesenchymal stem cells modulate B-cell functions. Blood, 107, 367-372.

Crisostomo, P.R., Wang, Y., Markel, T.A., Wang, M., Lahm, T., and Meldrum, D.R. 2008. Human mesenchymal stem cells stimulated by TNF-α, LPS, or hypoxia produce growth factors by an NF-κB-but not JNK-dependent mechanism. Am J Physiol Cell Physiol, 294, C675-C682.

Croitoru-Lamoury, J., Lamoury, F.M., Caristo, M., Suzuki, K., Walker, D., Takikawa, O., Taylor, R., and Brew, B.J. 2011. Interferon-γ regulates the proliferation and differentiation of mesenchymal stem cells via activation of indoleamine-2,3-dioxygenase (IDO). PloS One, 6, e14698.

da Silva Meirelles, L., Caplan, A.I., and Nardi, N.B. 2008. In search of the *in vivo* identity of mesenchymal stem cells. Stem Cells, 26, 2287-2299.

da Silva Meirelles, L., Chagastelles, P.C., and Nardi, N.B. 2006. Mesenchymal stem cells reside in virtually all post-natal organs and tissues. J Cell Sci, 119, 2204-2213.

Danese, S., Colombel, J.F., Peyrin Biroulet, L., Rutgeerts, P., and Reinisch, W. 2013. The role of anti TNF in the management of ulcerative colitis – past, present and future. Aliment Pharmacol Ther, 37, 855-866.

De Becker, A., and Van Riet, I. 2016. Homing and migration of mesenchymal stromal cells: How to improve the efficacy of cell therapy? World J Stem Cells, 8, 73.

Deshmane, S.L., Kremlev, S., Amini, S., and Sawaya, B.E. 2009. Monocyte chemoattractant protein-1 (MCP-1): An overview. J interferon Cytokine Res, 29, 313-326.

Djouad, F., Charbonnier, L.M., Bouffi, C., Louis Plence, P., Bony, C., Apparailly, F., Cantos, C., Jorgensen, C., and Noel, D. 2007. Mesenchymal stem cells inhibit the differentiation of dendritic cells through an interleukin-6-dependent mechanism. Stem Cells, 25, 2025-2032.

Dohadwala, M., Batra, R.K., Luo, J., Lin, Y., Krysan, K., Pold, M., Sharma, S., and Dubinett, S.M. 2002. Autocrine/paracrine prostaglandin E_2 production by non-small cell lung cancer cells regulates matrix metalloproteinase-2 and CD44 in cyclooxygenase-2-dependent invasion. J Biol Chem, 277, 50828-50833.

Duffy, M.M., Pindjakova, J., Hanley, S.A., McCarthy, C., Weidhofer, G.A., Sweeney, E.M., English, K., Shaw, G., Murphy, J.M., Barry, F.P., Mahon, B.P., Belton, O., Ceredig, R., and Griffin, M.D. 2011. Mesenchymal stem cell inhibition of T-helper 17 cell-differentiation is triggered by cell-cell contact and mediated by prostaglandin E_2 via the EP4 receptor. Eur J Immunol, 41, 2840-2851.

Duijvestein, M., Wildenberg, M.E., Welling, M.M., Hennink, S., Molendijk, I., van Zuylen, V.L., Bosse, T., Vos, A.C., de Jonge-Muller, E.S., Roelofs, H., van der Weerd, L., Verspaget, H.W., Fibbe, W.E., te Velde, A.A., van den Brink, G.R., and Hommes, D.W. 2011. Pretreatment with interferon-γ enhances the therapeutic activity of mesenchymal stromal cells in animal models of colitis. Stem Cells, 29, 1549-1558.

Dwyer, R., Potter-Beirne, S., Harrington, K., Lowery, A., Hennessy, E., Murphy, J., Barry, F., O'Brien, T., and Kerin, M. 2007. Monocyte chemotactic protein-1 secreted by primary breast tumors stimulates migration of mesenchymal stem cells. Clin Cancer Res, 13, 5020-5027.

Eibl, G., Bruemmer, D., Okada, Y., Duffy, J.P., Law, R.E., Reber, H.A., and Hines, O.J. 2003. PGE_2 is generated by specific COX-2 activity and increases VEGF production in COX-2-expressing human pancreatic cancer cells. Biochem Biophys Res Commun, 306, 887-897.

Fan, H., Zhao, G., Liu, L., Liu, F., Gong, W., Liu, X., Yang, L., Wang, J., and Hou, Y. 2012. Pre-treatment with IL-1β enhances the efficacy of MSC transplantation in DSS-induced colitis. Cell Mol Immunol, 9, 473.

Fehrer, C., and Lepperdinger, G. 2005. Mesenchymal stem cell aging. Exp Gerontol, 40, 926-930.

Forbes, G.M., Sturm, M.J., Leong, R.W., Sparrow, M.P., Segarajasingam, D., Cummins, A.G., Phillips, M., and Herrmann, R.P. 2014. A phase 2 study of allogeneic mesenchymal stromal cells for luminal Crohn's disease refractory to biologic therapy. Clin Gastroenterol Hepatol, 12, 64-71.

Fossett, E., and Khan, W. 2012. Optimising human mesenchymal stem cell numbers for clinical application: A literature review. Stem Cells Int, 2012, 1-5.

Franquesa, M., Mensah, F.K., Huizinga, R., Strini, T., Boon, L., Lombardo, E., DelaRosa, O., Laman, J.D., Grinyo, J.M., Weimar, W., Betjes, M.G., Baan, C.C., and Hoogduijn, M.J. 2015. Human adipose tissue-derived mesenchymal stem cells abrogate plasmablast formation and induce regulatory B cells independently of T helper cells. Stem Cells, 33, 880-891.

Frith, J.E., Thomson, B., and Genever, P.G. 2009. Dynamic three-dimensional culture methods enhance mesenchymal stem cell properties and increase therapeutic potential. Tissue Eng Part C Methods, 16, 735-749.

Garcia, K.d.O., Ornellas, F.L., Matsumoto, P., Patti, C.d.L., Mello, L.E., Frussa-Filho, R., Han, S.W., and Longo, B.M. 2014. Therapeutic effects of the transplantation of VEGF overexpressing bone marrow mesenchymal stem cells in the hippocampus of murine model of Alzheimer's disease. Front Aging Neurosci, 6, 30.

Ge, W., Jiang, J., Baroja, M., Arp, J., Zassoko, R., Liu, W., Bartholomew, A., Garcia, B., and Wang, H. 2009. Infusion of mesenchymal stem cells and rapamycin synergize to attenuate alloimmune responses and promote cardiac allograft tolerance. Am J Transplant, 9, 1760-1772.

Ghannam, S., Pène, J., Torcy-Moquet, G., Jorgensen, C., and Yssel, H. 2010. Mesenchymal stem cells inhibit human Th17 cell differentiation and function and induce a T regulatory cell phenotype. J Immunol, 185(1), 302-312.

Ginn, S.L., Alexander, I.E., Edelstein, M.L., Abedi, M.R., and Wixon, J. 2013.

Gene therapy clinical trials worldwide to 2012 – An update. J Gene Med, 15, 65-77.

Girvan, R.C., Knight, D.A., O'loughlin, C.J., Hayman, C.M., Hermans, I.F., and Webster, G.A. MIS416, a non-toxic microparticle adjuvant derived from *Propionibacterium acnes* comprising immunostimulatory muramyl dipeptide and bacterial DNA promotes cross-priming and Th1 immunity. Vaccine, 29, 545-557.

Giuliani, M., Bennaceur-Griscelli, A., Nanbakhsh, A., Oudrhiri, N., Chouaib, S., Azzarone, B., Durrbach, A., and Lataillade, J.J. 2014. TLR ligands stimulation protects MSC from NK killing. Stem Cells, 32, 290-300.

Gonzalez-King, H., García, N.A., Ontoria-Oviedo, I., Ciria, M., Montero, J.A., and Sepúlveda, P. 2017. Hypoxia inducible factor-1α potentiates Jagged 1-mediated angiogenesis by mesenchymal stem cell-derived exosomes. Stem Cells, 35, 1747-1759.

Guo, B., Chang, E.Y., and Cheng, G. 2008. The type I IFN induction pathway constrains Th17-mediated autoimmune inflammation in mice. J Clin Invest, 118, 1680-1690.

Hahn, J.Y., Cho, H.J., Kang, H.J., Kim, T.S., Kim, M.H., Chung, J.H., Bae, J.W., Oh, B.H., Park, Y.B., and Kim, H.S. 2008. Pre-treatment of mesenchymal stem cells with a combination of growth factors enhances gap junction formation, cytoprotective effect on cardiomyocytes, and therapeutic efficacy for myocardial infarction. J Am Coll Cardiol, 51, 933-943.

Haller, M.J., Viener, H.-L., Wasserfall, C., Brusko, T., Atkinson, M.A., and Schatz, D.A. 2008. Autologous umbilical cord blood infusion for type 1

diabetes. Exp Hematol, 36, 710-715.

Haller, M.J., Wasserfall, C.H., Hulme, M.A., Cintron, M., Brusko, T.M., McGrail, K.M., Sumrall, T.M., Wingard, J.R., Theriaque, D.W., and Shuster, J.J. 2011. Autologous umbilical cord blood transfusion in young children with type I diabetes fails to preserve C-peptide. Diabetes Care, 34(12), 2567-2569.

Hamidouche, Z., Fromigue, O., Nuber, U., Vaudin, P., Pages, J.C., Ebert, R., Jakob, F., Miraoui, H., and Marie, P.J. 2010. Autocrine fibroblast growth factor 18 mediates dexamethasone-induced osteogenic differentiation of murine mesenchymal stem cells. J Cell Physiol, 224, 509-515.

He, B., Qiao, X., and Cerutti, A. 2004. CpG DNA induces IgG class switch DNA recombination by activating human B cells through an innate pathway that requires TLR9 and cooperates with IL-10. J Immunol, 173, 4479-4491.

Hemmingsen, M., Vedel, S., Skafte-Pedersen, P., Sabourin, D., Collas, P., Bruus, H., and Dufva, M. 2013. The role of paracrine and autocrine signaling in the early phase of adipogenic differentiation of adipose-derived stem cells. PLoS One, 8, e63638.

Herrmann, J.L., Wang, Y., Abarbanell, A.M., Weil, B.R., Tan, J., and Meldrum, D.R. 2010. Preconditioning mesenchymal stem cells with transforming growth factor-α improves mesenchymal stem cell-mediated cardioprotection. Shock, 33, 24-30.

Hnatiuk, A.P., Ong, S.G., Olea, F.D., Locatelli, P., Riegler, J., Lee, W.H., Jen, C.H., De Lorenzi, A., Giménez, C.S., and Laguens, R. 2016. Allogeneic mesenchymal stromal cells overexpressing mutant human HIF-1α in an ovine

model of acute myocardial infarction. J Am Heart Assoc, 5, e003714.

Hodgkinson, C.P., Naidoo, V., Patti, K.G., Gomez, J.A., Schmeckpeper, J., Zhang, Z., Davis, B., Pratt, R.E., Mirotsou, M., and Dzau, V.J. 2013. Abi3bp is a multifunctional autocrine/paracrine factor that regulates mesenchymal stem cell biology. Stem Cells, 31, 1669-1682.

HoWangYin, K.-Y., Loinard, C., Bakker, W., Guérin, C.L., Vilar, J., D'Audigier, C., Mauge, L., Bruneval, P., Emmerich, J., and Lévy, B.I. 2014. HIF-prolyl hydroxylase 2 inhibition enhances the efficiency of mesenchymal stem cell-based therapies for the treatment of critical limb ischemia. Stem Cells, 32, 231-243.

Hsu, P.D., Lander, E.S., and Zhang, F. 2014. Development and applications of CRISPR-Cas9 for genome engineering. Cell, 157, 1262-1278.

Hu, S., Chen, M., Wang, Y., Wang, Z., Pei, Y., Fan, R., Liu, X., Wang, L., Zhou, J., Zheng, S., Zhang, T., Lin, Y., Zhang, M., Tao, R., and Zhong, J. 2016. mTOR inhibition attenuates dextran sulfate sodium-induced colitis by suppressing T cell proliferation and balancing Th1/Th17/Treg profile. PLoS One, 11, e0154564.

Hu, X., Wu, R., Jiang, Z., Wang, L., Chen, P., Zhang, L., Yang, L., Wu, Y., Chen, H., and Chen, H. 2014. Leptin signaling is required for augmented therapeutic properties of mesenchymal stem cells conferred by hypoxia preconditioning. Stem Cells, 32, 2702-2713.

Huang, G.J., Gronthos, S., and Shi, S. 2009. Mesenchymal stem cells derived from dental tissues vs. those from other sources: Their biology and role in regenerative medicine. J Dent Res, 88, 792-806.

Huch, M., and Koo, B.K. 2015. Modeling mouse and human development using organoid cultures. Development, 142, 3113-3125.

Hung, S.C., Pochampally, R.R., Chen, S.C., Hsu, S.C., and Prockop, D.J. 2007a. Angiogenic effects of human multipotent stromal cell conditioned medium activate the PI3K-Akt pathway in hypoxic endothelial cells to inhibit apoptosis, increase survival, and stimulate angiogenesis. Stem Cells, 25, 2363-2370.

Hung, S.C., Pochampally, R.R., Hsu, S.C., Sanchez, C., Chen, S.C., Spees, J., and Prockop, D.J. 2007b. Short-term exposure of multipotent stromal cells to low oxygen increases their expression of CX3CR1 and CXCR4 and their engraftment *in vivo*. PLoS One, 2, e416.

Ikegame, Y., Yamashita, K., Hayashi, S.-I., Mizuno, H., Tawada, M., You, F., Yamada, K., Tanaka, Y., Egashira, Y., and Nakashima, S. 2011. Comparison of mesenchymal stem cells from adipose tissue and bone marrow for ischemic stroke therapy. Cytotherapy, 13, 675-685.

Jang, M.W., Yun, S.P., Park, J.H., Ryu, J.M., Lee, J.H., and Han, H.J. 2012. Cooperation of Epac1/Rap1/Akt and PKA in prostaglandin E_2-induced proliferation of human umbilical cord blood derived mesenchymal stem cells: Involvement of c-Myc and VEGF expression. J Cell Physiol, 227, 3756-3767.

Jeon, Y.K., Jang, Y.H., Yoo, D.R., Kim, S.N., Lee, S.K., and Nam, M.J. 2010. Mesenchymal stem cells' interaction with skin: Wound healing effect on fibroblast cells and skin tissue. Wound Repair Regen, 18, 655-661.

Jeong, S.Y., Ha, J., Lee, M., Jin, H.J., Kim, D.H., Choi, S.J., Oh, W., Yang, Y.S., Kim, J.S., Kim, B.G., Chang, J.H., Cho, D.H., and Jeon, H.B. 2015.

Autocrine action of thrombospondin-2 determines the chondrogenic differentiation potential and suppresses hypertrophic maturation of human umbilical cord blood-derived mesenchymal stem cells. Stem Cells, 33, 3291-3303.

Johnson, R.L., and Fleet, J.C. 2013. Animal models of colorectal cancer. Cancer Metastasis Rev, 32, 39-61.

Kaji, E.H., and Leiden, J.M. 2001. Gene and stem cell therapies. JAMA, 285, 545-550.

Kalinski, P. 2012. Regulation of immune responses by prostaglandin E_2. J Immunol, 188, 21-28.

Kang, I., Lee, B.C., Choi, S.W., Lee, J.Y., Kim, J.J., Kim, B.E., Kim, D.H., Lee, S.E., Shin, N., Seo, Y., Kim, H.S., Kim, D.I., and Kang, K.S. 2018. Donor-dependent variation of human umbilical cord blood mesenchymal stem cells in response to hypoxic preconditioning and amelioration of limb ischemia. Exp Mol Med, 50, 35.

Kang, S., Bhang, S.H., Hwang, S., Yoon, J.-K., Song, J., Jang, H.-K., Kim, S., and Kim, B.S. 2015a. Mesenchymal stem cells aggregate and deliver gold nanoparticles to tumors for photothermal therapy. ACS Nano, 9, 9678-9690.

Kang, T.W., Kim, H.S., Lee, B.C., Shin, T.H., Choi, S.W., Kim, Y.J., Lee, H.Y., Jung, Y.K., Seo, K.W., and Kang, K.S. 2015b. Mica nanoparticle, STB-HO eliminates the human breast carcinoma cells by regulating the interaction of tumor with its immune microenvironment. Sci Rep, 5, 17515.

Kanichai, M., Ferguson, D., Prendergast, P.J., and Campbell, V.A. 2008.

Hypoxia promotes chondrogenesis in rat mesenchymal stem cells: A role for AKT and hypoxia inducible factor (HIF)-1α. J Cell Physiol, 216, 708-715.

Karp, J.M., and Teo, G.S.L. 2009. Mesenchymal stem cell homing: The devil is in the details. Cell Stem Cell, 4, 206-216.

Karussis, D., Karageorgiou, C., Vaknin-Dembinsky, A., Gowda-Kurkalli, B., Gomori, J.M., Kassis, I., Bulte, J.W., Petrou, P., Ben-Hur, T., and Abramsky, O. 2010. Safety and immunological effects of mesenchymal stem cell transplantation in patients with multiple sclerosis and amyotrophic lateral sclerosis. Arch Neurol, 67, 1187-1194.

Katakowski, M., Buller, B., Zheng, X., Lu, Y., Rogers, T., Osobamiro, O., Shu, W., Jiang, F., and Chopp, M. 2013. Exosomes from marrow stromal cells expressing miR-146b inhibit glioma growth. Cancer Lett, 335, 201-204.

Katakura, K., Lee, J., Rachmilewitz, D., Li, G., Eckmann, L., and Raz, E. 2005. Toll-like receptor 9-induced type I IFN protects mice from experimental colitis. J Clin Invest, 115, 695-702.

Kavanagh, D.P., Suresh, S., Newsome, P.N., Frampton, J., and Kalia, N. 2015. Pretreatment of mesenchymal stem cells manipulates their vasculoprotective potential while not altering their homing within the injured gut. Stem Cells, 33, 2785-2797.

Kawakami, T., Ando, T., Kimura, M., Wilson, B.S., and Kawakami, Y. 2009. Mast cells in atopic dermatitis. Curr Opin Immunol, 21, 666-678.

Kay, A.G., Long, G., Tyler, G., Stefan, A., Broadfoot, S.J., Piccinini, A.M.,

Middleton, J., and Kehoe, O. 2017. Mesenchymal stem cell-conditioned medium reduces disease severity and immune responses in inflammatory arthritis. Sci Rep, 7, 18019.

Ke, F., Zhang, L., Liu, Z., Liu, J., Yan, S., Xu, Z., Bai, J., Zhu, H., Lou, F., Wang, H., Shi, Y., Jiang, Y., Su, B., and Wang, H. 2014. Autocrine interleukin-6 drives skin-derived mesenchymal stem cell trafficking via regulating voltage-gated Ca^{2+} channels. Stem Cells, 32, 2799-2810.

Kern, S., Eichler, H., Stoeve, J., Kluter, H., and Bieback, K. 2006. Comparative analysis of mesenchymal stem cells from bone marrow, umbilical cord blood, or adipose tissue. Stem Cells, 24, 1294-1301.

Kim, H.S., Shin, T.H., Lee, B.C., Yu, K.R., Seo, Y., Lee, S., Seo, M.S., Hong, I.S., Choi, S.W., Seo, K.W., Nunez, G., Park, J.H., and Kang, K.S. 2013. Human umbilical cord blood mesenchymal stem cells reduce colitis in mice by activating NOD2 signaling to COX-2. Gastroenterology, 145, 1392-1403.

Kim, H.S., Shin, T.H., Yang, S.R., Seo, M.S., Kim, D.J., Kang, S.K., Park, J.H., and Kang, K.S. 2010. Implication of NOD1 and NOD2 for the differentiation of multipotent mesenchymal stem cells derived from human umbilical cord blood. PLoS One, 5, e15369.

Kim, H.S., Yun, J.W., Shin, T.H., Lee, S.H., Lee, B.C., Yu, K.R., Seo, Y., Lee, S., Kang, T.W., Choi, S.W., Seo, K.W., and Kang, K.S. 2015. Human umbilical cord blood mesenchymal stem cell-derived PGE_2 and TGF-β1 alleviate atopic dermatitis by reducing mast cell degranulation. Stem Cells, 33, 1254-1266.

Kim, N., and Cho, S.G. 2013. Clinical applications of mesenchymal stem cells. Korean J Intern Med, 28, 387-402.

Kim, S.W., Han, H., Chae, G.T., Lee, S.H., Bo, S., Yoon, J.H., Lee, Y.S., Lee, K.S., Park, H.K., and Kang, K.S. 2006. Successful stem cell therapy using umbilical cord blood derived multipotent stem cells for Buerger's disease and ischemic limb disease animal model. Stem Cells, 24, 1620-1626.

Kim, Y.I., Ryu, J.-S., Yeo, J.E., Choi, Y.J., Kim, Y.S., Ko, K., and Koh, Y.G. 2014. Overexpression of TGF-β1 enhances chondrogenic differentiation and proliferation of human synovium-derived stem cells. Biochem Biophys Res Commun, 450, 1593-1599.

Kinnaird, T., Stabile, E., Burnett, M., Shou, M., Lee, C., Barr, S., Fuchs, S., and Epstein, S. 2004. Local delivery of marrow-derived stromal cells augments collateral perfusion through paracrine mechanisms. Circulation, 109, 1543-1549.

Klaschik, S., Tross, D., Shirota, H., and Klinman, D.M. 2010. Short- and long-term changes in gene expression mediated by the activation of TLR9. Mol Immunol, 47, 1317-1324.

Kleiveland, C.R., Kassem, M., and Lea, T. 2008. Human mesenchymal stem cell proliferation is regulated by PGE_2 through differential activation of cAMP-dependent protein kinase isoforms. Exp Cell Res, 314, 1831-1838.

Kortesidis, A., Zannettino, A., Isenmann, S., Shi, S., Lapidot, T., and Gronthos, S. 2005. Stromal-derived factor-1 promotes the growth, survival, and development of human bone marrow stromal stem cells. Blood, 105, 3793-3801.

Krampera, M., Cosmi, L., Angeli, R., Pasini, A., Liotta, F., Andreini, A., Santarlasci, V., Mazzinghi, B., Pizzolo, G., and Vinante, F. 2006. Role for interferon-γ in the immunomodulatory activity of human bone marrow mesenchymal stem cells. Stem Cells, 24, 386-398.

Kwon, Y.W., Heo, S.C., Jeong, G.O., Yoon, J.W., Mo, W.M., Lee, M.J., Jang, I.H., Kwon, S.M., Lee, J.S., and Kim, J.H. 2013. Tumor necrosis factor-α -activated mesenchymal stem cells promote endothelial progenitor cell homing and angiogenesis. Biochim Biophys Acta, 1832, 2136-2144.

Lai, R.C., Arslan, F., Lee, M.M., Sze, N.S.K., Choo, A., Chen, T.S., Salto-Tellez, M., Timmers, L., Lee, C.N., and El Oakley, R.M. 2010. Exosome secreted by MSC reduces myocardial ischemia/reperfusion injury. Stem Cell Res. 4, 214-222.

Lai, T., Li, M., Zheng, L., Song, Y., Xu, X., Guo, Y., Zhang, Y., Zhang, Z., and Mei, Y. 2012. Over-expression of VEGF in marrow stromal cells promotes angiogenesis in rats with cerebral infarction via the synergistic effects of VEGF and Ang-2. J Huazhong Univ Sci Technol Med Sci, 32, 724-731.

Lazarus, H., Haynesworth, S., Gerson, S., Rosenthal, N., and Caplan, A. 1995. *Ex vivo* expansion and subsequent infusion of human bone marrow-derived stromal progenitor cells (mesenchymal progenitor cells): Implications for therapeutic use. Bone Marrow Transplant, 16, 557-564.

Lazarus, H.M., Koc, O.N., Devine, S.M., Curtin, P., Maziarz, R.T., Holland, H.K., Shpall, E.J., McCarthy, P., Atkinson, K., and Cooper, B.W. 2005. Cotransplantation of HLA-identical sibling culture-expanded mesenchymal stem cells and hematopoietic stem cells in hematologic malignancy patients. Biol

Blood Marrow Transplant, 11, 389-398.

Le Blanc, K., and Davies, L.C. 2015. Mesenchymal stromal cells and the innate immune response. Immunol Lett. 168, 140-146.

Le Blanc, K., and Mougiakakos, D. 2012. Multipotent mesenchymal stromal cells and the innate immune system. Nat Rev Immunol, 12, 383-396.

Le Blanc, K., Tammik, L., Sundberg, B., Haynesworth, S., and Ringden, O. 2003. Mesenchymal stem cells inhibit and stimulate mixed lymphocyte cultures and mitogenic responses independently of the major histocompatibility complex. Scand J Immunol, 57, 11-20.

Leadbetter, E.A., Rifkin, I.R., Hohlbaum, A.M., Beaudette, B.C., Shlomchik, M.J., and Marshak-Rothstein, A. 2002. Chromatin-IgG complexes activate B cells by dual engagement of IgM and Toll-like receptors. Nature, 416, 603-607.

Leahy, K.M., Ornberg, R.L., Wang, Y., Zweifel, B.S., Koki, A.T., and Masferrer, J.L. 2002. Cyclooxygenase-2 inhibition by celecoxib reduces proliferation and induces apoptosis in angiogenic endothelial cells *in vivo*. Cancer Res, 62, 625-631.

Lee, B.C., Kim, H.S., Shin, T.H., Kang, I., Lee, J.Y., Kim, J.J., Kang, H.K., Seo, Y., Lee, S., Yu, K.R., Choi, S.W., and Kang, K.S. 2016. PGE_2 maintains self-renewal of human adult stem cells via EP2-mediated autocrine signaling and its production is regulated by cell-to-cell contact. Sci Rep, 6, 26298.

Lee, B.C., Shin, N., Lee, J.Y., Kang, I., Kim, J.J., Lee, S.E., Choi, S.W., Webster, G.A., and Kang, K.S. MIS416 enhances therapeutic functions of

human umbilical cord blood-derived mesenchymal stem cells against experimental colitis by modulating systemic immune milieu. Front Immunol, 9, 1078.

Lee, J., Rachmilewitz, D., and Raz, E. 2006. Homeostatic effects of TLR9 signaling in experimental colitis. Ann N Y Acad Sci, 1072, 351-355.

Lee, J.S., Hong, J.M., Moon, G.J., Lee, P.H., Ahn, Y.H., and Bang, O.Y. 2010. A long term follow up study of intravenous autologous mesenchymal stem cell transplantation in patients with ischemic stroke. Stem Cells. 28, 1099-1106.

Lee, S., Kim, H.S., Roh, K.H., Lee, B.C., Shin, T.H., Yoo, J.M., Kim, Y.L., Yu, K.R., Kang, K.S., and Seo, K.W. 2015. DNA methyltransferase inhibition accelerates the immunomodulation and migration of human mesenchymal stem cells. Sci Rep, 5, 8020.

Li, L., Chen, X., Wang, W.E., and Zeng, C. 2016a. How to improve the survival of transplanted mesenchymal stem cell in ischemic heart? Stem Cells Int, 2016, 9682757.

Li, M.O., Wan, Y.Y., and Flavell, R.A. 2007. T cell-produced transforming growth factor-β1 controls T cell tolerance and regulates Th1- and Th17-cell differentiation. Immunity, 26, 579-591.

Li, S., Wang, X., Li, J., Zhang, J., Zhang, F., Hu, J., Qi, Y., Yan, B., and Li, Q. 2016b. Advances in the treatment of ischemic diseases by mesenchymal stem cells. Stem Cells Int, 2016, 5896061.

Liang, J., Zhang, H., Hua, B., Wang, H., Lu, L., Shi, S., Hou, Y., Zeng, X.,

Gilkeson, G.S., and Sun, L. 2010. Allogenic mesenchymal stem cells transplantation in refractory systemic lupus erythematosus: A pilot clinical study. Ann Rheum Dis, 69, 1423-1429.

Lu, X., Han, J., Xu, X., Xu, J., Liu, L., Huang, Y., Yang, Y., and Qiu, H. 2017. PGE_2 promotes the migration of mesenchymal stem cells through the activation of FAK and ERK1/2 pathway. Stem Cells Int, 2017, 8178643.

Luo, G., Cheng, W., He, W., Wang, X., Tan, J., Fitzgerald, M., Li, X., and Wu, J. 2010. Promotion of cutaneous wound healing by local application of mesenchymal stem cells derived from human umbilical cord blood. Wound Repair Regen, 18, 506-513.

Luz-Crawford, P., Djouad, F., Toupet, K., Bony, C., Franquesa, M., Hoogduijn, M.J., Jorgensen, C., and Noel, D. 2016. Mesenchymal stem cell-derived interleukin 1 receptor antagonist promotes macrophage polarization and inhibits B cell differentiation. Stem Cells, 34, 483-492.

Luz-Crawford, P., Kurte, M., Bravo-Alegría, J., Contreras, R., Nova-Lamperti, E., Tejedor, G., Noël, D., Jorgensen, C., Figueroa, F., and Djouad, F. 2013. Mesenchymal stem cells generate a $CD4^+CD25^+Foxp3^+$ regulatory T cell population during the differentiation process of Th1 and Th17 cells. Stem Cell Res Ther, 4, 65.

Lv, F.J., Tuan, R.S., Cheung, K.M., and Leung, V.Y. 2014. Concise review: The surface markers and identity of human mesenchymal stem cells. Stem Cells, 32, 1408-1419.

Macho Fernandez, E., Valenti, V., Rockel, C., Hermann, C., Pot, B., Boneca,

I.G., and Grangette, C. 2011. Anti-inflammatory capacity of selected *lactobacilli* in experimental colitis is driven by NOD2-mediated recognition of a specific peptidoglycan-derived muropeptide. Gut, 60, 1050-1059.

Mao, F., Wu, Y., Tang, X., Wang, J., Pan, Z., Zhang, P., Zhang, B., Yan, Y., Zhang, X., and Qian, H. 2017. Human umbilical cord mesenchymal stem cells alleviate inflammatory bowel disease through the regulation of 15-LOX-1 in macrophages. Biotechnol Lett. 39, 929-938.

Marigo, I., and Dazzi, F. 2011. The immunomodulatory properties of mesenchymal stem cells. Semin Immunopathol, 33, 593-602.

Markel, T.A., Wang, Y., Herrmann, J.L., Crisostomo, P.R., Wang, M., Novotny, N.M., Herring, C.M., Tan, J., Lahm, T., and Meldrum, D.R. 2008. VEGF is critical for stem cell-mediated cardioprotection and a crucial paracrine factor for defining the age threshold in adult and neonatal stem cell function. Am J Physiol Heart Circ Physiol, 295, H2308-H2314.

Marquez-Curtis, L.A., and Janowska-Wieczorek, A. 2013. Enhancing the migration ability of mesenchymal stromal cells by targeting the SDF-1/CXCR4 axis. Biomed Res Int, 2013, 561098.

Masferrer, J.L., Leahy, K.M., Koki, A.T., Zweifel, B.S., Settle, S.L., Woerner, B.M., Edwards, D.A., Flickinger, A.G., Moore, R.J., and Seibert, K. 2000. Antiangiogenic and antitumor activities of cyclooxygenase-2 inhibitors. Cancer Res, 60, 1306-1311.

McKee, C., and Chaudhry, G.R. 2017. Advances and challenges in stem cell culture. Colloids Surf B Biointerfaces, 159, 62-77.

Meisel, R., Zibert, A., Laryea, M., Göbel, U., Däubener, W., and Dilloo, D. 2004. Human bone marrow stromal cells inhibit allogeneic T-cell responses by indoleamine-2,3-dioxygenase-mediated tryptophan degradation. Blood, 103, 4619-4621.

Mohyeddin Bonab, M., Yazdanbakhsh, S., Lotfi, J., Alimoghaddom, K., Talebian, F., Hooshmand, F., Ghavamzadeh, A., and Nikbin, B. 2007. Does mesenchymal stem cell therapy help multiple sclerosis patients? Report of a pilot study. Iran J Immunol, 4, 50-57.

Moschen, A.R., Geiger, S., Krehan, I., Kaser, A., and Tilg, H. 2008. Interferon-α controls IL-17 expression *in vitro* and *in vivo*. Immunobiol, 213, 779-787.

Mueller, S.M., and Glowacki, J. 2001. Age-related decline in the osteogenic potential of human bone marrow cells cultured in three-dimensional collagen sponges. J Cell Biochem, 82, 583-590.

Murphy, M.B., Moncivais, K., and Caplan, A.I. 2013. Mesenchymal stem cells: Environmentally responsive therapeutics for regenerative medicine. Exp Mol Med, 45, e54.

Najar, M., Raicevic, G., Boufker, H.I., Kazan, H.F., De Bruyn, C., Meuleman, N., Bron, D., Toungouz, M., and Lagneaux, L. 2010. Mesenchymal stromal cells use PGE_2 to modulate activation and proliferation of lymphocyte subsets: Combined comparison of adipose tissue, Wharton's Jelly and bone marrow sources. Cell Immunol, 264, 171-179.

Nemeth, K., Wilson, T., Rada, B., Parmelee, A., Mayer, B., Buzas, E., Falus, A., Key, S., Masszi, T., Karpati, S., and Mezey, E. 2012. Characterization and

function of histamine receptors in human bone marrow stromal cells. Stem Cells, 30, 222-231.

Newman, R.E., Yoo, D., LeRoux, M.A., and Danilkovitch-Miagkova, A. 2009. Treatment of inflammatory diseases with mesenchymal stem cells. Inflamm Allergy Drug Targets, 8, 110-123.

Ni, X., Ou, C., Guo, J., Liu, B., Zhang, J., Wu, Z., Li, H., and Chen, M. 2017. Lentiviral vector-mediated co-overexpression of VEGF and Bcl-2 improves mesenchymal stem cell survival and enhances paracrine effects *in vitro*. Int J Mol Med, 40, 418-426.

Nie, C., Yang, D., Xu, J., Si, Z., Jin, X., and Zhang, J. 2011. Locally administered adipose-derived stem cells accelerate wound healing through differentiation and vasculogenesis. Cell Transplant, 20, 205-216.

Ning, H., Yang, F., Jiang, M., Hu, L., Feng, K., Zhang, J., Yu, Z., Li, B., Xu, C., and Li, Y. 2008. The correlation between cotransplantation of mesenchymal stem cells and higher recurrence rate in hematologic malignancy patients: Outcome of a pilot clinical study. Leukemia. 22, 593-599.

Nitzsche, F., Müller, C., Lukomska, B., Jolkkonen, J., Deten, A., and Boltze, J. 2017. Concise review: MSC adhesion cascade-insights into homing and transendothelial migration. Stem Cells, 35, 1446-1460.

Noguchi, M., Taniya, T., Koyasaki, N., Kumaki, T., Miyazaki, I., and Mizukami, Y. 1991. Effects of the prostaglandin synthetase inhibitor indomethacin on tumorigenesis, tumor proliferation, cell kinetics, and receptor contents of 7,12-dimethylbenz(α)anthracene-induced mammary carcinoma in

Sprague-Dawley rats fed a high- or low-fat diet. Cancer Res, 51, 2683-2689.

Ogura, Y., Bonen, D.K., Inohara, N., Nicolae, D.L., Chen, F.F., Ramos, R., Britton, H., Moran, T., Karaliuskas, R., Duerr, R.H., Achkar, J.P., Brant, S.R., Bayless, T.M., Kirschner, B.S., Hanauer, S.B., Nunez, G., and Cho, J.H. 2001. A frameshift mutation in NOD2 associated with susceptibility to Crohn's disease. Nature, 411, 603-606.

Opitz, C.A., Litzenburger, U.M., Lutz, C., Lanz, T.V., Tritschler, I., Köppel, A., Tolosa, E., Hoberg, M., Anderl, J., and Aicher, W.K. 2009. Toll-like receptor engagement enhances the immunosuppressive properties of human bone marrow-derived mesenchymal stem cells by inducing indoleamine-2,3-dioxygenase-1 via interferon-β and protein kinase R. Stem Cells, 27, 909-919.

Orozco, L., Munar, A., Soler, R., Alberca, M., Soler, F., Huguet, M., Sentís, J., Sánchez, A., and García-Sancho, J. 2013. Treatment of knee osteoarthritis with autologous mesenchymal stem cells: A pilot study. Transplantation, 95, 1535-1541.

Park, J., Kim, B., Han, J., Oh, J., Park, S., Ryu, S., Jung, S., Shin, J.-Y., Lee, B.S., and Hong, B.H. 2015. Graphene oxide flakes as a cellular adhesive: Prevention of reactive oxygen species mediated death of implanted cells for cardiac repair. ACS Nano, 9, 4987-4999.

Park, J.Y., Pillinger, M.H., and Abramson, S.B. 2006. Prostaglandin E_2 synthesis and secretion: The role of PGE_2 synthases. Clin Immunol, 119, 229-240.

Payne, N.L., Dantanarayana, A., Sun, G., Moussa, L., Caine, S., McDonald, C.,

Herszfeld, D., Bernard, C.C., and Siatskas, C. 2012. Early intervention with gene-modified mesenchymal stem cells overexpressing interleukin-4 enhances anti-inflammatory responses and functional recovery in experimental autoimmune demyelination. Cell Adh Migr, 6, 179-189.

Peng, Y., Ke, M., Xu, L., Liu, L., Chen, X., Xia, W., Li, X., Chen, Z., Ma, J., and Liao, D. 2013. Donor-derived mesenchymal stem cells combined with low-dose tacrolimus prevent acute rejection after renal transplantation: A clinical pilot study. Transplantation, 95, 161-168.

Perin, E.C., Murphy, M.P., March, K.L., Bolli, R., Loughran, J., Yang, P.C., Leeper, N.J., Dalman, R.L., Alexander, J., and Henry, T.D. 2017. Evaluation of cell therapy on exercise performance and limb perfusion in peripheral artery disease. Circulation. 135:1417-1428.

Pevsner-Fischer, M., Morad, V., Cohen-Sfady, M., Rousso-Noori, L., Zanin-Zhorov, A., Cohen, S., Cohen, I.R., and Zipori, D. Toll-like receptors and their ligands control mesenchymal stem cell functions. Blood, 109, 1422-1432.

Phinney, D.G., Kopen, G., Righter, W., Webster, S., Tremain, N., and Prockop, D.J. 1999. Donor variation in the growth properties and osteogenic potential of human marrow stromal cells. J Cell Biochem, 75, 424-436.

Polchert, D., Sobinsky, J., Douglas, G., Kidd, M., Moadsiri, A., Reina, E., Genrich, K., Mehrotra, S., Setty, S., and Smith, B. 2008. IFN-γ activation of mesenchymal stem cells for treatment and prevention of graft versus host disease. Eur J Immunol, 38, 1745-1755.

Prasanna, S.J., Gopalakrishnan, D., Shankar, S.R., and Vasandan, A.B. 2010.

Pro-inflammatory cytokines, IFNγ and TNFα, influence immune properties of human bone marrow and Wharton jelly mesenchymal stem cells differentially. PloS One, 5, e9016.

Pulendran, B., Tang, H., and Manicassamy, S. 2010. Programming dendritic cells to induce Th2 and tolerogenic responses. Nat Immunol, 11, 647-655.

Qiu, Y., Guo, J., Mao, R., Chao, K., Chen, B., He, Y., Zeng, Z., Zhang, S., and Chen, M. 2017. TLR3 preconditioning enhances the therapeutic efficacy of umbilical cord mesenchymal stem cells in TNBS-induced colitis via the TLR3-Jagged-1-Notch-1 pathway. Mucosal Immunol. 10, 727-742.

Rachmilewitz, D., Katakura, K., Karmeli, F., Hayashi, T., Reinus, C., Rudensky, B., Akira, S., Takeda, K., Lee, J., Takabayashi, K., and Raz, E. 2004. Toll-like receptor 9 signaling mediates the anti-inflammatory effects of probiotics in murine experimental colitis. Gastroenterology, 126, 520-528.

Raval, Z., and Losordo, D.W. 2013. Cell therapy of peripheral arterial disease. Circ Res, 112, 1288-1302.

Ravanidis, S., Bogie, J.F.J., Donders, R., Deans, R., Hendriks, J.J.A., Stinissen, P., Pinxteren, J., Mays, R.W., and Hellings, N. 2017. Crosstalk with inflammatory macrophages shapes the regulatory properties of multipotent adult progenitor cells. Stem Cells Int, 2017, 2353240.

Rojas-Cartagena, C., Flores, I., and Appleyard, C.B. 2005. Role of tumor necrosis factor receptors in an animal model of acute colitis. Cytokine, 32, 85-93.

Sala, E., Genua, M., Petti, L., Anselmo, A., Arena, V., Cibella, J., Zanotti, L., D'Alessio, S., Scaldaferri, F., and Luca, G. 2015. Mesenchymal stem cells reduce colitis in mice via release of TSG6, independently of their localization to the intestine. Gastroenterology, 149, 163-176.

Saller, M.M., Prall, W.C., Docheva, D., Schönitzer, V., Popov, T., Anz, D., Clausen-Schaumann, H., Mutschler, W., Volkmer, E., and Schieker, M. 2012. Increased stemness and migration of human mesenchymal stem cells in hypoxia is associated with altered integrin expression. Biochem Biophys Res Commun, 423, 379-385.

Saparov, A., Ogay, V., Nurgozhin, T., Jumabay, M., and Chen, W.C. 2016. Preconditioning of human mesenchymal stem cells to enhance their regulation of the immune response. Stem Cells Int, 2016, 3924858.

Saraswati, S., Guo, Y., Atkinson, J., and Young, P.P. 2015. Prolonged hypoxia induces monocarboxylate transporter 4 expression in mesenchymal stem cells resulting in a secretome that is deleterious to cardiovascular repair. Stem Cells, 33, 1333-1344.

Sato, K., Ozaki, K., Oh, I., Meguro, A., Hatanaka, K., Nagai, T., Muroi, K., and Ozawa, K. 2007. Nitric oxide plays a critical role in suppression of T-cell proliferation by mesenchymal stem cells. Blood, 109, 228-234.

Schajnovitz, A., Itkin, T., D'Uva, G., Kalinkovich, A., Golan, K., Ludin, A., Cohen, D., Shulman, Z., Avigdor, A., Nagler, A., Kollet, O., Seger, R., and Lapidot, T. 2011. CXCL12 secretion by bone marrow stromal cells is dependent on cell contact and mediated by connexin-43 and connexin-45 gap junctions. Nat Immunol, 12, 391-398.

Scherjon, S.A., Kleijburg van der Keur, C., de Groot Swings, G.M., Claas, F.H., Fibbe, W.E., and Kanhai, H.H. 2004. Isolation of mesenchymal stem cells of fetal or maternal origin from human placenta. Stem Cells, 22, 1338-1345.

Scholich, K., and Geisslinger, G. 2006. Is mPGES-1 a promising target for pain therapy? Trends Pharmacol Sci, 27, 399-401.

Seno, H., Oshima, M., Ishikawa, T.O., Oshima, H., Takaku, K., Chiba, T., Narumiya, S., and Taketo, M.M. 2002. Cyclooxygenase 2- and prostaglandin E_2 receptor EP2-dependent angiogenesis in $Apc^{\Delta 716}$ mouse intestinal polyps. Cancer Res, 62, 506-511.

Seo, B.M., Miura, M., Gronthos, S., Bartold, P.M., Batouli, S., Brahim, J., Young, M., Robey, P.G., Wang, C.Y., and Shi, S. 2004. Investigation of multipotent postnatal stem cells from human periodontal ligament. Lancet, 364, 149-155.

Shao, Z., Zhang, X., Pi, Y., Wang, X., Jia, Z., Zhu, J., Dai, L., Chen, W., Yin, L., and Chen, H. 2012. Polycaprolactone electrospun mesh conjugated with an MSC affinity peptide for MSC homing *in vivo*. Biomaterials, 33, 3375-3387.

Sheng, H.M., Wang, Y., Jin, Y.Q., Zhang, Q.Y., Zhang, Y., Wang, L., Shen, B., Yin, S., Liu, W., Cui, L., and Li, N.L. 2008. A critical role of IFNγ in priming MSC-mediated suppression of T cell proliferation through up-regulation of B7-H1. Cell Res, 18, 846-857.

Shi, Y., Hu, G., Su, J., Li, W., Chen, Q., Shou, P., Xu, C., Chen, X., Huang, Y., and Zhu, Z. 2010. Mesenchymal stem cells: A new strategy for immunosuppression and tissue repair. Cell Res, 20, 510-518.

Shin, T.H., Kim, H.S., Kang, T.W., Lee, B.C., Lee, H.Y., Kim, Y.J., Shin, J.H., Seo, Y., Choi, S.W., Lee, S., Shin, K., Seo, K.W., and Kang, K.S. 2016. Human umbilical cord blood-stem cells direct macrophage polarization and block inflammasome activation to alleviate rheumatoid arthritis. Cell Death Dis, 7, e2524.

Shin, T.H., Lee, B.C., Choi, S.W., Shin, J.H., Kang, I., Lee, J.Y., Kim, J.J., Lee, H.K., Jung, J.E., Choi, Y.W., Lee, S.H., Yoon, J.S., Choi, J.S., Lee, C.S., Seo, Y., Kim, H.S., and Kang, K.S. 2017. Human adipose tissue-derived mesenchymal stem cells alleviate atopic dermatitis via regulation of B lymphocyte maturation. Oncotarget, 8, 512-522.

Shoji, Y., Takahashi, M., Kitamura, T., Watanabe, K., Kawamori, T., Maruyama, T., Sugimoto, Y., Negishi, M., Narumiya, S., Sugimura, T., and Wakabayashi, K. 2004. Downregulation of prostaglandin E receptor subtype EP3 during colon cancer development. Gut, 53, 1151-1158.

Siddappa, R., Licht, R., van Blitterswijk, C., and de Boer, J. 2007. Donor variation and loss of multipotency during *in vitro* expansion of human mesenchymal stem cells for bone tissue engineering. J Orthop Res, 25, 1029-1041.

Siegel, G., Kluba, T., Hermanutz-Klein, U., Bieback, K., Northoff, H., and Schäfer, R. 2013. Phenotype, donor age and gender affect function of human bone marrow-derived mesenchymal stromal cells. BMC Med, 11, 146.

Soland, M., Colletti, E.J., Bego, M., Sanada, C., Porada, C.D., Zanjani, E.D., Jeor, S.S., and Almeida-Porada, G. 2010. Modulation of mesenchymal stem cell MHC-I complex increases engraftment *in vivo*. Blood, 116, 1457.

Sotiropoulou, P.A., Perez, S.A., Gritzapis, A.D., Baxevanis, C.N., and Papamichail, M. 2006. Interactions between human mesenchymal stem cells and natural killer cells. Stem Cells, 24, 74-85.

Spaggiari, G.M., Abdelrazik, H., Becchetti, F., and Moretta, L. 2009. MSCs inhibit monocyte-derived DC maturation and function by selectively interfering with the generation of immature DCs: Central role of MSC-derived prostaglandin E_2. Blood, 113, 6576-6583.

Spaggiari, G.M., Capobianco, A., Becchetti, S., Mingari, M.C., and Moretta, L. 2006. Mesenchymal stem cell-natural killer cell interactions: Evidence that activated NK cells are capable of killing MSCs, whereas MSCs can inhibit IL-2-induced NK-cell proliferation. Blood, 107, 1484-1490.

Sriramulu, S., Banerjee, A., Di Liddo, R., Jothimani, G., Gopinath, M., Murugesan, R., Marotta, F., and Pathak, S. 2018. Concise review on clinical applications of conditioned medium derived from human umbilical cord-mesenchymal stem cells (UC-MSCs). Int J Hematol Oncol Stem Cell Res, 12, 229-233.

Su, W., Wan, Q., Huang, J., Han, L., Chen, X., Chen, G., Olsen, N., Zheng, S.G., and Liang, D. 2015. Culture medium from TNF-α-stimulated mesenchymal stem cells attenuates allergic conjunctivitis through multiple antiallergic mechanisms. J Allergy Clin Immunol, 136, 423-432 e428.

Suga, H. 2009. IFATS series: FGF-2-induced HGF secretion by adipose-derived stromal cells inhibits post-injury fibrogenesis through a JNK-dependent mechanism. Stem Cells, 27, 238-249.

Sugiyama, T., Kohara, H., Noda, M., and Nagasawa, T. 2006. Maintenance of the hematopoietic stem cell pool by CXCL12-CXCR4 chemokine signaling in bone marrow stromal cell niches. Immunity, 25, 977-988.

Sung, Y.M., He, G., and Fischer, S.M. 2005. Lack of expression of the EP2 but not EP3 receptor for prostaglandin E_2 results in suppression of skin tumor development. Cancer Res, 65, 9304-9311.

Takeyama, H., Mizushima, T., Uemura, M., Haraguchi, N., Nishimura, J., Hata, T., Matsuda, C., Takemasa, I., Ikenaga, M., and Murata, K. 2017. Adipose-derived stem cells ameliorate experimental murine colitis via TSP-1-dependent activation of latent TGF-β. Dig Dis Sci, 62, 1963-1974.

Tang, J., Xie, Q., Pan, G., Wang, J., and Wang, M. 2006. Mesenchymal stem cells participate in angiogenesis and improve heart function in rat model of myocardial ischemia with reperfusion. Eur J Cardiothoracic Surg, 30, 353-361.

Tatara, R., Ozaki, K., Kikuchi, Y., Hatanaka, K., Oh, I., Meguro, A., Matsu, H., Sato, K., and Ozawa, K. 2011. Mesenchymal stromal cells inhibit Th17 but not regulatory T-cell differentiation. Cytotherapy, 13, 686-694.

Tomchuck, S.L., Zwezdaryk, K.J., Coffelt, S.B., Waterman, R.S., Danka, E.S., and Scandurro, A.B. 2008. Toll-like receptors on human mesenchymal stem cells drive their migration and immunomodulating responses. Stem Cells, 26, 99-107.

Turinetto, V., Vitale, E., and Giachino, C. 2016. Senescence in human mesenchymal stem cells: Functional changes and implications in stem cell-based therapy. Int J Mol Sci, 17, 1164.

Uccelli, A., Moretta, L., and Pistoia, V. Mesenchymal stem cells in health and disease. Nat Rev Immunol, 8, 726-736.

Uhlig, H.H., McKenzie, B.S., Hue, S., Thompson, C., Joyce-Shaikh, B., Stepankova, R., Robinson, N., Buonocore, S., Tlaskalova-Hogenova, H., Cua, D.J., and Powrie, F. 2006. Differential activity of IL-12 and IL-23 in mucosal and systemic innate immune pathology. Immunity, 25, 309-318.

Wang, D., Zhang, H., Liang, J., Li, X., Feng, X., Wang, H., Hua, B., Liu, B., Lu, L., and Gilkeson, G.S. 2013. Allogeneic mesenchymal stem cell transplantation in severe and refractory systemic lupus erythematosus: 4 years of experience. Cell transplant. 22, 2267-2277.

Wang, L., Li, Y., Chen, X., Chen, J., Gautam, S.C., Xu, Y., and Chopp, M. 2002. MCP-1, MIP-1, IL-8 and ischemic cerebral tissue enhance human bone marrow stromal cell migration in interface culture. Hematology, 7, 113-117.

Wang, T., Xu, Z., Jiang, W., and Ma, A. 2006. Cell-to-cell contact induces mesenchymal stem cell to differentiate into cardiomyocyte and smooth muscle cell. Int J Cardiol, 109, 74-81.

Wang, W., Itaka, K., Ohba, S., Nishiyama, N., Chung, U.I., Yamasaki, Y., and Kataoka, K. 2009a. 3D spheroid culture system on micropatterned substrates for improved differentiation efficiency of multipotent mesenchymal stem cells. Biomaterials, 30, 2705-2715.

Wang, X., Zhao, T., Huang, W., Wang, T., Qian, J., Xu, M., Kranias, E.G., Wang, Y., and Fan, G.C. 2009b. Hsp20-engineered mesenchymal stem cells are resistant to oxidative stress via enhanced activation of Akt and increased

secretion of growth factors. Stem Cells, 27, 3021-3031.

Waskewich, C., Blumenthal, R.D., Li, H., Stein, R., Goldenberg, D.M., and Burton, J. 2002. Celecoxib exhibits the greatest potency amongst cyclooxygenase (COX) inhibitors for growth inhibition of COX-2-negative hematopoietic and epithelial cell lines. Cancer Res, 62, 2029-2033.

Watanabe, T., Kitani, A., Murray, P.J., and Strober, W. 2004. NOD2 is a negative regulator of Toll-like receptor 2-mediated T helper type 1 responses. Nat Immunol, 5, 800-808.

Watanabe, T., Kitani, A., Murray, P.J., Wakatsuki, Y., Fuss, I.J., and Strober, W. 2006. Nucleotide binding oligomerization domain 2 deficiency leads to dysregulated TLR2 signaling and induction of antigen-specific colitis. Immunity, 25, 473-485.

Wei, X., Du, Z., Zhao, L., Feng, D., Wei, G., He, Y., Tan, J., Lee, W.H., Hampel, H., Dodel, R., Johnstone, B.H., March, K.L., Farlow, M.R., and Du, Y. 2009. IFATS collection: The conditioned media of adipose stromal cells protect against hypoxia-ischemia-induced brain damage in neonatal rats. Stem Cells, 27, 478-488.

Wei, X., Yang, X., Han, Z.P., Qu, F.F., Shao, L., and Shi, Y.F. 2013. Mesenchymal stem cells: A new trend for cell therapy. Acta Pharmacol Sin, 34, 747-754.

Wenzel, S., Ford, L., Pearlman, D., Spector, S., Sher, L., Skobieranda, F., Wang, L., Kirkesseli, S., Rocklin, R., and Bock, B. 2013. Dupilumab in persistent asthma with elevated eosinophil levels. N Engl J Med, 368,

2455-2466.

White, M., Webster, G., O'Sullivan, D., Stone, S., and La Flamme, A.C. 2014. Targeting innate receptors with MIS416 reshapes Th responses and suppresses CNS disease in a mouse model of multiple sclerosis. PloS One, 9, e87712.

White, M.P.J., Webster, G., Leonard, F., and La Flamme, A.C. 2018. Innate IFN-γ ameliorates experimental autoimmune encephalomyelitis and promotes myeloid expansion and PDL-1 expression. Sci Rep, 8, 259.

Widera, D., Holtkamp, W., Entschladen, F., Niggemann, B., Zanker, K., Kaltschmidt, B., and Kaltschmidt, C. 2004. MCP-1 induces migration of adult neural stem cells. Eur J Cell Biol, 83, 381-387.

Wong, K.L., Lee, K.B.L., Tai, B.C., Law, P., Lee, E.H., and Hui, J.H. 2013. Injectable cultured bone marrow-derived mesenchymal stem cells in varus knees with cartilage defects undergoing high tibial osteotomy: A prospective, randomized controlled clinical trial with 2 Years' follow-up. Arthroscopy, 29, 2020-2028.

Wu, G., Luo, J., Rana, J.S., Laham, R., Sellke, F.W., and Li, J. 2006. Involvement of COX-2 in VEGF-induced angiogenesis via P38 and JNK pathways in vascular endothelial cells. Cardiovasc Res, 69, 512-519.

Wu, Y., Chen, L., Scott, P.G., and Tredget, E.E. 2007. Mesenchymal stem cells enhance wound healing through differentiation and angiogenesis. Stem Cells, 25,2648-2659.

Wynn, R.F., Hart, C.A., Corradi-Perini, C., O'Neill, L., Evans, C.A., Wraith,

J.E., Fairbairn, L.J., and Bellantuono, I. 2004. A small proportion of mesenchymal stem cells strongly expresses functionally active CXCR4 receptor capable of promoting migration to bone marrow. Blood, 104, 2643-2645.

Xu, C., Wang, J., Zhu, T., Shen, Y., Tang, X., Fang, L., and Xu, Y. 2016. Cross-talking between PPAR and WNT signaling and its regulation in mesenchymal stem cell differentiation. Curr Stem Cell Res Ther, 11, 247-254.

Yagi, H., Soto-Gutierrez, A., Parekkadan, B., Kitagawa, Y., Tompkins, R.G., Kobayashi, N., and Yarmush, M.L. 2010. Mesenchymal stem cells: Mechanisms of immunomodulation and homing. Cell Transplant, 19, 667-679.

Yang, J.X., Zhang, N., Wang, H.W., Gao, P., Yang, Q.P., and Wen, Q.P. 2015. CXCR4 receptor overexpression in mesenchymal stem cells facilitates treatment of acute lung injury in rats. J Biol Chem, 290, 1994-2006.

Yang, Z., Fuss, I.J., Watanabe, T., Asano, N., Davey, M.P., Rosenbaum, J.T., Strober, W., and Kitani, A. 2007. NOD2 transgenic mice exhibit enhanced MDP-mediated down-regulation of TLR2 responses and resistance to colitis induction. Gastroenterology, 133, 1510-1521.

Ylostalo, J.H., Bartosh, T.J., Coble, K., and Prockop, D.J. 2012. Human mesenchymal stem/stromal cells cultured as spheroids are self-activated to produce prostaglandin E_2 that directs stimulated macrophages into an anti-inflammatory phenotype. Stem Cells, 30, 2283-2296.

Yousefi, F., Ebtekar, M., Soleimani, M., Soudi, S., and Hashemi, S.M. 2013. Comparison of *in vivo* immunomodulatory effects of intravenous and intraperitoneal administration of adipose-tissue mesenchymal stem cells in

experimental autoimmune encephalomyelitis (EAE). Int Immunopharmacol, 17, 608-616.

Yu, B., Gong, M., He, Z., Wang, Y.-G., Millard, R.W., Ashraf, M., and Xu, M. 2013. Enhanced mesenchymal stem cell survival induced by GATA-4 overexpression is partially mediated by regulation of the miR-15 family. Int J Biochem Cell Biol, 45, 2724-2735.

Yu, K.R., Lee, J.Y., Kim, H.S., Hong, I.S., Choi, S.W., Seo, Y., Kang, I., Kim, J.J., Lee, B.C., Lee, S., Kurtz, A., Seo, K.W., and Kang, K.S. 2014. A p38 MAPK-mediated alteration of COX-2/PGE_2 regulates immunomodulatory properties in human mesenchymal stem cell aging. PLoS One, 9, e102426.

Zappia, E., Casazza, S., Pedemonte, E., Benvenuto, F., Bonanni, I., Gerdoni, E., Giunti, D., Ceravolo, A., Cazzanti, F., Frassoni, F., Mancardi, G., and Uccelli, A. 2005. Mesenchymal stem cells ameliorate experimental autoimmune encephalomyelitis inducing T-cell anergy. Blood, 106, 1755-1761.

Zhang, B., Wang, M., Gong, A., Zhang, X., Wu, X., Zhu, Y., Shi, H., Wu, L., Zhu, W., Qian, H., and Xu, W. 2015. HucMSC-exosome mediated-Wnt4 signaling is required for cutaneous wound healing. Stem Cells, 33, 2158-2168.

Zhang, Q.Z., Su, W.R., Shi, S.H., Wilder Smith, P., Xiang, A.P., Wong, A., Nguyen, A.L., Kwon, C.W., and Le, A.D. 2010. Human gingiva derived mesenchymal stem cells elicit polarization of M2 macrophages and enhance cutaneous wound healing. Stem Cells, 28, 1856-1868.

Zhao, L., Hu, C., Zhang, P., Jiang, H., and Chen, J. 2018. Novel preconditioning strategies for enhancing the migratory ability of mesenchymal

stem cells in acute kidney injury. Stem Cell Res Ther. 9, 225.

Zhou, J., Tan, X., Tan, Y., Li, Q., Ma, J., and Wang, G. 2018. Mesenchymal stem cell derived exosomes in cancer progression, metastasis and drug delivery: A comprehensive review. J Cancer, 9, 3129-3137.

Zhu, G.H., Wong, B.C., Slosberg, E.D., Eggo, M.C., Ching, C.K., Yuen, S.T., Lai, K.C., Soh, J.W., Weinstein, I.B., and Lam, S.K. 2000. Overexpression of protein kinase C-β1 isoenzyme suppresses indomethacin-induced apoptosis in gastric epithelial cells. Gastroenterology, 118, 507-514.

Zhu, Y., Liu, T., Song, K., Fan, X., Ma, X., and Cui, Z. 2008. Adipose-derived stem cell: A better stem cell than BMSC. Cell Biochem Funct, 26, 664-675.

Zimmermann, J.A., and Mcdevitt, T.C. 2014. Pre-conditioning mesenchymal stromal cell spheroids for immunomodulatory paracrine factor secretion. Cytotherapy, 16, 331-345.

Zippel, N., Schulze, M., and Tobiasch, E. 2010. Biomaterials and mesenchymal stem cells for regenerative medicine. Recent Pat Biotechnol, 4, 1-22.

국문 초록

인간 중간엽 줄기세포의 면역 조절능을 통한 치료 효율 향상 연구

서울대학교 대학원

수의학과

수의병인생물학 및 예방수의학 전공

이병철

(지도교수: 강경선)

인간 중간엽 줄기세포는 면역 조절능 및 조직 재생능을 촉진하는 바이오-의료적 특성을 지니고 있어, 최근 다양한 면역 이상 질환에

대한 대체 치료제로서 각광을 받고 있다. 하지만 다년간의 기초 및 전임상 연구에도 불구하고, 위 세포를 이용한 임상 실험의 결과는 편차가 크고, 그 기대에 부응하지 못하는 경우가 많다. 이와 같은 연구 결과와 임상 시험 결과 간의 차이는 이식된 세포의 병변부로의 생착 실패, 낮은 체내 생존율, 공여자에 따라 상이한 세포의 특성 등의 요인으로 인하여 유발된다. 그러므로 현재 중간엽 줄기세포 기반 치료가 직면하고 있는 문제들을 극복하고, 더 향상된 치료 효과를 얻기 위해서 중간엽 줄기세포의 항상성과 치료효능을 증대시킬 수 있는 방안을 개발해야 한다.

인간 제대혈 및 지방조직 유래 중간엽 줄기세포는 다양한 계통의 면역세포를 억제할 수 있는 것으로 알려져 있다. 또한 많은 연구를 통해 위 중간엽 줄기세포의 자가 면역성 질환에 대한 치료 효능 및 관련 치료 기전이 밝혀졌다. 실제로 중간엽 줄기세포로부터 분비되는 Prostaglandin E_2 (PGE_2)와 같은 면역 조절 인자가 질병을 유발하는 데 핵심 역할을 하는 면역 세포의 작용을 억제할 수 있으며, 이와 관련된 작용 기전이 다각도로 규명되어 왔다. 그러나 이러한 분비인자들의 중간엽 줄기세포에 대한 직접적인 영향과 배양 환경 등의 변화에 따른 면역조절 인자들의 생산 조절에 대해서는 명확히 밝혀진 바 없다. 그러므로 본 연구의 첫 번째 장에서는 자가 분비된 PGE_2가 인간 제대혈 및 지방조직 유래 중간엽 줄기세포의 생장과 줄기세포능에 미치는 직접적인 영향, 더 나아가 세포간 접촉에 의한 PGE_2 생산 조절, 이로 인해 발생하는

줄기세포의 면역 조절능 변화 양상을 조사하였다. PGE_2의 분비를 선택적으로 억제하기 위해 COX-2 혹은 mPGES-1에 대한 억제제를 처치하고 중간엽 줄기세포의 증식율을 측정하였다. 그 결과, 중간엽 줄기세포에서 EP2 수용체를 통해 PGE_2의 분비를 조절하며, 이는 세포의 생장과 직접적인 관련이 있음을 밝혀냈다. 실제로 PGE_2의 분비를 억제하였을 경우, G_1 cell cycle arrest를 통하여 생포의 증식이 억제되며, 중간엽 줄기세포 유래 PGE_2가 이러한 성장 억제를 해소하여 줄 수 있는 것을 밝혔다. 또 동일 수의 세포로부터 생산되는 PGE_2의 양은 Gap junction 세포간 신호전달 (Gap junction intercellular communication, GJIC)에 의하여 감소되는 것을 밝혔다. 세포간 접촉에 의한 PGE_2 분비량의 감소는 곧 줄기세포의 면역억제능의 저하로 이어진다. 결과적으로 중간엽 줄기세포에 의해 분비된 PGE_2는 EP2 수용체를 통해 줄기세포의 자가 증식능의 유지에 기여한다. PGE_2의 분비는 세포간 접촉에 의해 저해될 수 있으며, 이는 줄기세포의 면역조절능의 감소를 야기한다.

본 연구의 두 번째 장에서는 NOD2 및 TLR9 수용체의 작용제로 이루어진 MIS416 microparticle의 공동 적용을 통해 염증성 장염에 대한 제대혈 유래 중간엽 줄기세포의 치료 효능을 증진시킬 수 있는지를 조사하였다. 장염 동물실험 모델은 3% Dextran sulfate sodium (DSS) 용액을 음수로 공급하여 유발하며, MIS416과 제대혈 유래 중간엽 줄기세포를 차례로 체내로 주입하였다. 실험동물의 상태를 육안적으로 검사

하고, 안락사 후에 추가적인 검사를 위해 혈액, 비장, 결장 조직을 채취한다. MIS416의 작용기전을 분석하기 위해서 제대혈 유래 중간엽 줄기세포 뿐 아니라 혈액으로부터 분리해 낸 면역세포와의 공배양을 진행하고 추가적인 검사를 수행하였다. 그 결과, MIS416을 줄기세포와 공동주입해 준 실험군에서 염증성 장염의 증상이 더욱 효과적으로 완화되며, 복합처치를 통하여 줄기세포의 치료능을 증진할 수 있었다. 그러나 MIS416의 직접 처치는 제대혈 유래 중간엽 줄기세포의 면역 조절능에 대한 변화를 유발하지 않았다. 대신 체내로 주입된 MIS416은 장내 면역환경의 변화가 줄기세포가 더욱 쉽게 병변부로 이동할 수 있도록 도우며, 염증반응을 효과적으로 억제할 수 있도록 한다. 이에 더하여, MIS416과 중간엽 줄기세포의 상호 작용을 통하여 억제성 T 세포의 장내 침착 및 조절작용이 증대되는 것을 확인하였다. 이 연구 결과를 통해 MIS416의 공동 적용은 체내 염증 반응을 조절하여 제대혈 유래 중간엽 줄기세포의 치료효능이 증진될 수 있음을 증명하였고, 이는 현재 임상분야에서 줄기세포 기반 연구가 마주한 장애를 극복할 수 있는 효과적인 방안이 될 수 있다.

이 연구 결과들을 통해 (1) 세포간 접촉에 의해 조절되는 PGE_2의 분비와 EP2 수용체의 발현은 중간엽 줄기세포의 세포 증식과 면역억제능에 관여하며, 줄기세포 및 줄기세포 배양액을 이용한 치료제 생산과정에 이러한 세포 생리학적인 특성이 고려되어야 함을 제안하였고, (2)

MIS416와의 복합처치를 통해 중간엽 줄기세포의 생착과 면역 억제능을 간접적으로 증진시킬 수 있음을 증명하였다. 결론적으로 본 연구를 통해 중간엽 줄기세포의 면역조절능 저하를 막기 위해 과도한 세포간 접촉을 지양해야 하며, 면역조절물질의 공동 적용을 통해 중간엽 줄기세포의 치료효율이 증강될 수 있음을 밝혔다.

주요어 : 중간엽줄기세포, 세포간 접촉, PGE_2, 세포 증식, 면역억제, MIS416, 염증성 장질환, 세포 이동

학번 : 2012-21544